ACIDITY AND CATALYTIC ACTIVITY OF

ZEOLITE CATALYSTS BOUND WITH SILICA AND ALUMINA

A Dissertation

by

XIANCHUN WU

Submitted to the Office of Graduate Studies of
Texas A&M University
in partial fulfillment of the requirements for the degree of

DOCTOR OF PHILOSOPHY

December 2003

Major Subject: Chemical Engineering

ACIDITY AND CATALYTIC ACTIVITY OF

ZEOLITE CATALYSTS BOUND WITH SILICA AND ALUMINA

A Dissertation

by

XIANCHUN WU

Submitted to Texas A&M University
in partial fulfillment of the requirements
for the degree of

DOCTOR OF PHILOSOPHY

Approved as to style and content by:

Rayford G. Anthony (Chair of Committee)	Aydin Akgerman (Member)
David M. Ford (Member)	Michael P. Rosynek (Member)
	Kenneth R. Hall (Head of Department)

December 2003

Major Subject: Chemical Engineering

ABSTRACT

Acidity and Catalytic Activity of Zeolite Catalysts Bound with Silica and Alumina.

(December 2003)

Xianchun Wu, B.S., Daqing Petroleum Institute, China;

M.S., Daqing Petroleum Institute, China

Chair of Advisory Committee: Dr. Rayford G. Anthony

Zeolites ZSM-5 (SiO_2/Al_2O_3=30~280) and Y(SiO_2/Al_2O_3=5.2~80) are bound with silica gel (Ludox HS-40 and Ludox AS-40) and alumina (γ- Al_2O_3 and boehmite) by different binding methods, namely, gel-mixing, powder-mixing and powder-wet-mixing methods. The acidities of the bound catalysts and the zeolite powder are determined by NH_3-TPD and FTIR. The textures of these catalysts are analyzed on a BET machine with nitrogen as a probe molecule. The micropore surface area and micropore volume are determined by t-plot method. Micropore volume distribution is determined by Horvath-Kawazoe approach with a cylindrical pore model. Mesopore volume distribution is determined by BJH method from the nitrogen desorption isotherm.

Silica from the binder may react with extra-framework alumina in zeolites to form a new protonic acid. SiO_2-bound catalysts have less strong acidity, Bronsted acidity and Lewis acidity than the zeolite powder. Also, the strength of strong acid sites of the zeolites is reduced when silica is embedded. Micropore surface area and micropore

volume are reduced by about 19% and 18%, respectively, indicating some micropores of ZSM-5 are blocked on binding with silica. SiO_2-bound ZSM-5 catalysts have less catalytic activity for butane transformation (cracking and disproportionation) and ethylene oligomerization than ZSM-5 powder.

When alumina is used as a binder, both the total acid sites and Lewis acid sites are increased. Micropore surface area and micropore volume of ZSM-5 powder are reduced by 26% and 23%, respectively, indicating some micropores of ZSM-5 are blocked by the alumina binder. Alumina-bound catalysts showed a lower activity for butane transformation and ethylene oligomerization than ZSM-5 powder.

Alkaline metals content in the binder is a crucial factor that influences the acidity of a bound catalyst. The metal cations neutralize more selectively Bronsted acid sites than Lewis acid sites. Alkaline metal cations in the binder and micropore blockage cause the bound catalysts to have a lower catalytic activity than the zeolite powder.

Dedicated to

My Wife: Linlin

And

My Daughter: Mo

ACKNOWLEDGEMENTS

I am very grateful to my committee chair and research advisor, Dr. Rayford G. Anthony, for his continual interest, guidance, and support throughout the course of this research. His invaluable insight and encouragement during my study and research are greatly appreciated. I also appreciate his valuable time spent on deliberating and discussing this project with me. I also thank him for allowing me to take on the Ph.D. program while I was a full-time employee working under his direction. Additionally, I am also grateful to my committee members, Dr. Aydin Akgerman, Dr. David M. Ford, and Dr. Michael P. Rosynek for their suggestions, advice, ideas, and assistance on my research.

I thank Prof. Jack Lunsford in the Chemistry Department of Texas A&M University, Profs. Daniel Shantz and Gilbert F. Froment in the Chemical Engineering Department of Texas A&M Univeristy, Prof. Miki Niwa at the Department of Materials Science, Faculty of Engineering of Tottori University, Japan, and Dr. Ferenc Lonyi at the Institute of Chemistry, Chemical Research Center, Hungarian Academy of Science, Hungary, for their helpful comments and advice on zeolite physiochemical properties and measurement.

I extend my special thanks to Dr. C.V Philip for his kind help whenever I needed it. His encouragement and assistance made my research work easier to conduct and progress in a smooth manner. I learned so much from him about gas chromatographic science. Special thanks go to former graduates Drs. Sirirat Jitkarnka, Michael Abraha,

and Ammar Alkhawaldeh for their support and help through the years. I would also like to thank Dr. Roberto Flores for showing me how to use the NH_3-TPD apparatus. I would also like to thank the current members of the kinetics group: Dr. Bo Wang, Dr. Jagannathan Govindhakannan, Saeed Al-Wahabi, Won-jae Lee, Sung Hyun Kim, Rogelio Sotelo-Boyas, Hemendra Khakhar, Hans Kumar, Luis Castaneda, and Celia Marin for making the laboratory a lively research place to work. Working in such a big group with each member being specialized in one or two areas, allowed me to benefit so much from the group.

I would like to thank the staff of the Chemical Engineering Department at Texas A&M University for their kind assistance. A special thank you to Randy Marek for all the help he provided in setting up the experimental apparatus.

I owe a special gratitude to my Mom who, even though she did not have a chance to go to school before she died in 1981, always managed to create ways to allow me to go to school, so I would have an opportunity to be educated. She has been a source of inspiration for me. Special thanks also go to my parents-in-law and my brothers and sisters for their concerns for me and my family.

Finally I would like to express my gratitude to my best friend and former collegemate, Minghui Zhu, for his friendship and encouragement.

TABLE OF CONTENTS

CHAPTER Page

LIST OF FIGURES

FIGURE Page

FIGURE Page

FIGURE Page

FIGURE Page

LIST OF TABLES

CHAPTER I

INTRODUCTION

1.1 Zeolite Development and Properties

The word “Zeolite” was first used by a Swedish mineralogist Axel Cronstadt. In 1756, he discovered the very first zeolite mineral “stilbite”. This mineral visibly lost water when heated. Accordingly, he named this class of mineral “zeolite” from the classical Creek words “zeo”, meaning to boil, and “lithos”, meaning stone. Since then, about 40 different kinds of natural zeolites have been identified (Hewin International, 2000). They vary in crystal structure and chemical composition, and some physical properties as well. Today, most natural zeolites have been successfully synthesized in laboratory or in commercial plants. Besides natural zeolites, man-made or synthetic zeolites have also added many new members to the zeolite family. Scientists have synthesized many zeolites that do not exist naturally or at least have not been discovered on the earth (Hewin International, 2000).

Zeolite is defined by J.V. Smith (1963) as “an aluminosilicate with a framework structure enclosing cavities occupied by large ions and water molecules, both of which have considerable freedom of movement, permitting ion-exchange and reversible dehydration.” Other definitions can also be found. P. A. Jacobs (1977) gave such a definition: “zeolites as synthesized or formed in nature are crystalline, hydrated alumino-

---

This dissertation follows the format of *Industrial Engineering and Chemical Research*.

silicates of group I and II elements. Structurally, they comprise a framework based on an infinitely extending three-dimensional network of SiO_4 and AlO_4 tetrahedra linked together through common oxygen atoms." R. Szostak (1989) stated that "structurally, zeolite is a crystalline aluminosilicate with a framework based on an extensive three-dimensional network of oxygen ions." Recently, Corma (2003) defined zeolite as "crystalline silicalites and aluminosilicates linked through oxygen atoms, producing a three-dimensional network containing channels and cavities of molecular dimensions." Although the four definitions are stated differently, the main characteristics of a zeolite are either clearly expressed or implied as a crystalline material of aluminosilicate featured by a three-dimensional microporous framework structure built of the primary SiO_4 and AlO_4 tetrahedra, and ion-exchange capability. Apparently, Corma extended the definition to silicates.

Common examples of zeolites are A, X, Y, ZSM-5, β, chabazite, and erionite. Because of the unique sizes of pore openings and the channels in zeolites, zeolites are also called molecular sieves. Molecular sieves are materials that can selectively adsorb molecules based on molecule shape and size (R. Szostak, 1989). Molecular sieve materials involve a variety of micropore and mesopore materials, such as zeolites, metalloaluminates, silicates, metallosilicates, aluminophosphates (AlPO), silicoalumino-phosphates (SAPO), carbon sieves, and MCM-41. By definition, any material that can "screen" molecules based on the molecular size can be referred to as molecular sieve. Unlike zeolites that are crystalline material composed of SiO_4 and AlO_4 tetrahydra, molecular sieves are crystalline or amorphous materials composed of any elements.

Since the first man-made zeolite A and X were synthesized and commercially used as adsorbents by Union Carbide Co. (UCC) in 1948 (Corma, 2003), the development of synthetic zeolites have been fast paced, especially in recent years. In 1972, Mobil Company (now merged with Exxon to ExxonMobil) synthesized a medium pore, high silica content zeolite, the so-called ZSM-n series. Before this invention, either synthetic or natural zeolites had never had a silica-to-alumina ratio of more than 9. Since then, the synthesis of new zeolites or molecular sieves has been a major research area, especially since 1982 when UCC synthesized $AlPO_4$-n and SAPO-n molecular sieves. The invention of $AlPO_4$-n and SAPO-n molecular sieves by the researchers at UCC enlightened and inspired scientists all over the world to make many new hybrid zeolites or molecular sieves. From this invention, scientists learned it is possible to make hybrid zeolites, such as metalloaluminates, silicates, metallosilicates, etc., by isomorphic substitution. So, many hybrid zeolites or molecular sieves have been prepared. However, the channel openings (apertures) of zeolites or molecular sieves, either natural or man-made, were mainly composed of either 8-, 10-, or 12-member rings. In 1988, Davis et al. (1988) synthesized an aluminophosphate molecular sieve (VPI-5) with a channel opening of 18-member ring. Three years later in 1991, Esterman et al. (1991) synthesized a gallophosphate (Cloverite) with a bigger channel opening that is composed of 20-member rings. One year later in 1992, researchers at Mobil Research and Development Co. developed a series of novel, mesoporous molecular sieves. One member of this series, MCM-41, possesses uniformly sized mesopores of 1.5 - 10 nm (Beck et al, 1992). In addition to zeolite or zeolite-type crystalline materials with pore openings of 8-, 10-,

12-, 18, and 20-membered rings, a 14-membered ring zeolite-type material, $AlPO_4$-8, was prepared in 1990 (Dessau et al.,1990). Currently, research has been focusing on the catalysis and application of these new zeolites or molecular sieves materials.

As stated previously, synthetic zeolites or molecular sieves have pore openings of from 8-member to 20-member rings. However, natural zeolites are mainly of 8- or 12-member ring openings, such as chabazite and mordenite. The largest pore openings of a natural zeolitic material, cacoxenite, has been found to be 1.4 nm. It is a highly hydrated basic ferric oxyphosphate (Moore et al., 1983).

By the definition of zeolites, $AlPO_4$-n, SAPO-n, metallosilicates, metalloaluminates, silicates, borosilicates, etc., showed not be referred to as zeolites. Sometimes, these materials are referred to zeolite-type or zeolitic materials, because they have many similar properties as zeolites, such as crystallinity, unique pore structure system, and ion-exchangeability (except for $AlPO_4$-n and silicates), etc.

Since zeolites are composed of SiO_4 and AlO_4 tetrahedra, the AlO_4 tetrahedra cause the zeolite framework to possess negative charges. Positive charges are required to balance the negative framework charges to allow the zeolite to be a neutral material. Such positive charges can be metal ions or protons. Because of the presence of metal cations or protons in zeolite structures, zeolites have cation-exchange ability or acidic properties. The ion-exchange properties of zeolites play an important role when zeolites are used as catalysts or adsorbents. The acidic property of a zeolite takes the major role in zeolitic catalytic materials for acid-catalyzed reactions.

Structurally, zeolites are built of primary and secondary building units. The primary unit is simply the SiO_4 or AlO_4 tetrahedron. Si or Al atom sits at the center of the tetrahedron with 4 oxygen atoms co-valently bonded to the centered Si or Al atom (so-called T-atom). From this primary unit, a number of secondary building units can be built by a linkage through the oxygen atom covalent bonding, which is called an oxygen bridge. The secondary building units are featured by simple geometric shapes such as those shown in Fig.1.1.1. A zeolite structure is finally constructed from the secondary units. A pore channel system is formed during the systematically packing of the secondary units. A schematic representation of the structuring process of a zeolite is shown in Fig.1.1.1, where the final zeolite structure of Y is taken as an example.

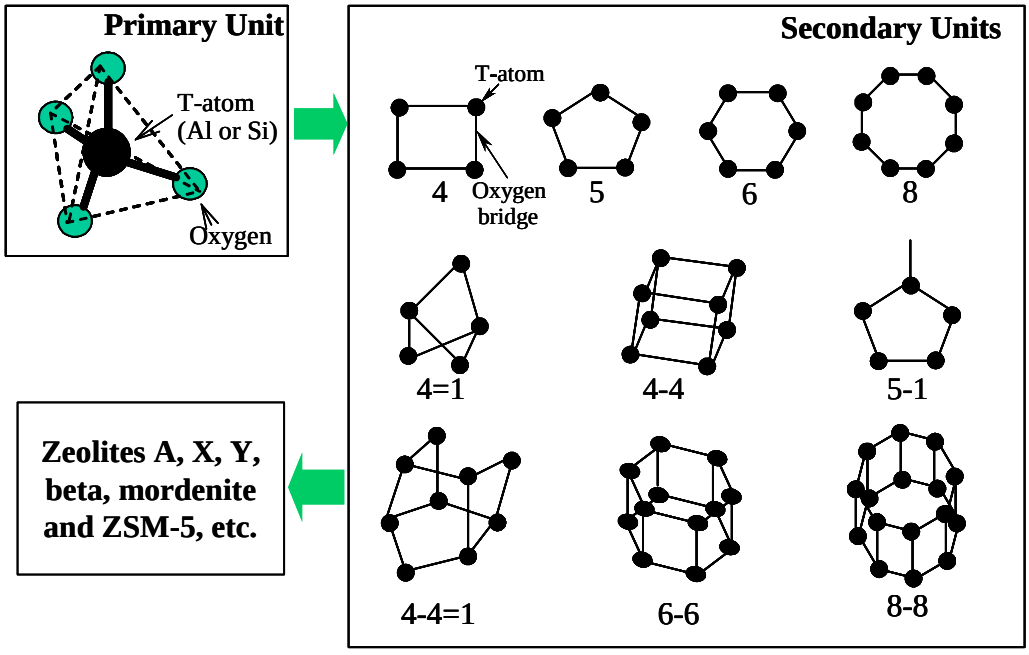

Fig.1.1.1 Schematic representation of building zeolites.

Zeolite Y has the same structure as the natural zeolite, faujasite. Inside its structure, there is a super-cage of internal diameter of 1.25nm with free apertures (constructed of 12-member rings) of 0.74 nm. The micropore channels are three-dimensional (Jacob, 1977). ZSM-5 does not have this kind of super-cages. It has three-dimensional microporous channels with pore openings (10-member rings) of 0.53×0.56 nm for sinusoidal channels and 0.51×0.55 nm for straight channels (Meier et al., 1996).

Zeolites have Bronsted and Lewis acid sites. Bronsted acid can donate protons, while Lewis acid can accept a pair of electrons. Bronsted acid sites in zeolites can change into Lewis acid sites through dehydroxylation on heating. And the reverse reaction takes place when water is present in the zeolite (Jacob, 1977), as shown in Fig.1.1.2.

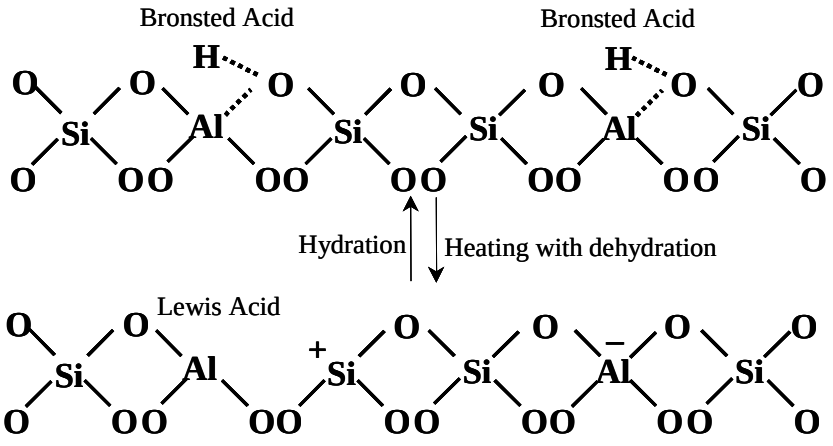

Fig.1.1.2 Inter-conversion of Bronsted and Lewis acid sites.

Zeolites have unique channels (one-dimension, two-dimension, or three-dimension) with pore opening from about 0.3 nm to 0.8 nm (however, synthetic zeolite-type crystalline materials have pore openings up to about 1.3 nm, such as Cloverite). Because of the presence of micropores, zeolites have high surface areas of up to 1000 m^2/g. The unique micropores and high surface areas of zeolites play an important role in the application of zeolites in catalysis and adsorption.

As a summary, zeolites have the following unique properties.

- ♦Acidity and basicity—Bronsted and Lewis acid sites with their conjugated bases.
- ♦Ion-exchange ability— due to the presence of AlO_4 tetrahedra
- ♦Shape selective adsorption—due to the unique channels of molecular dimensions
- ♦High surface area—due to the micro- and meso-porous structure
- ♦Micropores—resulting high surface area, shape-selective adsorption and catalysis
- ♦Structural stability—stable in acidic or basic medium
- ♦Thermal stability—withstanding temperatures up to 1000^oC

Because of their unique properties, zeolites or zeolite-type materials have been found for many applications. Although many natural zeolites have been found around the world, they have found less commercial applications than synthetic zeolites or zeolite-type materials because natural zeolites often contain impurity components that restrict their commercial applications. The following section will only discuss the applications of synthetic materials.

1.2 Application of Synthetic Zeolites or Zeolite-type Materials

Synthetic zeolite or zeolite-type materials have been found for applications in various areas. The major applications include using zeolites or zeolite-type materials as ion-exchangers, adsorbents, and catalysts. However, there are some other new applications that have been developed in recent years, such as using zeolites to make molecular wires, nano-devices, optical devices and membranes. Only the major applications will be described.

In the United States in Year 2000, the production of synthetic zeolites totaled 465 $\times 10^3$ metric tons, among which, 365 $\times 10^3$ tons (78.5%) were for detergent builders, 70 $\times 10^3$ (15.0%) tons for catalysts, and 30 $\times 10^3$ tons (6.5%) for adsorbents and desiccants. On the worldwide basis, Fig.1.2.1 shows the projected productions of synthetic and natural zeolites. It is clearly shown that the production and use of synthetic zeolite materials will increase by about 15% annually. Fig.1.2.2 shows the utilization and sales of synthetic zeolites on the world. Apparently, even though zeolite catalysts take only about 8% of the total synthetic zeolite volume production, their sales represent more than half of the total sales of the synthetic zeolites, because zeolite catalysts are much more expensive than ion-exchangers and adsorbents. Fig.1.2.3 depicts the prices (Hewin International, 2000).

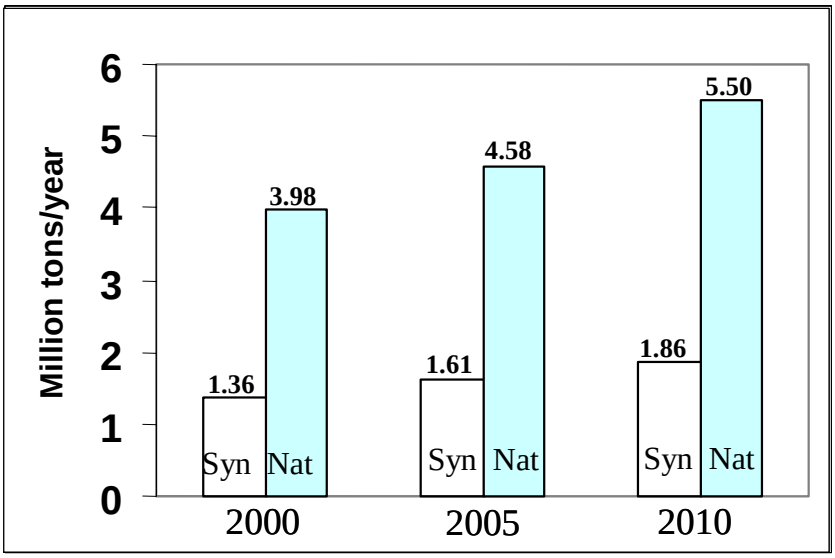

Fig.1.2.1 Worldwide production of synthetic and natural zeolites projected to year 2010 (Data taken from Hewin International, 2000). Legends: Syn and Nat stand for synthetic and natural zeolites, respectively.

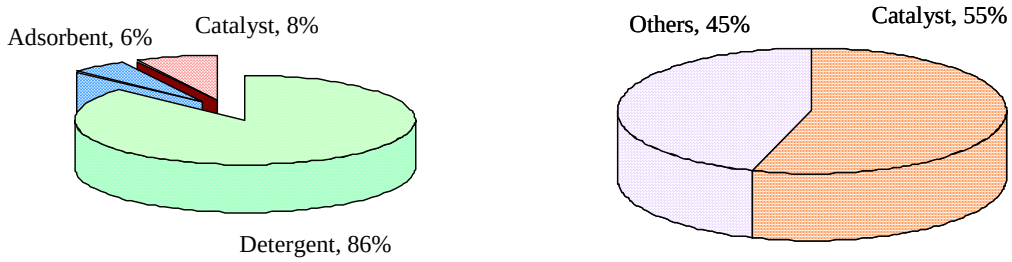

(A) Synthetic zeolites production percentage (B) Synthetic zeolites sales percentage

Fig.1.2.2 Utilizations and sales of synthetic zeolites on worldwide zeolite market (Data taken from Hewin International, 2000).

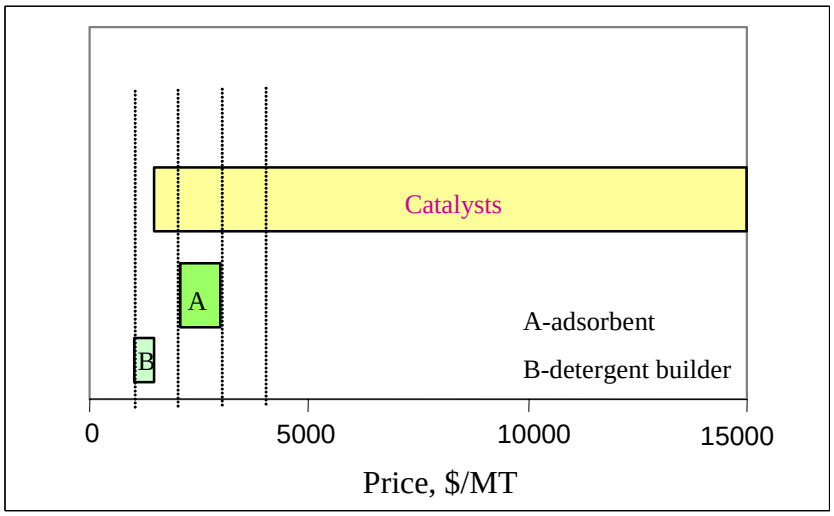

Fig.1.2.3 Prices of synthetic zeolites used for different purposes (Data taken from Hewin International, 2000).

1.2.1 Zeolites as Ion-exchangers

As stated previously, zeolites have ion-exchange ability because they contain exchangeable cations to balance electronically the negative charged framework. This property has allowed zeolites to have industrial applications as ion-exchangers. Traditionally, a detergent builder was sodium tripolyphosphate, and it was used primarily from 1940s-1970s. Sodium tripolyphosphate was found to have the potential to contribute to eutrophication. Therefore, it is banned in many countries for use as a detergent builder. Zeolites are a good alternative.

Zeolites as ion-exchangers are mainly used in detergent production. They are used as a “softener” or “hardness carrier”. The zeolite used as a detergent builder is in the sodium form. The hardness of wash water, namely the calcium and magnesium ions, are extracted and bound to the zeolite and the sodium ion on the zeolite is released into the

washing water. Today, zeolites are the major detergent builder, especially in Western Europe, the United States, and Japan. Zeolites used as detergent builder are zeolites A and X in the form of Na. About 86% of synthetic zeolites are used as detergent builder through out the world.

1.2.2 Zeolites as Adsorbents

The unique channels and high surface area of zeolites or zeolite-type materials provide these materials with a high adsorption capacity and shape-selective adsorption. Zeolites have been used as desiccants for drying air, natural gas, other light hydrocarbon gaseous streams, and some liquid streams to remove water. Zeolites have a high adsorption capacity of moisture and a strong power to remove water from gases. The dew-point of a gas steam can be achieved to below $-100^{o}C$. For example, in the cryogenic separation of the hydrocarbons in a steam cracker of naphtha, zeolite A is used to remove trace amounts of water in the hydrocarbon stream to achieve a low dew point to avoid blocking of pipelines which may happen due to freezing water.

Zeolites are also used for separation or purification. For instance, zeolite Ag-X is used to recover ethylene from a dilute ethylene stream; zeolite A is used to remove water, CO_2 and H_2S from natural gas; zeolite X is used to remove aromatics from naphtha; zeolite A is used for separation of oxygen and nitrogen from air; ZSM-5 is used in separation of para-xylene from a C_8 aromatic hydrocarbon mixture; zeolite A is used to separate normal paraffins from their isomers. Some other recent applications of zeolites as adsorbents may be found in environmental control and protection, such as in

the application of catalytic converters in automobiles, removal of volatile organic compounds from air, and odor control in restrooms.

When zeolites are used for separation or purification, the molecules to be removed or separated should have a difference in one or more of the following properties from the other molecules:

- ♦molecular size and shape;
- ♦polarity for polar molecules;
- ♦induced-dipole moment for non-polar molecules;
- ♦boiling point;
- ♦saturation of hydrocarbons (saturated and unsaturated hydrocarbons);
- ♦aromaticity of hydrocarbons (aromatics and non-aromatics).

Theoretically, if the molecules in a mixture distinguish in one or more of the above properties, a zeolite or a modified zeolite could be found to facilitate to the separation. The zeolites used as adsorbents are mainly A and X type zeolites. About six percent of synthetic zeolites in the world are used as adsorbents.

1.2.3 Zeolites as Catalysts

The biggest sales in the synthetic zeolite market come from the catalyst sector, even though the volume of synthetic zeolites in the catalysts sector is much smaller than the detergent builder sector. This is because zeolite catalysts are much more expensive. More importantly, zeolites play an important role in the catalyst world. Today, about 80 to 90% of the products we use in our daily life are somehow related to catalysts

somewhere in their manufacturing process (Marchilly, 2003). About 40% of catalysts used in the chemical and petrochemical industrial processes are zeolite or zeolitic catalysts (Tanabe et al., 1999). Zeolite and zeolite-type catalysts will play a more important role in the catalyst world by finding new applications and synthesizing zeolites of new structures and properties (Corma, 2003).

Zeolites as a solid catalyst (a solid acid and a solid base) have many unique properties. Among these properties, acidity, shape-selective catalysis, high surface area and structure stability are the most important ones in zeolite catalysts. Recently, basicity in zeolite and its catalysis have drawn researchers' attention (Corma, 2003).

Zeolites as acidic catalysts have been used commercially in petroleum refining and petrochemical processing (Jacob, 1977). In petroleum refining, zeolite catalysts are used in catalytic cracking, catalytic reforming, lube dewaxing, and hydrocracking; in chemical processing, zeolites are used as catalysts for a number of processes, such as isomerization (xylene or C_4-C_6 alkanes), alkylation (alkyl aromatics production), disproportionation (toluene to xylene, especially to p-xylene), methanol conversion (to olefin or gasoline), oligomerization (propylene or butenes to gasoline or diesel), aromatization (C_3-C_7 alkanes), hydration of olefins (propylene to di-methyl ether), and dehydrogenation (butane to butenes). There are several recent detailed reviews on zeolite and zeolite-type catalysts (Tanabe et al., 1999; Hewin International, 2000; Marcilly, 2003; Degnan, Jr, 2003).

In recent years, zeolites used as catalysts for fine chemical synthesis started to obtain researchers' attention (Climent et al, 2000 and 2001; Clerici, 2001; Guisnet et al.,

2002), because zeolite or zeolite-type catalysts are more active, selective, environmentally benignant and easier to separate from products than traditional Friedel-Crafts catalysts. Traditionally, the fine chemicals were synthesized, in case it needs an acid catalyst, using Friedel-Crafts catalysts such as $AlCl_3$, which is not environmentally benignant. Some fine chemicals can be prepared with zeolite or zeolite-type catalysts at a higher selectivity and yield than a traditional catalyst. For example, benzyl methyl ether and benzyl alcohol can be selectively synthesized from benzene and formaldehyde on zeolite ZSM-5. The channels of ZSM-5 restrict the bulky tri-phenyl methane formation. While on Friedel-Crafts catalyst such as $AlCl_3$, the reaction product is tri-phenyl methane and it is difficult to stop the reaction at the benzyl methyl ether stage (Wu et al., 1999; 2001).

1.3 Bound Zeolite Catalysts and Research Purposes

Zeolites Y and ZSM-5 have been employed in a vast array of applications as catalysts in the petroleum refining and chemical industry. Because of their poor self-binding property, they need to be bound with a binder (matrix) such as silica, alumina, clay, or their mixture to produce a desired physical shape and mechanical strength for industrial applications. Among the binders for zeolites, silica and alumina are most widely used. A proper physical shape and mechanical strength of a commercial catalyst would give a reasonable stream pressure drop and low mechanical loss of the catalyst due to attrition.

Although synthetic zeolites have had a history of about a half century, the effects of a binder on zeolite physicochemical and catalytic properties have not drawn as much researchers' attention as zeolites themselves (without a binder) have done (Romero et al., 1997; Dorado et al., 2002). Research has been focused on the synthesis, acidic properties and catalysis with zeolites. There have been several books dedicated to this area, in addition to a tremendous number of papers in journals and professional proceedings. Compared to the research work done on the acidic and catalytic properties of zeolites, much less work has been done on the physicochemical, acidic and catalytic properties of bound zeolites, which will be used if there are commercial applications. In academia, the acidic and catalytic properties or even a kinetic model were studied primarily based on a pure zeolite (unbound zeolite). The binder effects were skipped or neglected. Any commercial zeolite catalysts have to be bound with a binder into a desired physical form and strong enough to resist attrition. Catalyst manufactures might have realized that a binder has effects on acidic and catalytic properties, but kept the detailed information secret.

In most catalysis cases, zeolites are applied as an acidic catalyst. For a solid acidic catalyst, three important acidic properties should be addressed, that is, acid site density, nature of acid sites (i.e., Bronsted acid and Lewis acid), and the strength of acid sites. Since most zeolite catalysts are utilized in the bound form, a question should be asked whether the binder has any effects on the physical and chemical properties such as surface area, pore volume, and acidities, and further on the catalytic properties of the zeolites. One might think that zeolite would not experience any change on binding

because the binder that is used is often assumed to be “inert” and the zeolite is “mechanically” mixed with the binder. Others may believe that zeolite would experience some changes in its properties when it is bound. Therefore, a better understanding of the changes in the physical and acidic properties of the bound zeolite catalysts would be a great help for catalyst research and for successfully preparing commercial zeolite catalysts.

The purpose of this research is to study the changes of zeolites Y and ZSM-5 in important properties with respect to catalysis, which are the surface area, pore volume, acidity, after binding with silica and alumina binders. Further, model reactions using butane transformation (cracking and disproportionation) and ethylene oligomerization are performed on the zeolites and their binder-embedded counterparts to investigate how these changes affect the catalytic activity for the acid-catalyzed reactions. Butane transformation (cracking and disproportionation) occurs on strong acid sites (Guisnet et al., 1996), while ethylene oligomerization may take place on both weak acid sites and strong acid sites.

CHAPTER II

LITERATURE REVIEW

A zeolite or zeolite-type material is in fine powder form when it is synthesized. Therefore, it has to be incorporated into a matrix, namely a binder, in order to obtain a large and rigid catalyst of some physical forms to avoid a high pressure drop in a fixed-bed reactor or attrition in a moving-bed or fluidized-bed reactor, if the catalyst is to be applied at the industrial level. The most commonly used binders have included refractory oxides such as alumina and silica, and clay such as kaolin and montmorillonite. These binders are thermally stable and fairly easy to extrude and provide extrudates of good physical strength. The presence of a binder may affect the acidic and physical properties of a zeolite and thus the catalytic performance of the final catalyst such as activity, selectivity and deactivation. The change in the catalyst performance may be a result of the changes in alkaline metal contents of zeolite, blockage of zeolite channels, decrease in surface area, and trapping of coke precursors on binders. However, even though the catalytic properties of a zeolite catalyst could be greatly affected by a binder, the effect of the binder on the acidity, physical properties and activity of a zeolite "has been rarely studied" (Romero et al., 1997; Dorado et al., 2002).

Researchers at former Mobil Oil Corp. did some pioneering work on embedding ZSM-5 in oxides. Chang et al. (1984) and Shihabi et al. (1985) investigated the acidity and activity change of high silica content ZSM-5 ($SiO_2/Al_2O_3 \geq 1600$) after reaction with aluminum halides or embedding on alumina matrix, respectively. If the high silica ZSM-

5 was treated with $AlCl_3$ or $AlBr_3$ in solid-gas phase reaction or with aluminum fluoride in liquid phase reaction (pH = 5.9~10.5), a new Bronsted acid was formed that is similar to the bridged Bronsted acid found in a common ZSM-5. The high silica ZSM-5 thus treated showed a higher activity for acid-catalyzed reactions and a higher NH_4^+-exchange capacity (thus higher acidity). On alumina-bound ZSM-5, they used α-alumina monohydrate as the binder. The bound catalyst was made by first wet-mulling the binder with the zeolite powder, extrudating the paste, calcining the extrudates at 538°C, NH_4^+-exchanging and finally calcining again at 538°C. They found the alumina-bound high silica ZSM-5 had a higher acidity and activity than the ZSM-5 powder for acid-catalyzed reactions such as cracking, oligomerization, lube hydrodewaxing and methanol conversion. The bound catalyst also had a higher ion-exchange capacity. Based on the results, they proposed that Al from aluminum halides or the binder migrated into the zeolite framework, resulting in new Bronsted acid sites. These sites are not associated with some new alumino-silicate phases formed at the grain boundaries. This Al migration resulted in all of these enhancements in acidity, activity and ion-exchange capacity. For the case of alumina binder, by comparing wet v.s. dry binding, they believed the Al migration occurred in the extrudation process through a soluble species rather than in a solid-solid reaction. However, the alumina-bound ZSM-5 showed an even higher ion-exchange capacity after steaming, which may indicate more Bronsted acid sites were formed.

In the late 1980's and early 1990's, researchers at the former Mobil Oil Corp. (now the ExxonMobil Corp.) filed a number of patents on how to make oxide-bound

zeolite catalysts. Absil et al. (1991) and Marler (1993) claimed that low acidity oxide binders such as SiO_2, TiO_2, and ZrO_2 do not interact with zeolite to increase the acid catalytic activity. More particularly, the binders may reduce the intrinsic acid catalytic activity of zeolites such as ZSM-5, Y, beta of SiO_2/Al_2O_3 ratio of 70 or less. They stated in the patents that the oxides may replace alumina in the zeolite, resulting in a higher silica content in the framework, smaller ion-exchange capacity, lower hexane cracking rate, and lower α (alpha) valve*. Unlike the low acidity oxide binders, an alumina binder gives a zeolite a higher intrinsic acid catalytic activity, which is indicated by a higher hexane cracking rate and a higher α value. These patents did not disclose how acidity changes due to the different binders in terms of acid nature, number of acid sites, and strength of acid sites. When the silica-bound catalysts were further ammonium ion-exchanged three times to bring sodium content of the catalysts from 1.8~1.9 wt% to 0.1~0.2 wt%, the activity of these catalysts for hexane cracking that is indicated by the α value increased.

Uguina et al. (1991) studied the acidity and activity of ZSM-5 bound with montmorillonite (15~45 wt%) for toluene disproportionation. They mixed ZSM-5 powder with sodium montmorillonite in distillate water at 80°C for 1 hour and then filtered and dried at 120°C overnight. The dried catalyst was then calcined at 550°C for 5 hours. IR spectroscopy for adsorption/desorption of pyridine was used to investigate acidity. The binder itself (either in Na or H form) did not have any activity for toluene disproportionation. The bound catalyst showed a dramatic decrease in activity for

* α value is a ratio of cracking rate of hexane of a catalyst to that of a standard amorphous aluminosilicate.

toluene conversion because of sodium from the binder neutralizing the acidic sites in ZSM-5 during preparation of the bound catalyst. To increase the activity, the bound catalyst was reactivated by ion-exchanging with 0.6 M/L HCl solution and calcining at 550^{o}C. The catalyst activity was greatly increased and close to, but still lower than the activity of ZSM-5 itself. They referred the slight decrease of activity of the reactivated bound catalyst to pore blockage by the binder deposition. The dramatic decrease of acidity and activity of the bound catalyst (without reactivation) mainly came from the partial ion-exchange between protons of ZSM-5 and sodium ions of the montmorillonite in the gel solution during the embedding process. Their result shows that ion-exchange in water solution is primarily responsible for the decreased activity of the bound catalyst while pore blocking by the binder makes a small contribution.

Zholobenko et al. (1992) studied the acidity of pentasil zeolite (Si/Al=21) with different contents (30-70 wt%) of Al_2O_3 binder with diffuse scattering IR spectroscopy. The zeolite was embedded with γ-Al_2O_3 by mixing the suspension of γ-Al_2O_3 and the suspension of the NH_4^+ form zeolite, followed by drying and calcining at 500^{o}C for 5 hours. The hydroxyl groups of the bound zeolite catalysts were found to be superpositioned from the binder and the zeolite. No new Bronsted centers were formed from Al_2O_3 binding, which is different to the observation on alumina-bound high silica ZSM-5 by Chang et al. (1984) and Shihabi et al. (1985). Using H_2 and CH_4 as probe molecules for FTIR study, Zholobenko et al. found a new Lewis center Al^+=O located in the zeolite channel, which they believed came from the aluminum ion migration from the Al_2O_3 surface into the zeolite channels. Al^+=O cations may enter the cationic

positions of the zeolite. Therefore, the bound catalysts showed a higher Lewis acidity, which is consistent to the results of Cao et al. (1997) and Wu et al. (2002). The new Lewis center was believed to be active in cracking and aromatization, and the possibility of pore blockage at the formation of this new Lewis center was also proposed.

Fougerit and Gnep et al. (1994) studied the acidity, activity and coke formation of kaolinite-bound mordenite. The kaolinite binder contained 0.05 wt% (Na + K) and 0.5 wt% (Ca + Mg). They used NH_3-TPD method (step-wise from 150^{o}C to 550^{o}C) to determine acid site densities at different acid strengths. The bound catalyst had more weak acid sites and less strong acid sites than the predicted values from the binder and the mordenite. However, if they just simply mixed the binder powder and the zeolite powder, they obtained a mixture with an activity similar to the zeolite powder. Based on these results, they believed that the activity decrease was due to the neutralization of the acidic sites of the mordenite by the alkaline metals in wet ion-exchange (during preparation of the bound catalysts) but not in the thermal-treatment, which implied that solid-ion-exchange occurred to a limited extend. On model reactions, the bound catalyst showed lower conversion than the zeolite for dimethyl ether conversion into hydrocarbons, n-heptane cracking and m-xylene isomerization. However, the bound catalyst showed better activity stability (slower deactivation rate) than the zeolite alone. The binder acted like a coke sink. A similar result was found on zeolite 5A bound with kaolin (20 wt%) by Misk et al. (2000), who found a lower coking rate on bound 5A catalysts than on 5A powder for propylene oligomerization at 350^{o}C.

Cao et al. (1997) studied γ-Al_2O_3 made by different manufactures as a binder for mordenite. The bound catalysts were prepared with a similar procedure to the one used by Shihabi et al. (1985). They used a step-wise temperature programmed pyridine adsorption/desorption technique to determine acidity and the strength of the acid sites. Pyridine desorption temperature was used as an indication of the strength of acid sites. They defined strong, medium and weak acid sites with desorption temperatures ≥300^{o}C, 200~300^{o}C, and ≤ 200^{o}C, respectively. Pyridine desorption was monitored by FTIR. Both strong and medium Lewis acid site densities increased significantly with all three γ-Al_2O_3 samples, while for Bronsted acid site density, two samples of γ-Al_2O_3 showed a reduction and only one sample showed a slight increase. Unfortunately, they did not report alkaline metal contents for the alumina binders and the zeolite powder.

Choudhary et al. (1997) and Devadas et al.(1998) investigated the effects of silica, alumina and kaolin binders on the acidity and activity of H-gallosilicate. Unlike the binding method used by former researchers, that was the wet-binding method, they prepared the catalysts by a dry-binding method, that is, by physically mixing the binder powder and the zeolite powder, followed by pressing, crushing and finally calcining at 600^{o}C under nitrogen for 1 hour. The strong acidity of the catalysts with or without a binder was determined with GC adsorption/desorption of pyridine at 400^{o}C. They also used two model reactions, iso-octane cracking and toluene disproportionation, to check the external acidity and intra-crystalline acidity, respectively, of the bound catalysts. They concluded that the alumina binder had no significant effect on the intra-crystalline acidity but caused an appreciate increase in external acidity. The increase in external

acidity was believed due to the creation of new zeolitic acid sites at the external surface of the zeolite crystals by substitution of framework Si with Al from the binder. However, external surface of a zeolite is only a very small portion of the total surface, hence; the increase in external acidity would not make a significant contribution to the total acidity. This result does not seem consistent with Shihabi et al.'s (1985) and Cao et al.'s (1997) results, that is because Choudary et al. used a dry-mixing method while Shihabi et al. and Cao et al. used a wet-mixing method. Shihabi et al. (1985) believed that Al migrated into the zeolite framework in the extrudation process rather than in a solid-solid reaction. In this aspect, both of the results are consistent. In the cases of silica binder and kaolin binder, both external and intra-crystalline acidities decreased appreciably, resulting in a marked decrease in total acidity. From propane aromatization activity test, Choudhary et al. further concluded that all of the bound catalysts showed better shape-selective catalysis and a lower deactivation rate than the zeolite itself; however, kaolin and silica-bound catalysts showed a lower aromatization activity than the zeolite while alumina-bound catalyst showed a similar activity to the zeolite. The increase in shape-selective catalysis indicated the decrease in effective channel diameter of the zeolite. They supposed this was due to the migration of alkaline and alkaline-earth metal cations from the binders into the zeolite channels and/or due to the formation of non-framework Ga-oxide species formed from degalliation of the zeolite.

Romero et al (1997) studied the change of acidity of ZSM-5 (SiO_2/Al_2O_3 ratio of 15-43) after binding with a clay (montmorillonite). They used a similar procedure (wet-binding method) to the one used by Uguina et al. (1991) to embed ZSM-5 to the binder.

Sodium montmorillonite and NaZSM-5 were agglomerated in water (suspension), filtered out the solid, dried and calcined the solid at 550 ^{o}C for 12 hours. Then the bound catalysts was transformed into an acid form by proton-exchange with a dilute HCl solution (1.0 M/L). They did not agglomerate the acid form of montmorillonite because only the sodium form of montmorillonite could give good binding properties. Ammonia-TPD (200^{o}C to 550^{o}C with a ramping rate of 10^{o}C/min) technique was used to measure acid site density (weak and strong acids) and the strength of the acid sites indicated by the peak temperature obtained through Gaussian deconvolution of ammonia desorption profile. Their results were similar to Uguina et al.'s (1991) and Fougerit and Gnep et al.'s (1994) results, that the strong acid site density and total acid site density were lower and weak acid site density was higher than the predicted acid site densities from the partial contribution of the raw materials. They attributed these changes to solid-state ion exchange between montmorillonite and zeolite and pore mouth blockage of zeolite by physical deposition of montmorillonite on zeolite external surface. Since the montmorillonite showed only weak acidity, the result of solid-state ion exchange between clay and zeolite would be more weak acids (proton transfers to montmorillonite) and less strong acids (sodium moves in and replaces proton in zeolite) on the bound catalyst. However, the acid site density of bound ZSM-5 could be close to or even higher than the predicted value from the contributions of the raw materials, if the bound zeolite was further proton-exchanged three times or more. They further concluded that the solid-state ion exchange played a more important role than the pore blockage in

the changes of acidity of ZSM-5 on binding. Unfortunately, no sodium content, surface area and pore volume were reported for all of their samples.

Like other researchers using a clay as a binder for zeolite, Canizares et al. (2000) used a sodium form of montmorillonite (Na 2.9 wt%) to embed Na-ZSM-5 and Na-mordenite(Na 4.21 wt%) by suspending the powders in 80^{o}C water for 1 hour. Then the catalyst was filtered, dried, crashed into 0.5-1.0 mm particles, proton-exchanged with HCl solution, and finally calcined at 550^{o}C for 14 hours. Since both the zeolite and the binder were in sodium form, post-proton-exchange was needed after binding to transform the catalyst into an acidic form. A dilute HCl solution (0.6M/L) was used for the proton-exchange. The NH_3-TPD technique was used to determine acid site density. Acidity change was found to be similar to the results of Uguina et al. (1991) and Romero et al. (1997), that strong acidity was reduced. And also, butane transformation reactions (cracking and disproportionation) activity was found to decrease on the bound catalyst. They referred the change in acidity and activity to solid-state ion exchange in calcination of the catalyst, as proposed by Romero et al. (1997). Since the surface area and pore volume (both micropores and mesopores) were in line with the prediction from the binder and the zeolites, they proposed pore blockage did not occur during embedding the binder to the zeolites, which is different to Uguina et al.'s (1991) presumption. Also, Canizares et al. believed the sodium in the binder or in the zeolites affect only weak acidity. On Na-ZSM-5 or Na-mordenite, only weak acid sites were found from NH_3-TPD measurement with ammonia desorption peak temperature less than 275^{o}C. While FTIR pyridine showed that only Lewis acid sites were found on the Na-form zeolites.

Butane transformation was used as a probe reaction, because the conversion depends on the density of strong acid sites. Strong acid sites of bound zeolites could be closed to or higher than the predicted values from the binder and zeolite after the bound catalysts were proton-exchanged one more time or two more times, which is similar to the finding by Romero et al. (1997).

Dorado et al. (2002) recently studied the acidity and activity of zeolites beta (SiO_2/Al_2O_3 ratio of 12-75) and ZMS-5 (SiO_2/Al_2O_3 ratio of 15-40) bound with bentonite (65 wt% in the bound catalyst). The bound catalysts were tested for activity for hydroisomerization of n-butane. They used a fixed-bed reactor to conduct the reaction and the NH_3-TPD (180^oC to 600^oC with a ramping rate of 15^oC/min) technique to measure the site densities of weak and strong acids. The bound-catalysts had a higher weak acid density and a lower strong acid density than the values predicted from the zeolites and the binder even though the bound catalysts were post proton-exchanged once with a diluted HCl (0.6 M/L) solution. They attributed the decrease of strong acid density to the ion-exchange of Na^+ in bentonite (left after the treatment with the HCl solution) with the proton in the zeolite during the calcination process. That was the solid-state ion-exchange. They proposed an equilibrium between the zeolites and the binder: $Na^+_{binder} + H^+_{zeolite} \leftrightharpoons Na^+_{zeolite} + H^+_{binder}$. The higher the strong acid density of the zeolites and the stronger the strong acid sites of the zeolites, the more right displacement the equilibrium reaction undergoes. Therefore, the deviation of strong acid density from the prediction from the weighed contribution of the zeolite and the binder may depend on the strong acid density and the strength of acid sites in the zeolite. However, they did

not find significant changes in BET surface area after binding. The BET surface area of bound catalysts was very close to the prediction from the raw materials (within 3% of difference), and therefore no micro-pore blockage was proposed. Due to the decrease of the strong acidity, bound catalysts showed higher butane isomerization activity and lower butane disproportionation activity since strong acid sites lead to more disproportionation and less isomerization.

Wu et al. (2002) studied the acidities of alumina- and silica-bound ZSM-5 and Y of different SiO_2/Al_2O_3 molar ratios (from 5 to 280). They used the NH_3-TPD technique to determine acid site density. They found that alumina-bound ZSM-5 and Y had more total acidity than the unbound counterparts, which is consistent with most of the previous researchers' results. The increase in total acidity of alumina-bound zeolites primarily came from the increase in Lewis acidity, which may support Zholobenko et al.'s (1992) finding of a new Lewis center. The strength of acid sites, which was indicated by the peak temperature in ammonia desorption profile, did not change after the zeolites were bound with alumina. While with silica binder, the total acidity, strong acid site density, and strength of strong acid sites are all reduced. The result on the silica-bound zeolites are similar to the results of Absil et al. (1991), Marler (1993), Choudhary et al. (1997), and Devadas et al.(1998). However, Falabella et al. (1996) studied ultra-stable Y zeolite bound with silica, and found that the extra-framework alumina of the zeolite underwent reactions with the silica-binder, generating an acidic silica-alumina compound.

Dagade et al. (2002) studied Al_2O_3-bound zeolite beta for nitration of toluene. The bound catalyst showed a higher acidity and activity at the same selectivity to para-isomers and a longer life than the unbound beta. The bound catalyst was found to have a larger BET surface area, which is different to most of previous observations, and a smaller total pore volume. They attributed the activity increase to the increased acidity by the alumina binder which they believed made a contribution of Lewis acidity to the zeolite beta sample which had only Bronsted acid sites.

Fluidized Catalytic Cracking (FCC) catalyst contains about 50~90 wt% of a binder (matrix) and 10~50 wt% of zeolite (Scherzer, 1993). Research has been conducted to study the influence of a matrix on the physicochemical and catalytic properties of the matrix-embedded zeolite catalyst. Most FCC catalysts were steam-treated to enhance stability, and this treatment may provide a condition in which some components in a matrix would react with zeolite. Therefore, the results on embedded FCC catalyst might be of some help in understanding the relation between binder and zeolite.

Corma et al. (1990a, 1990b, 1990c) did research on embedding Y zeolites with silica and stream-treated the embedded catalysts. The catalysts were used for gas oil cracking. They found silicon from the matrix reacted with extra-framework aluminum if zeolite Y to form a new silica/alumina phase, which was external to the zeolite crystal and showed weak Bronsted acidity. The steamed silica-embedded Y promoted activity and improved gasoline and especially diesel selectivity. Acid leaching which removed extra-framework aluminum produced catalysts with more micropore volume and acidic

sites (Corma et al., 1990b; de la Puente et al., 2003), which resulted in a higher activity in cyclohexene cracking (de la Puente et al. 2003).

Gelin and Gueguen (1988) found that REY and offretite were stabilized by embedding them into a silica-alumina matrix. The final catalysts could sustain high temperature steaming without loss of zeolite structure. Since steaming treatment resulted in dealumination of zeolites, they proposed that Si in the matrix was responsible to replace to the Al expelled in the zeolite framework during steaming, thus stabilizing the zeolite structure. Intimate contact between the zeolite and the matrix was necessary since only intimate contact could allow a rapid diffusion of silicon into the zeolite component, preventing the zeolite structure from collapsing. With an isotopic labeling technique, Gelin and Des Courieres (1991) found the evidence of silicon migration from a silica-alumina matrix into zeolite La-Y channels and further into its structure to replace the expelled zeolite aluminum during streaming. They also found that the crystallinity of La-Y zeolite was totally preserved on streaming when the zeolite was embedded into the silica-alumina matrix, however, if not embedded, the zeolite would lose about 55% of its crystallinity after stream treating at 750^{o}C for 17 hours under 100% stream atmosphere. Recently, Noronha et al. (1998) studied mordenite embedded with a silica-alumina gel. They obtained similar results as on the embedded La-Y. By comparing a physical mixture of the mordenite and the matrix with the catalyst made by binding with the silica-alumina gel (wet-binding method), they further demonstrated that “intimate” contact between the matrix and the zeolite is necessary for the matrix to have the protecting effect on the zeolite structure (the wet-binding method would provide an

"intimate" contact between the matrix and the zeolite). The analysis on the volume of micropores (determined by the t-plot method) showed that the catalyst (only calcined at 500^{o}C with no additional steaming) made from a gel-mixture had a slightly smaller micropore volume (0.031 cc/g-cat) than the micropore volume (0.035 cc/g-cat) of the physical mixture. The later value was closely in line with the predicted value. They therefore concluded that zeolite pores were not significantly blocked. However, the gel-mixed catalyst had a larger mesopore volume of 0.341cc/g-cat (determined by the BJH method) than the mesopore volume of 0.309 cc/g-cat of the physically-mixed catalyst. The gel-mixed catalyst had a smaller BET surface area and smaller micropore and mesopore surface areas than the physically-mixed catalyst. However, these properties of the physical mixture were close to the predicted values from the matrix and the zeolite.

Kubicek at al. (1998) also obtained similar results on zeolite beta embedded with silica-alumina to Gelin et al's results. Microactivity test and hexane cracking test showed that, the mechanical mixture (just calcination at 500^{o}C without additional steaming treatment) had almost the same activity and acidity as pure zeolite beta. BET surface area and micropore volume were lower and mesopore volume was higher than the prediction. However, steaming the silica-alumina embedded catalyst caused the activity and acidity to increase. They concluded that the catalyst made by wet-embedding in alumina or silica-alumina gels followed by a calcination at 600^{o}C leads to the generation of new zeolite acidic sites which are active sites in cracking reactions. Moreover, the changes of textural properties occurring during the catalyst preparation, particularly when both aluminum and silicon were available in the matrix, supported the assumption

that these new sites are created via extensive recrystallization of the zeolite component. Or put it in another way, the aluminum from the matrix incorporates into the zeolite crystals, generating new Bronsted acid sites. This re-crystallization could occur at mild temperatures say around 330^{o}C. Only the wet-embedding method can lead to this effect, while the mechanical mixing method does not provide any significant stabilization of acid sites and textural structure. The alumina-containing matrix preserved the acidity and also increased the acid sites by dealumination---insertion of AlO_4 tetrahedra into the vacancies (defect silanol groups) of the framework and thus improved the crystallinity and decreased the micropore volume. Pure-silica matrix-embedded beta did not have these effects. Kubecek et al.'s proposal on the function of Al in the matrix was similar to the one proposed by Shihabi et al.(1985), who assumed the Bronsted acid sites were in the zeolite structure.

Klint and Bovin (1999) studied pore size distribution of USY embedded with kaolinite. Dealuminated ultrastable zeolite Y, kaolin and distilled water were mixed and ground in a mortar in a thick suspension. The suspension was then dried, pelletized (under pressure of 750MN/m^2), and calcined at 800^{o}C (48 hours) or 1000^{o}C (24 hours). They found that pore volume at pore diameters less than 3.8 nm decreased by about 50%, and the pore volume of pore diameters of 20 ~ 80 nm increased. They attributed the decrease of pore volume of small pores to the pore blockage by kaolin binder and the increase of pore volume of bigger pores to interparticle voids.

Very recently, de la Puente et al.(2003) also found that silica from matrix reacted with extra-framework alumina of zeolite during steam treatment to form new

silica/alumina phase for USY, which is similar to the previous observation by Corma et al.(1990a and 1990b). Hydrogen transfer capacity of the catalysts was found dependent on the paired acid sites in the zeolite, not on the matrix or extra-framework aluminum. The newly formed silica/alumina phase increased the catalyst hydride transfer rate of an adsorbed species relatively to the desorption of the species.

In a matrix-base zeolite catalyst, the pore system is also an important factor for reactants and products to diffuse in and out of the zeolite channels. If the matrix or the binder can establish a pore system with a smooth change in pore diameters, that is the so-called "funnel-shaped" pore configuration, the molecules of reactants and products would have a much less surface diffusion barrier. To have such a pore system, the binder or the matrix is necessary to be in intimate contact with the zeolite. With this thought, Le Van Mao (1999) and his coworkers have conducted research and the results show that the catalysts (silica or alumina bound ZSM-5) made under this idea have higher activity and selectivity for aromatization of n-butane than the parent ZSM-5 catalyst.

In most applications of zeolites as catalysts, they are used as solid acidic catalysts, or as materials to provide acidic properties. For a solid acid, acid site density, acid site nature, and acid site strength are the three most important properties. All of the three properties play important roles in acidic catalytic reactions in addition to pore surface area and pore volume. Therefore, if a binder would affect one of these properties of a zeolite, the catalytic property of the zeolite would be altered after it is bound with the binder. Consequently, the results obtained from the unbound zeolite may not be directly applicable to the bound zeolite.

Based on what has been reported, one can find some similarities and differences as well. The major similarities are: when a binder contains alkaline metals, the acidity of a bound zeolite is reduced significantly; silica-binder reduces acidity and catalytic activity; alumina binder increases Lewis acidity. The different observations and results are on the followings: whether silica or alumina from a binder reacts with alumina or silica in zeolites; whether a silica or alumina binder blocks micropores of zeolites; whether solid-state ion-exchange occurs to a significant degree to reduce the acidity of zeolites.

Embedding the powder of a zeolite into a binder involves complicated physical and chemical processes. Binder sources, binder properties, binding methods (dry or wet), and calcination processes (either in air or in steam or in an inert atmosphere) can all affect the properties of the final catalyst. Those could be the reasons that different results have been reported. Therefore, more research is still needed especially on how the binding methods affect zeolite physicochemical properties since only the binding method could lead to different catalyst if using the same binder.

CHAPTER III

CATALYST PREPARATION AND CHARACTERIZATION

3.1 Catalyst Preparation

3.1.1 Zeolite and Binder

Zeolite ZSM-5 and Y with different SiO_2/Al_2O_3 ratios were purchased from Zeolyst International Inc. They were in powder form. Zeolite Y samples were already in acidic form, so that no further ion-exchange was necessary to transfer them into H-form. Zeolite ZSM-5 samples were in NH_4^+ form, so they were converted into H-form by calcining at 550^{o}C for 4 hours before binding them with a binder. The properties of the zeolite samples are listed in Table 3.1.1.

Table 3.1.1 Zeolite Y and ZSM-5 and their manufacture assay data.

Zeolite Trade name	Type	SiO_2/Al_2O_3 Mole ratio*	Na+K, wt%		Unit cell size*, A	BET Area, m^2/g	
			Manuf.*	Anal.**		Manuf.*	Anal.**
CBV 3024E	NH_4-ZSM-5	30	0.05	0.067	-	440	411
CBV 8014	NH_4-ZSM-5	80	0.05	0.052	-	425	475
CBV 28014G	NH_4-ZSM-5	280	0.05	0.040	-	425	417
CBV 600	HY	5.2	0.03	-	24.35	660	592
CBV 720	HY	30	0.03	-	24.28	780	817
CBV 780	HY	80	0.03	-	24.24	780	805

* Manufacture's data; ** Our laboratory analysis.

The silica sources used to bind the zeolites were the silica gels, Ludox AS-40 and HS-40, purchased from Aldrich Chemical Co. Ludox HS-40 contained sodium cation as a stabilizing counterion for the gel, while Ludox AS-40 contained ammonium cation as the

counterion. Therefore, AS-40 contained much less sodium cation than HS-40, which can be seen from Table 3.1.2. Alumina used to bind the zeolites were γ-Al_2O_3 (HiQ7214F, Q1-1819) and boehmite (HiQ-31, Q-1818) from Alcoa Co. Both of them were in powder form. The properties of these binders are listed in Table 3.1.2.

Table 3.1.2 Binder properties.

Binder Trade name	SiO_2 Content wt%	Al_2O_3 Content wt%	Surface area m^2/g	(Na+K)* wt%	Average Particle size
Ludox HS-40 (SiO_2)	40	-	220	0.352	0.012 μm
Ludox AS-40 (SiO_2)	40	-	135	0.068	-
HiQ-31, Q-1818 (Boehmite)	0.007	76.9	247	0.104	<90 μm
HiQ7214F, Q1-1819 (γ-Al_2O_3)	0.01	98.8	151	0.104	<1000 μm

* Our laboratory analysis.

3.1.2 Preparation of Bound Zeolite Catalysts

Generally, three methods were used to embed zeolites into binders. These were gel-mixing, powder-wet-mixing, and powder-mixing. *Gel-mixing* is to mix a gel of a binder with the powder of a zeolite in de-ionized water (forming a thick suspension) under vigorously stirring. In the case of Ludox HS-40, the suspension had a pH value of 9.8; while in the case of Ludox AS-40, the suspension had a pH value of 9.1. Dry the suspension at 110^oC to evaporate water and calcine the dried material at 550^oC for 4 hours. Then press and sieve the calcined solid into small particles (0.5~1.17 mm). *Powder-wet-mixing* is to mix the powder of a binder with the powder of a zeolite in de-ionized water (forming a thick suspension) under vigorously stirring. In the case of using

silica powder obtained from calcining Ludox HS-40 at 550°C, the suspension had a pH value of about 7.0. In the cases of calcined Ludox AS-40 and alumina binders, the suspensions had pH values of about 5.3, which was the pH of the di-ionized water used for making the suspensions. Dry the suspension at 110°C and then calcine the dried material at 550°C for 4 hours. Press and sieve into 0.5~1.17 mm particles. *Powder-mixing* is to simply mix the powder of a binder with the powder of a zeolite in a plastic bottle. Shake the bottle strongly to make the powder to mix completely. Then press and sieve into small particles of 0.5~1.17 mm and calcine at 550°C for 4 hours. In the powder-mixing case, the moisture content of the binder and the zeolite would be less than 8% of the mixture. Fig. 3.1.1 depicts how the bound catalysts were made with binding ZSM-5 with silica as an example.

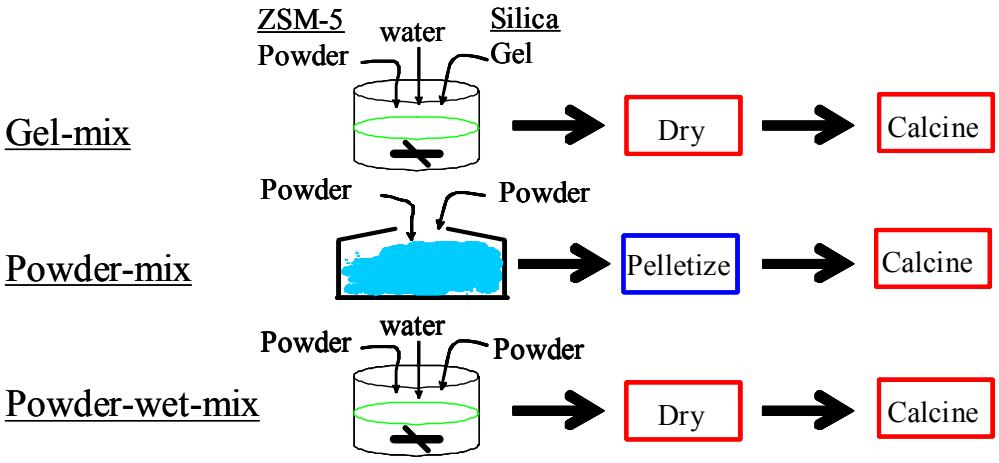

Fig.3.1.1 Schematic presentation of embedding ZSM-5 into silica.

3.1.2.1 Silica-bound Zeolite Catalysts

All of the silica-bound zeolite catalysts were made in the laboratory. Commercial HZSM-5 powder samples (obtained by calcining NH_4-ZSM-5) with SiO_2/Al_2O_3 ratios of 30, 80 and 280, and commercial HY powder samples with SiO_2/Al_2O_3 ratios of 5.2, 30 and 80 were purchased from Zeolyst International Inc. The properties of the zeolites are listed in Table 3.1.1. Ludox HS-40 and AS-40 (from Aldrich Chemical Co.) were used as a silica binder. The binder properties are listed in Table 3.1.2. Three embedding methods were used to bind zeolites ZSM-5 and Y with silica. The embedding procedures are depicted in Fig.3.1.1. The content of the silica binder in all of the bound catalysts was about 29 wt%.

The purpose to use different sources of silica gel is to investigate the effect of sodium content in the binder on acidity and catalytic reactivity of the bound zeolite catalysts. Ludox HS-40 contains sodium as a stabilizing counterion while Ludox AS-40 does not contain sodium but ammonium as the stabilizing counterion. Note the silica powder used in the powder-mixing method was obtained from drying and calcining the Ludox AS-40 and HS-40 gels at 550^{o}C for 4 hours, respectively. Information on an individual bound catalyst will be given on how it was made in the proceeding Chapters.

3.1.2.2 Alumina-bound Catalysts

Some alumina-bound zeolites of ZSM-5 and Y were purchased directly from Zeolyst International Inc. They contained 20 wt% of γ- Al_2O_3. The other alumina-bound ZSM-5 samples were made in the laboratory. ZSM-5 powder was the same as used in silica-bound ZSM-5 catalysts, also from Zeolyst International Inc. The alumina binder

was from Alcoa Co. It was either γ-Al_2O_3 (HiQ7214F, Q1-1819) or boehmite (HiQ-31, Q-1818). The properties of ZSM-5 and the alumina binders are listed in Tables 3.1.1 and 3.1.2, respectively.

The lab-made alumina-bound zeolite catalysts were made with the powder-mixing or the powder-wet-mixing method. Since both γ-Al_2O_3 (HiQ7214F, Q1-1819) and boehmite (HiQ-31, Q-1818) were in fine powder form, they were used directly without further grinding. The content of alumina binder in the bound catalysts was 30 wt%.

3.2 Catalyst Characterization

Catalysts used in this research were characterized for texture and acidity. To elucidate the texture of a zeolite and its bound counterpart, BET surface area, micropore surface area, mesopore/macropore surface area, micropore volume, mesopore/macropore volume, and pore size distribution were analyzed using a BET machine. To express a solid acid in terms of acid nature, acid site density, and acid strength, a combination of ammonia Temperature Programmed Desorption (NH_3-TPD) technique and Fourier Transform Infrared (FTIR) Spectroscopy was used. To measure metal contents in either zeolite or bound catalysts, Atomic Adsorption (AA) Spectrometer and Inductive Coupled Argon Plasma (ICAP) Spectrometer were used for alkaline metals and transition metals, respectively.

3.2.1 Measurement of Catalyst Texture

The catalyst surface area, pore size distribution, and pore volume were determined using an ASAP 2000 Micromeritics BET (Brunauer-Emmett-Teller) machine

using nitrogen as an adsorbate at the liquid nitrogen boiling temperature (77.35K). The machine was controlled by a computer, in which an ASAP 2010 software was installed. With this software, a lot of information on the texture of a porous material, such as BET surface area, micropore surface area, mesopore/macropore surface area, micropore volume, mesopore/macropore volume, and pore distribution can be obtained. The t-plot method and BJH method were used to obtain micropore and mesopore information, respectively (Webb and Orr, 1997).

The general procedure to conduct the measurement was: about 200 milligrams of a sample was loaded and degassed in vacuum at about 350^{o}C for at least 3 hours. Then analysis using N_2 as adsorbate at the liquid nitrogen boiling temperature began. N_2 incremental dose of 5 cm^3/g STP (standard temperature and pressure) was used. At the end of the experiment, ASAP 2010 software processed the N_2 adsorption and desorption isotherms to obtain surface areas, pore volumes, and pore distribution.

3.2.2 Determination of Solid Acidity

For a solid acid, three properties associated with the acid are the acid type or the nature of the acid (Bronsted acid or Lewis acid), the acid site density, and the strength of the acid site. Acid site density and strength of an acid site were determined from NH_3-TPD experiment, and the nature of an acid was determined from pyridine adsorption-FTIR. Figs. 3.2.1 and 3.2.2 show a typical NH_3-TPD profile and a pyridine adsorption FTIR spectrum, respectively.

Besides pyridine adsorption analysis, Fourier Transform Infrared (FTIR) technique was also used to obtain information on hydroxyl groups in the bound and

unbound zeolites. The IR adsorption band at about 3600 cm^{-1} that refers to bridged hydroxyl group was used to monitor Bronsted acidity in ZSM-5 (Kotrel et al, 1999). While for zeolite Y, the IR band around 3620 cm^{-1} was used to monitor Bronsted acidity (Corma, et al; 1990).

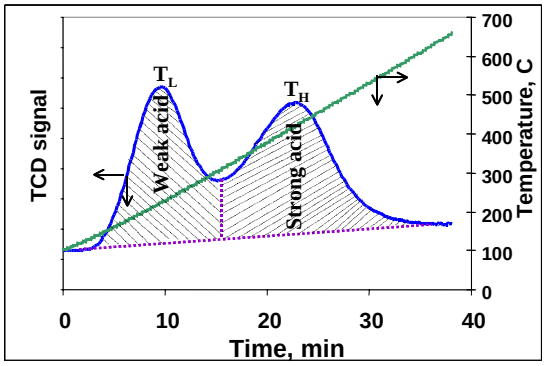

Fig.3.2.1 Typical NH_3-TPD profile.

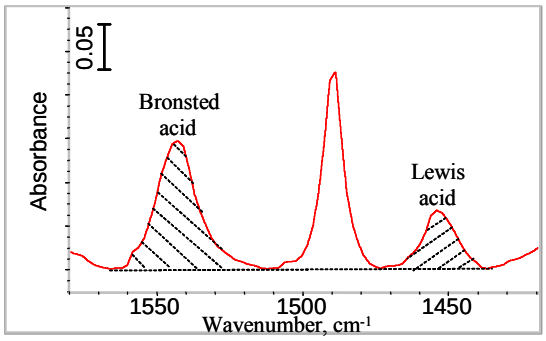

Fig.3.2.2 Adsorption of pyridine on Bronsted and Lewis acids detected by FTIR.

The weak acid site density and strong acid site density were determined from NH_3-TPD profiles, for example, from the areas under “weak acid” peak and “strong acid”

peak shown in Fig. 3.2.1. Total acid site density is then the summation of weak and strong acid site densities.

As shown in Fig. 3.2.2, adsorption of pyridine on Bronsted acid sites and on Lewis acid sites exhibits IR absorption bands around 1540cm^{-1} and 1450cm^{-1}, respectively (Jacob, 1977; Anderson and Pratt, 1985). From the pyridine IR absorption intensities at the two bands, relative density of these acid sites can be determined by the areas under the bands (as shown in Fig. 3.2.2), since the ratio of molar integrated absorption intensity at 1450cm^{-1} (Lewis acid) to that at 1540cm^{-1} (Bronsted acid) is about 1.08±0.1 for amorphous aluminosilicates and zeolites (Anderson and Pratt, 1985; Guisnet et al, 1997).

The following equations show how Bronsted acid density and Lewis acid density are determined. The molar integrated absorption intensity A_B of Bronsted acid at 1540 cm^{-1} and the molar integrated absorption intensity A_L of Lewis acid at 1450 cm^{-1} are expressed as follows (Anderson and Pratt, 1985):

$$A_B = \frac{1}{C_B L}\int \log\left(I_O/I\right)_B dv = \frac{Area_B}{C_B L} \tag{3-1}$$

$$A_L = \frac{1}{C_L L}\int \log\left(I_O/I\right)_L dv = \frac{Area_L}{C_L L} \tag{3-2}$$

where, $\left(I_O/I\right)_B$ and $\left(I_O/I\right)_L$ are relative IR light intensity at Bronsted acid and Lewis acid, respectively; v is wave frequency; C_B and C_L are Bronsted and Lewis acid site density, respectively; L is the sample thickness. $Area_B$ and $Area_L$ are peak area under Bronsted sites and Lewis sites, respectively, as shown in Fig. 3.2.2.

The ratio of molar integrated absorption intensity at Lewis acid sites and Bronsted acid sites is defined as:

$$K = \frac{A_L}{A_B} \tag{3-3}$$

K is about 1.08. Then the ratio of the Bronsted acid site density to Lewis acid site density is given by:

$$\frac{C_B}{C_L} = K\frac{Area_B}{Area_L} = 1.08\frac{Area_B}{Area_L} = 1.08R_{Area} \tag{3-4}$$

where, $R_{Area} = \frac{Area_B}{Area_L}$, denoting the area ratio.

Therefore, Lewis acid density and Bronsted acid density can be determined from Equations 3-5 and 3-6 if total acid site density is known.

$$C_L = \frac{C_T}{\left(1 + KR_{Area}\right)} \tag{3-5}$$

$$C_B = C_T - C_L = C_T\left(1 - \frac{1}{\left(1 + KR_{Area}\right)}\right) \tag{3-6}$$

where C_T stands for the total acid site density.

3.2.2.1 NH_3-TPD Experiment

NH_3-TPD (temperature programmed desorption) technique was employed to determine the acid site density and acid site strength. It was conducted on Micromeritics PulseChemiSorb 2705 equipped with a thermal conductivity detector (TCD). Fig. 3.2.3 depicts a simplified sketch of the apparatus. Helium was used as a carrier gas with a flowrate of 40 ml/min. About 100 milligrams of a powder sample was loaded into a U-

shape tube sample holder. The bottom part of this U-tube was a cylinder of about 8 mm (i.d.) × 36 mm (long). The catalyst sample powder was evenly distributed along the cylinder, and the sample tube was installed to the apparatus for dehydration of the sample. After the catalyst sample was dehydrated at 350°C and cooled down to 105°C, NH_3 was injected with a syringe until the sample was saturated with ammonia. The same flow of helium through the sample holder was maintained to eliminate free ammonia and physically adsorbed ammonia for about 2 hours at this temperature until no further change was found in the detector signal, i.e., constant baseline was achieved. Temperature programmed desorption (TPD) of the adsorbed ammonia was then conducted from 105°C to 685°C with a temperature ramping rate of 15°C/min. From the ammonia desorption profile, weak and strong acid site densities of the catalyst sample were calculated by integrating the area under the low temperature peak and the high temperature peak, respectively. The total acid site density of the catalyst sample was then obtained by summing the weak and strong acid site densities. The strength of acid sites is indicated by the peak temperature in the desorption profile; the higher the peak temperature, the stronger the acid sites are.

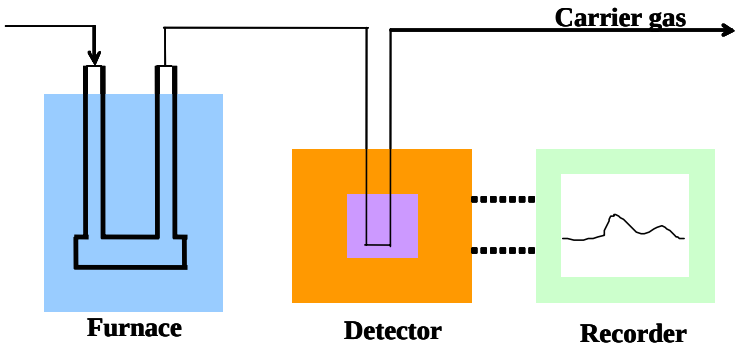

Fig.3.2.3 Schematic representation of NH_3-TPD experiment set-up.

In some NH_3-TPD experiments, injection of NH_3 was conducted at around 235^oC, and the temperature programmed desorption of the adsorbed ammonia started after purging with helium at this temperature until the TCD signal came back to the baseline (usually taking about 2 hours). These experiments were conducted in order to skip weak acid sites and to obtain only the strong acid sites. These experiments were necessary when low temperature peak and high temperature peak in NH_3-TPD profile were difficult to resolve since no peak deconvolution treatment was used in explanation of the desorption profiles.

3.2.2.2 FTIR Analysis

FTIR measurements were conducted on a Nicolet Magna-IR 560 spectrometer with a MCT (Mercury Cadmium Tellurium) detector and a KBr beam splitter by using Diffuse Reflectance Infrared Fourier Transform Spectroscopy (DRIFTS). The detector was cooled by cryogenic liquid nitrogen. Spectra were taken at a resolution of 4 cm^{-1} and an accumulation of 64 scans. A small amount (about 20-30 milligrams) of a catalyst sample (bound and unbound) was placed in the sample cup in the DRIFTS reactor and treated in situ for removal of adsorbed water under a flow of helium (about 20 ml/min). The sample was then cooled under a flow of helium and the spectra were taken at 25°C with KBr as background to obtain information about the hydroxyl groups in the catalyst sample. Pyridine was then brought into contact with the sample by bubbling the helium flow through a bottle of liquid pyridine. After the sample was saturated with pyridine, physically adsorbed pyridine and free pyridine molecules were removed by purging helium through the sample at about 200°C. IR spectra were taken again with KBr as

background to observe absorption bands near 1450 and 1540 cm^{-1}. OMNIC® FT-IR software was used to obtain individual area counts under each of the absorption bands at about 1450 cm^{-1} and 1540 cm^{-1}. The area count ratio of these two bands was used to calculate the ratio of Lewis acid sites to Bronsted acid sites. With this ratio and the total acidity obtained from the NH_3-TPD experiment, Bronsted acid site density and Lewis acid site density were calculated.

3.2.3 Metal Content Analysis

The bulk compositions of transition metals in the catalysts were analyzed on an Enviro II ICAP PolyScan 61E Spectrometer with a ThermoSPEC Version 6.20 software. The ICAP Spectrometer was manufactured by Thermo Jarrell Ash. Alkaline metals were analyzed on Varian SpectraAA-50 Atomic Absorption Spectrometer (AAS).

To prepare a solution of a catalyst sample for metal analysis, generally about 100 milligrams of a catalyst sample was dissolved in about 1.0 ml hydrofluoric acid in a plastic bottle. The dissolving process might take several minutes to several hours. Some times, shaking was forced to get a faster dissolution. After the dissolution was complete, de-ionized water was added to obtain a dilute solution which contained a concentration of the metal(s) to be measured in the range of standard metal solutions prepared for the analysis. From the standard metal solutions and the absorption intensity of the spectrometer, the concentrations of the metals in interest were determined and thus the metal contents in the catalyst were known.

CHAPTER IV

REACTION UNIT AND PRODUCT ANALYSIS

Bound zeolite catalysts and un-bound zeolite catalysts were tested for reaction activity with ethylene oligomerization and butane cracking and disproportionation.

4.1 Ethylene Oligomerization

4.1.1 Reactor System

Ethylene oligomerization was conducted in the Chemical Data Systems (CDS) unit manufactured by Autoclave Engineering Company. It was a complete gas/liquid phase reaction system designed to facilitate bench scale studies of both catalytic and non-catalytic processes with a degree of flexibility in both design and operation. It was functionally composed of three basic systems: the reactor system, the control system, and the analytical system. Figure 4.1.1 shows a simplified flow diagram of the CDS unit.

The reactor system was entirely placed in a temperature-controlled oven so that the feed can be preheated and well-mixed and the products can avoid condensation. The oven temperature was controlled at 200^{o}C. The reactor was a fixed-bed reactor. It was made of a stainlessness steel tube with inside diameter of 0.5 inch (12.7 mm) and length of 12 inch (305 mm). Inside the reactor tube, a thermocouple well was inserted along the axial direction. The thermocouple well was made of a stainlessness steel tube of 1/8 inch (3.2 mm) outside diameter. The reactor was heated by three individual furnaces at top, middle and bottom sections of the reactor tube, respectively.

The controlled system was basically composed of a computer, which controlled the furnace, switching valve, and mass flow meters. All of the process variables such as flow rate, temperature, and reaction time, etc. were set and monitored at the computer.

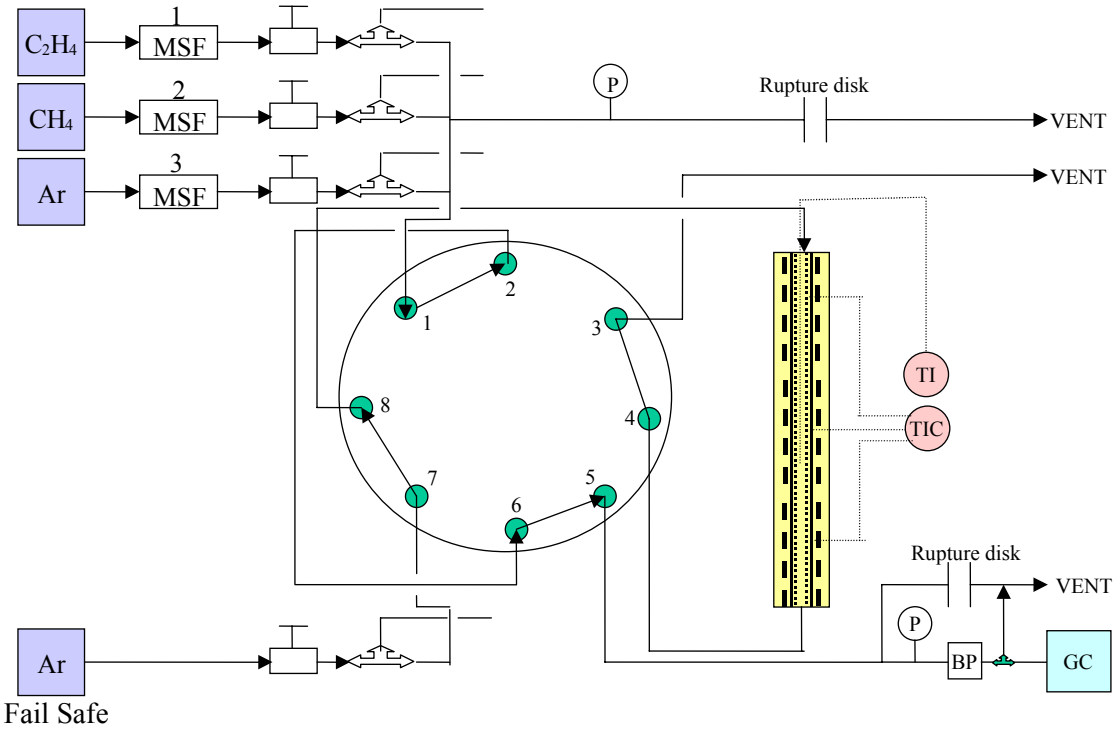

Fig. 4.1.1 Simplified flow diagram of CDS unit.

The flows of ethylene, methane and an inert gas, argon or nitrogen, were controlled through mass flow meters and monitored by the same computer in the CDS unit. The computer also monitored the reaction temperature. This unit had a maximum

reactor temperature of 650^{o}C. Also, the unit had a safe protection in case the temperature at any part of the reactor should rise higher than 650^{o}C, the computer would activate the fail safe function which would automatically turn the switching valve and allow a fail safe gas (an inert gas) to purge the reactor, and at the same time, the other flows are sent to vent and the furnace power is shut off automatically.

The pelletized catalyst particles of size of 0.5~1.17 mm were placed in the middle section of the reactor tube. The catalyst inventory was about 2~5 grams, depending on experimental requirement. The rest of the reactor space (the top and bottom sections) was filled with α-Al_2O_3 beads of size 1.0~1.5 mm. Between the catalyst and the α-Al_2O_3 beads was a thin layer of quartz wool.

4.1.2 Product Analysis

The reaction products were analyzed chromatographically by an on-line gas chromatograph (GC) of Varian GC 3400. The transfer line from the reactor to the GC was maintained isothermally at about 180^{o}C. The Varian GC3400 was redesigned with a complex valve and column system to facilitate a complicated separation. A special timing-program for switching the valves and a temperature program for the GC oven were run through the GC analysis. Note that the valve program and GC oven temperature program should be matched in order to accomplish a desired separation. If any one of the parameters in the programs is changed, the other parameters may need to be adjusted accordingly and the retention time of a component may change. With this GC configuration (as shown in Fig. 4.1.2) and the special programs, all of the reaction

products including hydrogen can be analyzed on this single GC in one run. The valve-timing and oven temperature programs are listed in Table 4.1.1.

Table 4.1.1 Programs for running Varian GC3400.

Valve Timing and Action		Oven Temperature Control	
Time, minute	Action	Time, minute	Oven temperature
0.00	Relays -1, -2, -3, -4	0.00	35°C
0.10	Relays 1, 2, 3	4.00	Start 10°C/min
6.00	Relays -2, -3	22.50	Final 220 °C, and hold
19.15	Relays -1,-2, -3	37.50	220 °C
40.00	Relays, -1, -2, -3, -4	40.00	Cool to 35 °C

Note: Relays 1, 2, 3, and 4 correspond to Valve 1, 2, 3, and 4 in Fig. 4.1.2, respectively. The negative sign " – " before the relay numbers means the relay (the valve) is at default position or "OFF" position (valve closed). If a positive sign or no sign is given before the number, the relay (the valve) is at "ON" position (valve opened).

The GC had a thermal conductivity detector (TCD) and flame ionization detector (FID). The set-up of the GC switching valves and columns is depicted in Fig. 4.1.2. From Fig. 4.1.2, it can be seen that the GC had two independent sample injection loops. One sample loop was for the TCD side, and the other one was for the FID side. The TCD side was equipped with Column 1 (Chromsorb® 107) and Column 2 (molecular sieve 13X), which were used to separate light components such as C_2H_6, CO_2 , and C_2H_4, and H_2, N_2, O_2, CO, and CH_4, respectively. The FID side was equipped with Column 3 (Alumina PLOT capillary column), which was used to separate hydrocarbons from CH_4 up to heavier compounds such as C_{9+}. The GC used argon and helium as carrier gases for TCD side and FID side, respectively. The reason that the reactor used

argon as an inert gas was that argon would not show a peak on the TCD since it was the carrier gas so that the calculation from GC peak would be easier and nitrogen could be used as an internal standard gas if needed.

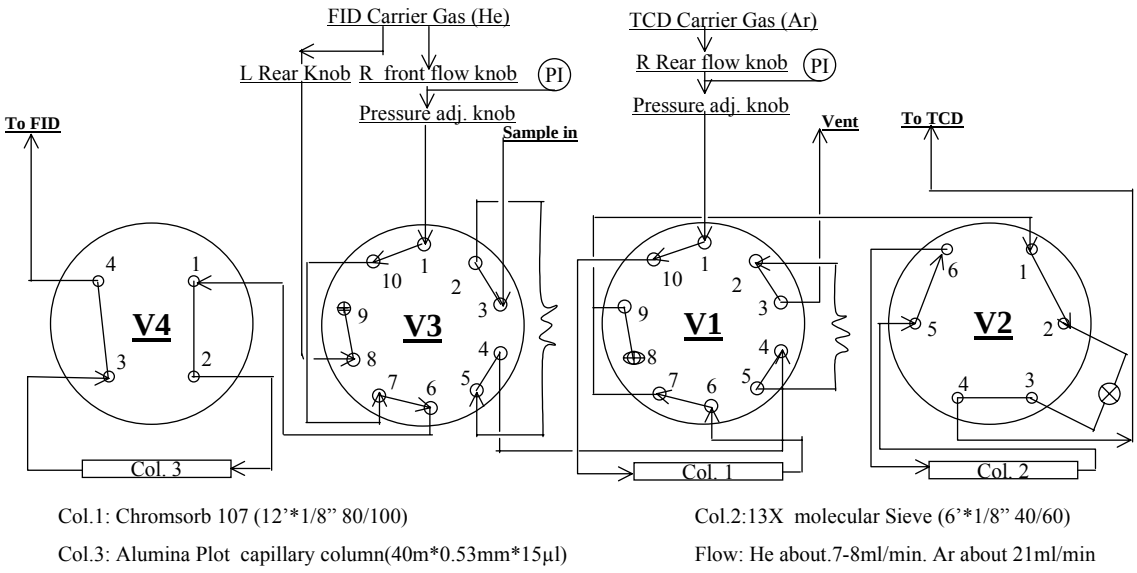

Fig. 4.1.2 Schematic representation of the configuration on Varian 3400 GC.

Since some components show up on the TCD side and the others only on the FID side, one component needs to be chosen as a tie component. This tie component links the TCD data and FID data together. This is necessary since the analysis on the TCD side and on the FID side is independent. The tie component should show up on both TCD side and FID side, and also have a good response on both TCD and FID. It should also take up a reasonable concentration in the mixture to be analyzed. A reasonable concentration here means that the tie component should be one of the major components

in the mixture. The tie component thus chosen would contribute less error than an otherwise-chosen tie component such as a minor component or a component that has a smaller response on the detectors. In ethylene oligomerization experiment, either ethylene or methane could be used as a tie component depending on their concentration in the product mixture.

4.1.3 GC Data Processing

After GC analysis is over, the retention times and peak areas of components in a sample are printed out for both TCD and FID. Based on the peak areas, the mixture composition can be calculated. A general calculation procedure for a tie component method of a GC analysis is described below. Note that this is a general calculation method. For a specific analysis, a more simplified method can be derived from this general method. A Microsoft® Excel® table can be used to perform the calculation.

For calculation, only those components that can not be detected on FID side will be accounted on the TCD side. This means that ethane and ethylene, even though they can be detected on the TCD side, will be determined from the FID (taking data from the FID) for product calculation.

Suppose the two sample loops contain exactly the same composition of a sample (which is a valid assumption since the sample is taken from the same sample line and injected at the same time). Therefore, the ratios of the weight fraction (or the molar fraction) of a component to the tie component determined from one sample loop should be equal to that determined from the other sample loop. Since one sample is analyzed on

TCD side, the other sample is analyzed on FID side. On TCD side, one can determined the weight or molar ratios that can not be determined on FID side, while on the FID side, one can determine the ratios that can not be determined on the TCD side. Therefore, from these ratios, one can determine the composition for the mixture. One thing that needs to be sure is that all of the components in the sample considered have to show up either on TCD or FID. Otherwise, the concentration determined would not present the real composition of the mixture. In this method, the size of the samples can be different, but it does not make any difference in the calculation results.

In the following demonstration of the tie component method, methane is used as a tie component. On TCD side, the weight fraction of a component to the tie component can be expressed as:

$$\left(\frac{w_{H_2}}{w_{CH_4}}\right)_{TCD} = \frac{A_{H_2,TCD}}{A_{CH_4,TCD}}\left(\frac{f_{H_2}}{f_{CH_4}}\right)_{TCD} \tag{4-1}$$

where w is weight fraction of a component in the sample, A the GC peak area, and f the GC peak area weight correction factor. The GC area correction factors for some compounds can be found in the literature (Dietz, 1967). The subscript denotes the component name or the detector. Similarly, other components can be expressed in terms of the tie component as follows.

$$\left(\frac{w_{N_2}}{w_{CH_4}}\right)_{TCD} = \frac{A_{N_2,TCD}}{A_{CH_4,TCD}}\left(\frac{f_{N_2}}{f_{CH_4}}\right)_{TCD} \tag{4-2}$$

$$\left(\frac{w_{CO_2}}{w_{CH_4}}\right)_{TCD} = \frac{A_{CO_2,TCD}}{A_{CH_4,TCD}}\left(\frac{f_{CO_2}}{f_{CH_4}}\right)_{TCD} \tag{4-3}$$

$$\left(\frac{w_{CO}}{w_{CH_4}}\right)_{TCD} = \frac{A_{CO\ ,TCD}}{A_{CH_4,TCD}}\left(\frac{f_{CO}}{f_{CH_4}}\right)_{TCD} \tag{4-4}$$

On FID side, similar expressions can also be derivated.

$$\left(\frac{w_{CH_4}}{w_{CH_4}}\right)_{FID} = \frac{A_{CH_4,FID}}{A_{CH_4,FID}}\left(\frac{f_{CH_4}}{f_{CH_4}}\right)_{FID} = 1 \tag{4-5}$$

$$\left(\frac{w_{C_2H_4}}{w_{CH_4}}\right)_{FID} = \frac{A_{C_2H_4,FID}}{A_{CH_4,FID}}\left(\frac{f_{C_2H_4}}{f_{CH_4}}\right)_{FID} \tag{4-6}$$

$$\left(\frac{w_{C_2H_6}}{w_{CH_4}}\right)_{FID} = \frac{A_{C_2H_6,FID}}{A_{CH_4,FID}}\left(\frac{f_{C_2H_6}}{f_{CH_4}}\right)_{FID} \tag{4-7}$$

$$\left(\frac{w_{C_3H_6}}{w_{CH_4}}\right)_{FID} = \frac{A_{C_3H_6,FID}}{A_{CH_4,FID}}\left(\frac{f_{C_3H_6}}{f_{CH_4}}\right)_{FID} \tag{4-8}$$

$$\left(\frac{w_{C_3H_8}}{w_{CH_4}}\right)_{FID} = \frac{A_{C_3H_8,FID}}{A_{CH_4,FID}}\left(\frac{f_{C_3H_8}}{f_{CH_4}}\right)_{FID} \tag{4-9}$$

Following the same way, the ratio for any other heavier hydrocarbon components detected on FID side can also be determined. A general formula for the FID side can then be expressed by the following equation:

$$\left(\frac{w_i}{w_{CH_4}}\right)_{FID} = \frac{A_{i,FID}}{A_{CH_4,FID}}\left(\frac{f_i}{f_{CH_4}}\right)_{FID} \tag{4-10}$$

The weight fraction of a component in the sample can be determined. For instance, the weight fraction of hydrogen can be determined as follows:

$$w_{H_2} = \frac{w_{H_2}}{w_{H_2} + w_{N_2} + w_{CO} + w_{CO_2} + w_{CH_4} + w_{C_2H_4} + w_{C_2H_6} + w_{C_3H_6} + w_{C_3H_8} + \ldots}$$

$$= \frac{\frac{w_{H_2}}{w_{CH_4}}}{\frac{w_{H_2}}{w_{CH_4}} + \frac{w_{N_2}}{w_{CH_4}} + \frac{w_{CO}}{w_{CH_4}} + \frac{w_{CO_2}}{w_{CH_4}} + 1 + \frac{w_{C_2H_4}}{w_{CH_4}} + \frac{w_{C_2H_6}}{w_{CH_4}} + \frac{w_{C_3H_6}}{w_{CH_4}} + \frac{w_{C_3H_8}}{w_{CH_4}} + \ldots}$$

$$= \frac{\frac{A_{H_2,TCD}}{A_{CH_4,TCD}}\left(\frac{f_{H_2}}{f_{CH_4}}\right)_{TCD}}{\frac{A_{H_2,TCD}}{A_{CH_4,TCD}}\left(\frac{f_{H_2}}{f_{CH_4}}\right)_{TCD} + \frac{A_{N_2,TCD}}{A_{CH_4,TCD}}\left(\frac{f_{N_2}}{f_{CH_4}}\right)_{TCD} + \ldots + 1 + \frac{A_{C_2H_4,FID}}{A_{CH_4,FID}}\left(\frac{f_{C_2H_4}}{f_{CH_4}}\right)_{FID} + \frac{A_{C_2H_6,FID}}{A_{CH_4,FID}}\left(\frac{f_{C_2H_6}}{f_{CH_4}}\right)_{FID} + \ldots} \quad (4\text{-}11)$$

Similarly, other components can be determined.

$$w_{N_2} = \frac{w_{N_2}}{w_{H_2} + w_{N_2} + w_{CO} + w_{CO_2} + w_{CH_4} + w_{C_2H_4} + w_{C_2H_6} + w_{C_3H_6} + w_{C_3H_8} + \ldots}$$

$$= \frac{\frac{A_{N_2,TCD}}{A_{CH_4,TCD}}\left(\frac{f_{N_2}}{f_{CH_4}}\right)_{TCD}}{\frac{A_{H_2,TCD}}{A_{CH_4,TCD}}\left(\frac{f_{H_2}}{f_{CH_4}}\right)_{TCD} + \frac{A_{N_2,TCD}}{A_{CH_4,TCD}}\left(\frac{f_{N_2}}{f_{CH_4}}\right)_{TCD} + \ldots + 1 + \frac{A_{C_2H_4,FID}}{A_{CH_4,FID}}\left(\frac{f_{C_2H_4}}{f_{CH_4}}\right)_{FID} + \frac{A_{C_2H_6,FID}}{A_{CH_4,FID}}\left(\frac{f_{C_2H_6}}{f_{CH_4}}\right)_{FID} + \ldots} \quad (4\text{-}12)$$

$$w_{CO} = \frac{w_{CO}}{w_{H_2} + w_{N_2} + w_{CO} + w_{CO_2} + w_{CH_4} + w_{C_2H_4} + w_{C_2H_6} + w_{C_3H_6} + w_{C_3H_8} + \ldots}$$

$$= \frac{\frac{A_{CO,TCD}}{A_{CH_4,TCD}}\left(\frac{f_{CO}}{f_{CH_4}}\right)_{TCD}}{\frac{A_{H_2,TCD}}{A_{CH_4,TCD}}\left(\frac{f_{H_2}}{f_{CH_4}}\right)_{TCD} + \frac{A_{N_2,TCD}}{A_{CH_4,TCD}}\left(\frac{f_{N_2}}{f_{CH_4}}\right)_{TCD} + \ldots + 1 + \frac{A_{C_2H_4,FID}}{A_{CH_4,FID}}\left(\frac{f_{C_2H_4}}{f_{CH_4}}\right)_{FID} + \frac{A_{C_2H_6,FID}}{A_{CH_4,FID}}\left(\frac{f_{C_2H_6}}{f_{CH_4}}\right)_{FID} + \ldots} \quad (4\text{-}13)$$

$$w_{CO_2} = \frac{w_{CO_2}}{w_{H_2} + w_{N_2} + w_{CO} + w_{CO_2} + w_{CH_4} + w_{C_2H_4} + w_{C_2H_6} + w_{C_3H_6} + w_{C_3H_8} + \ldots}$$

$$= \frac{\frac{A_{CO_2,TCD}}{A_{CH_4,TCD}}\left(\frac{f_{CO_2}}{f_{CH_4}}\right)_{TCD}}{\frac{A_{H_2,TCD}}{A_{CH_4,TCD}}\left(\frac{f_{H_2}}{f_{CH_4}}\right)_{TCD} + \frac{A_{N_2,TCD}}{A_{CH_4,TCD}}\left(\frac{f_{N_2}}{f_{CH_4}}\right)_{TCD} + \ldots + 1 + \frac{A_{C_2H_4,FID}}{A_{CH_4,FID}}\left(\frac{f_{C_2H_4}}{f_{CH_4}}\right)_{FID} + \frac{A_{C_2H_6,FID}}{A_{CH_4,FID}}\left(\frac{f_{C_2H_6}}{f_{CH_4}}\right)_{FID} + \ldots} \quad (4\text{-}14)$$

$$w_{CH_4} = \frac{w_{CH_4}}{w_{H_2} + w_{N_2} + w_{CO} + w_{CO_2} + w_{CH_4} + w_{C_2H_4} + w_{C_2H_6} + w_{C_3H_6} + w_{C_3H_8} + \ldots}$$

$$= \frac{1}{\frac{A_{H_2,TCD}}{A_{CH_4,TCD}}\left(\frac{f_{H_2}}{f_{CH_4}}\right)_{TCD} + \frac{A_{N_2,TCD}}{A_{CH_4,TCD}}\left(\frac{f_{N_2}}{f_{CH_4}}\right)_{TCD} + \ldots + 1 + \frac{A_{C_2H_4,FID}}{A_{CH_4,FID}}\left(\frac{f_{C_2H_4}}{f_{CH_4}}\right)_{FID} + \frac{A_{C_2H_6,FID}}{A_{CH_4,FID}}\left(\frac{f_{C_2H_6}}{f_{CH_4}}\right)_{FID} + \ldots} \quad (4\text{-}15)$$

$$w_{C_2H_4} = \frac{w_{C_2H_4}}{w_{H_2} + w_{N_2} + w_{CO} + w_{CO_2} + w_{CH_4} + w_{C_2H_4} + w_{C_2H_6} + w_{C_3H_6} + w_{C_3H_8} + \ldots}$$

$$= \frac{\frac{A_{C_2H_4,FID}}{A_{CH_4,FID}}\left(\frac{f_{C_2H_4}}{f_{CH_4}}\right)_{FID}}{\frac{A_{H_2,TCD}}{A_{CH_4,TCD}}\left(\frac{f_{H_2}}{f_{CH_4}}\right)_{TCD} + \frac{A_{N_2,TCD}}{A_{CH_4,TCD}}\left(\frac{f_{N_2}}{f_{CH_4}}\right)_{TCD} + \ldots + 1 + \frac{A_{C_2H_4,FID}}{A_{CH_4,FID}}\left(\frac{f_{C_2H_4}}{f_{CH_4}}\right)_{FID} + \frac{A_{C_2H_6,FID}}{A_{CH_4,FID}}\left(\frac{f_{C_2H_6}}{f_{CH_4}}\right)_{FID} + \ldots} \quad (4\text{-}16)$$

For any other heavier hydrocarbon, a general formula can be used:

$$w_i = \frac{w_i}{w_{H_2} + w_{N_2} + w_{CO} + w_{CO_2} + w_{CH_4} + w_{C_2H_4} + w_{C_2H_6} + w_{C_3H_6} + w_{C_3H_8} + \ldots}$$

$$= \frac{\dfrac{A_{i,FID}}{A_{CH_4,FID}}\left(\dfrac{f_i}{f_{CH_4}}\right)_{FID}}{\dfrac{A_{H_2,TCD}}{A_{CH_4,TCD}}\left(\dfrac{f_{H_2}}{f_{CH_4}}\right)_{TCD} + \dfrac{A_{N_2,TCD}}{A_{CH_4,TCD}}\left(\dfrac{f_{N_2}}{f_{CH_4}}\right)_{TCD} + \ldots + 1 + \dfrac{A_{C_2H_4,FID}}{A_{CH_4,FID}}\left(\dfrac{f_{C_2H_4}}{f_{CH_4}}\right)_{FID} + \dfrac{A_{C_2H_6,FID}}{A_{CH_4,FID}}\left(\dfrac{f_{C_2H_6}}{f_{CH_4}}\right)_{FID} + \ldots} \tag{4-17}$$

From weight fraction, mole fraction can be determined. The general formula is expressed in Equation 4-18.

$$y_i = \frac{\dfrac{w_i}{M_i}}{\sum_i \dfrac{w_i}{M_i}} \tag{4-18}$$

where y_i , w_i and M_i denote mole fraction, weight fraction, and molecular weight of component *i*, respectively.

By this method, we suppose all of the components at reactor effluent will either show up on TCD GC or FID GC.

If nitrogen is used as an internal standard, the reactor effluent flow rate can be determined based on a nitrogen balance. Because $F_{N_2,in} = F_{N_2,out}$, therefore

$$y_{N_2,in}F_{in} = y_{N_2,out}F_{out} \tag{4-19}$$

$$F_{out} = y_{N_2,in}F_{in} / y_{N_2,out} \tag{4-20}$$

where, F_{in} and F_{out} are the total molar flow rates at reactor inlet and outlet, respectively. $y_{N_2,in}$ and $y_{N_2,out}$ are mole fraction of nitrogen at reactor inlet and outlet, respectively.

Knowing F_{out} and y_i , a component flow rate at reactor outlet can be determined.

$$F_{i,out} = y_i F_{out} = y_i y_{N_2,in} F_{in} / y_{N_2,out} \quad (4\text{-}21)$$

where $F_{i,out}$ is the molar flow rate of component i at the reactor outlet.

4.2 Butane Cracking and Disproportionation

The reaction system, the GC analysis method and the GC data processing are the same as those used in ethylene oligomerization. Argon was used as an inert gas for the reaction.

CHAPTER V

ACIDITY OF BOUND ZEOLITES

In this chapter, the acidities of zeolites ZSM-5 and Y and their binder-embedded counterparts are measured and discussed. To investigate the acidity, NH_3-TPD and FTIR techniques were used. The binders used were silica and alumina, respectively. For silica binder, silica gels Ludox HS-40 and AS-40 were used. For alumina binder, γ-Al_2O_3 and boehmite were used. The properties of these binders are listed in Table 3.1.2. Note that Ludox AS-40 contained much less Na and K than Ludox HS-40 did. Binding methods were gel-mixing, powder-wet-mixing, and powder-mixing, which have been described in Chapter III. "HS-SiO_2-bound" denotes the binder is Ludox HS-40, while "AS-SiO_2-bound" denotes the binder is Ludox AS-40. In order to study the effect of alumina binder on the acidity of zeolites without the influence of alkaline metal cations, commercial alumina-bound zeolites of low sodium content were also examined.

5.1 Silica-bound Zeolites ZSM-5 and Y

5.1.1 Bound with Ludox HS-40

Hydroxyl groups on the surface of zeolites ZSM-5 and Y could be a source of Bronsted acid sites. Measurement of the surface hydroxyl groups is one of the common methods used to study acidity, especially protonic acidity, of zeolitic materials. Figs. 5.1.1 and 5.1.2 show the FTIR spectra in the range of hydroxyl group vibrations for zeolites ZSM-5 and Y of different SiO_2/Al_2O_3 ratios and their HS-SiO_2-bound counterparts made by the gel-mixing method.

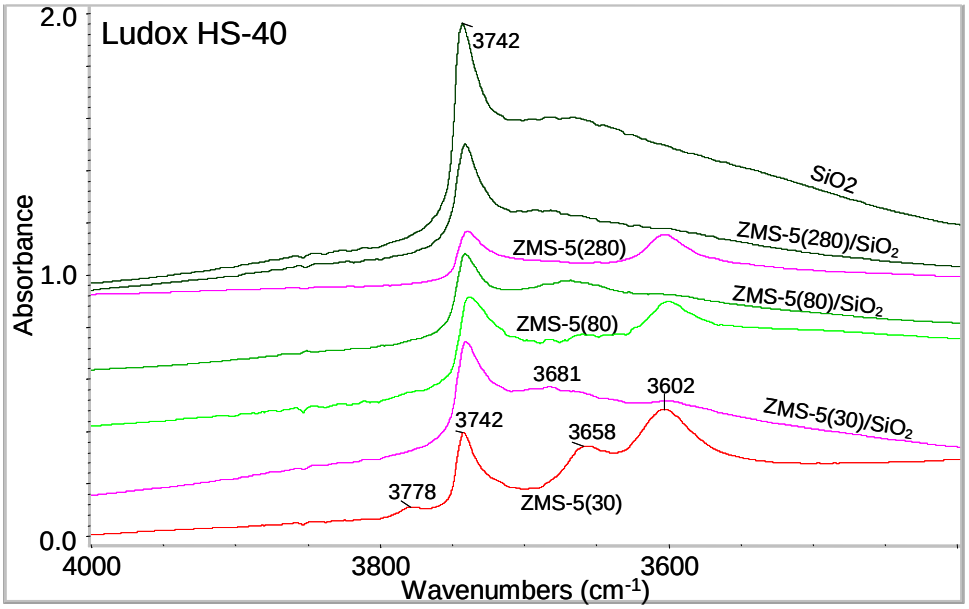

Fig. 5.1.1 FTIR spectra of ZSM-5 and SiO_2-bound ZSM-5. SiO_2: Ludox HS-40; ZSM-5: SiO_2/Al_2O_3 ratio of 30, 80, and 280; Binding method: gel-mixing; SiO_2-binder in bound catalyst: 29 wt%.

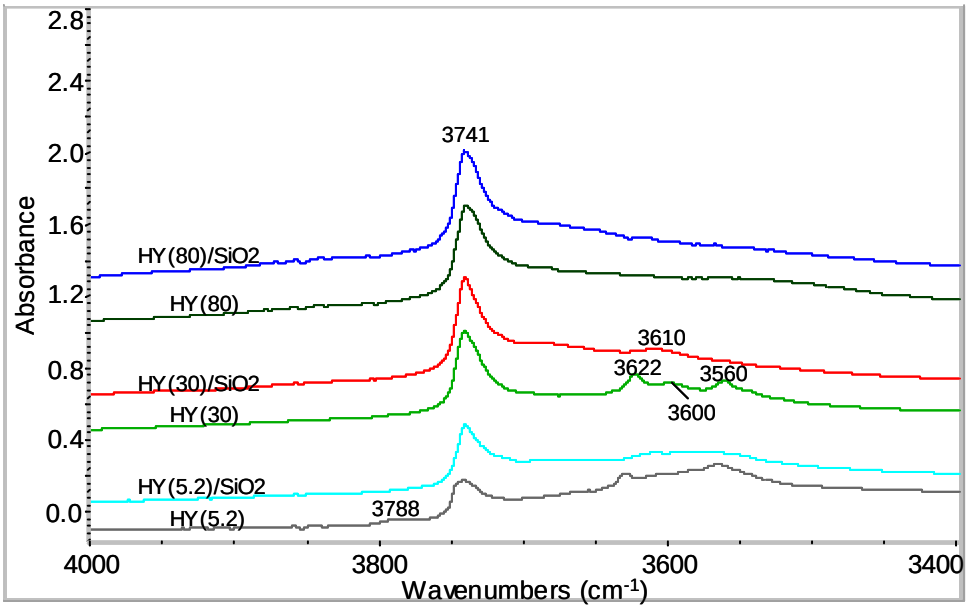

Fig. 5.1.2 FTIR spectra of Y and SiO_2-bound Y. SiO_2: Ludox HS-40; Y: SiO_2/Al_2O_3 ratio of 5.2, 30 and 80; Binding method: gel-mixing; SiO_2-binder in bound catalyst: 29 wt%.

Two IR absorption bands at around 3740 cm^{-1} and 3600 cm^{-1} exist on all of the tested ZSM-5 samples with different SiO_2/Al_2O_3 ratios, while the band near 3658 cm^{-1} is clearly observed only on a sample with the lowest SiO_2/Al_2O_3 ratio, as shown in Fig. 5.1.1. In ZSM-5, the bands at around 3740 cm^{-1} and 3600 cm^{-1} are attributed to terminal silanol (≡SiOH) on the external surface and bridged OH (≡Si-(OH)-Al≡) in the zeolite framework, respectively, and the 3658 cm^{-1} band is attributed to the hydroxyl group attached to extra-framework aluminum (Jacobs, 1977). While in zeolite Y, as shown in Fig. 5.1.2, the bands at 3622 and 3560 cm^{-1} are from the bridged OH groups, and the band at 3600 cm^{-1} (in HY with SiO_2/Al_2O_3 ratio of 30) is from the hydroxyl group attached to extra-framework aluminum (Corma et al., 1990). The band near 3740 cm^{-1} is observed on SiO_2 and all of the zeolite ZSM-5 and Y samples. While the band near 3780 cm^{-1} (about 3778 cm^{-1} in ZSM-5 and 3788 cm^{-1} in Y) is observed only on alumina and zeolites ZSM-5 and Y with low SiO_2/Al_2O_3 ratios. As SiO_2/Al_2O_3 ratio increases, this band disappears, as shown in Figs. 5.1.1 and 5.1.2. Therefore, the band may be due to a hydroxyl group originated from surface aluminum species. The band 3602 cm^{-1} in ZSM-5 and the bands at 3622 and 3560 cm^{-1} in Y represent Bronsted acid sites (Jacobs, 1977; Corma et al, 1990), so that the hydroxyl groups characterized by 3600 cm^{-1} in ZSM-5 and 3620 cm^{-1} and 3560 cm^{-1} in Y are protonic acidic sites. The IR absorption intensity at these sites corresponds to the Bronsted acidity. However, quantitative analysis based on the intensity is not feasible due to the difficulty in determining the extinction coefficients. Only qualitative analysis can be given.

It is obvious from Figs. 5.1.1 to 5.1.2 that the IR absorption intensity of the acidic hydroxyl groups is reduced significantly when zeolites ZSM-5 and Y are embedded on SiO_2. However, the band attributed to a hydroxyl group attached to extra-framework aluminum shifts to a position of a higher wavenumber. In zeolite Y, it shifts from 3600 to 3610 cm^{-1}; in ZSM-5, it shifts from 3658 to 3663 ~ 3681 cm^{-1}. This could be an indication that silica from the binder might react with extra-framework aluminum during preparation of the bound catalysts, forming new species that have an acidic property (Corma et al, 1990a, 1990b; Falabella, 1996; de la Puente et al., 2003).

Figs. 5.1.3 and 5.1.4 show NH_3-TPD profiles and total acid site density of zeolites ZSM-5 and Y and their HS-SiO_2–bound counterparts made by the gel-mixing method. After the zeolites are embedded on SiO_2 by the gel-mixing method, the density and the strength of the strong acid sites are significantly reduced, as indicated by the height (or the area under curve) and the temperature of the high temperature peak, respectively, as shown in Fig. 5.1.3. Total acid site density is also reduced compared to the parent zeolites, as shown in Fig. 5.1.4. However, the density and strength of weak acids do not change as significantly as those of the strong acids, as shown in Fig. 5.1.3.

Ludox HS-40 contained sodium and potassium as shown in Table 3.1.2. These alkaline metal cations are strongly basic and acidic site killers, especially for strong acid sites. One reason for the decreased acidity in HS-SiO_2-bound catalysts is the presence of alkaline metal cations in Ludox HS-40.

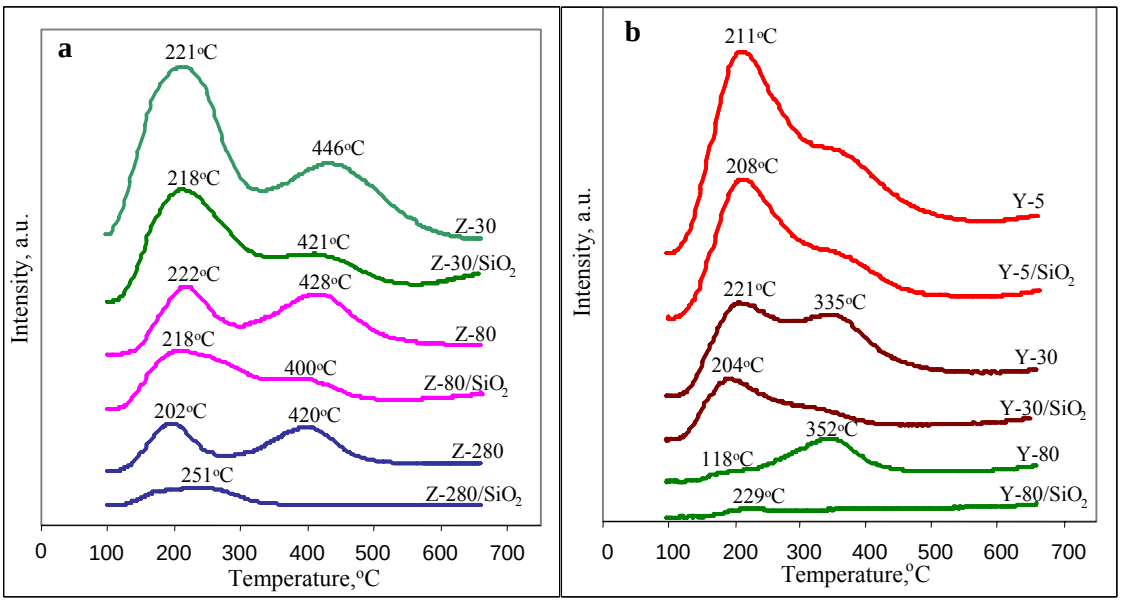

Fig. 5.1.3 NH_3-TPD profiles for (a) silica-bound ZSM-5 and (b) silica-bound Y. Numbers following the letter Z or Y denote SiO_2/Al_2O_3 molar ratio of the zeolite. Silica source: HS-40(Wu, et al., 2002).

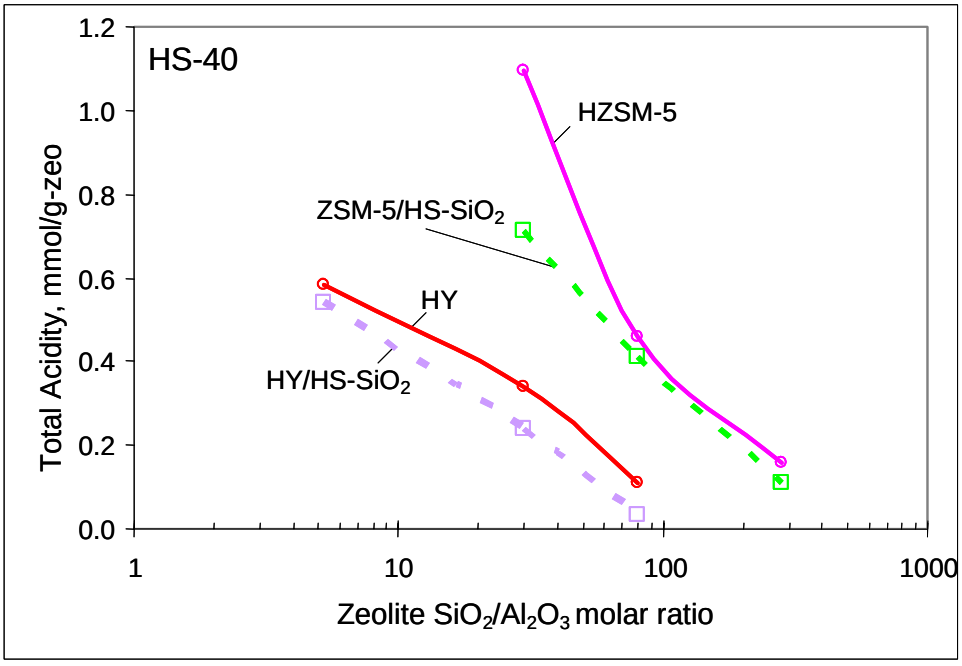

Fig. 5.1.4 Total acid site density of zeolites ZSM-5 and Y and their HS-SiO_2-bound counterparts. Silica source: HS-40; binding method: gel-mixing; SiO_2-binder in bound catalyst: 29 wt%.

When Ludox HS-40 is used as a binder, different binding methods are tested using HZSM-5 (SiO_2/Al_2O_3=30) in order to investigate how acidity is changed by the method of embedding. The binding methods are the gel-mixing, powder-mixing and powder-wet-mixing as described in Chapter III. It is found that the acidity of HS-SiO_2-bound ZSM-5 catalysts changes differently with the binding methods.

Fig. 5.1.5 shows IR spectra of HS-SiO_2-bound ZSM-5 made by different binding methods. The 3602 cm^{-1} band reduces its intensity dramatically for all of the three binding methods, but the catalyst made by the powder-mixing method shows a slightly higher intensity at 3602 cm^{-1} than the other catalysts made by the gel-mixing method and the powder-wet-mixing method, respectively. The band at 3658 cm^{-1} shifts to a higher wavenumber position. The band 3778 cm^{-1} disappears.

Fig. 5.1.6 shows the spectra of pyridine adsorption on the catalysts. 1543 cm^{-1} band corresponds to pyridine ion on Bronsted acid sites, and the 1454 cm^{-1} band to pyridine coordination to Lewis acid site. Both Bronsted acid sites and Lewis acid sites are reduced on all of the catalysts, however, Lewis acid sites almost totally vanish.

From the fact that 3778 cm^{-1} band vanishes and the 3658 cm^{-1} band shifts, one may propose that silica from the binder reacts with extra-framework aluminum during preparation of the bound catalysts.

Fig. 5.1.7 compares the difference between the profiles of NH_3-TPD of the catalysts made by the three different methods. The catalysts made by the powder-mixing and the powder-wet-mixing methods show similar profiles, while the catalyst made by the gel-mixing method has fewer strong acid sites (determined by NH_3-TPD experiment

ramping from 235°C), even though the strong acid site density of all of catalysts are reduced, as shown in Fig 5.1.8. The catalyst made by the gel-mixing method produces a catalyst with the lowest Bronsted acid site density and strong acid site density among the catalysts as indicated by Fig. 5.1.8.

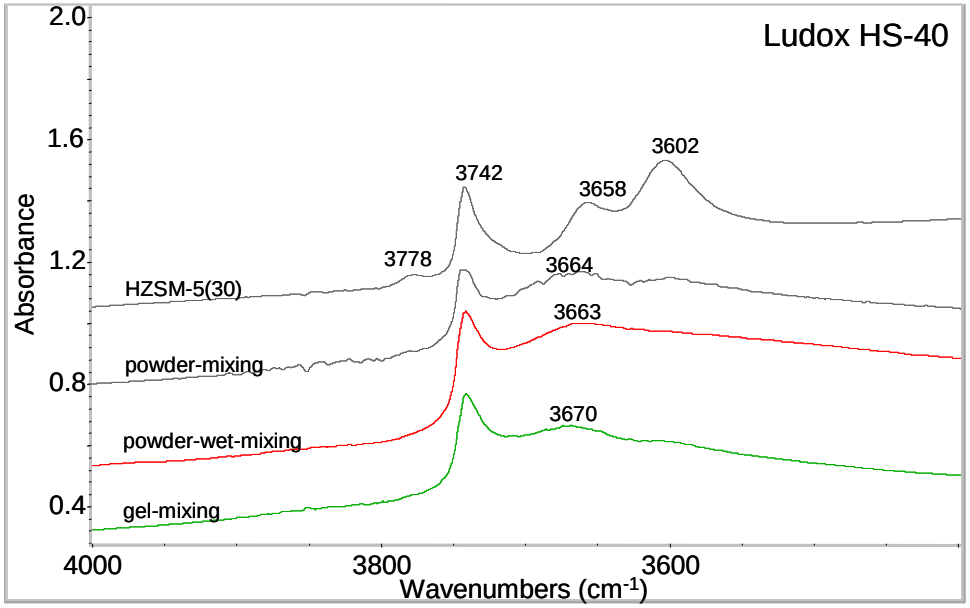

Fig. 5.1.5 IR spectra of SiO_2-bound ZSM-5 (SiO_2/Al_2O_3=30) catalysts made with different binding methods. Silica source: Ludox HS-40; SiO_2-binder in bound catalyst: 29 wt%.

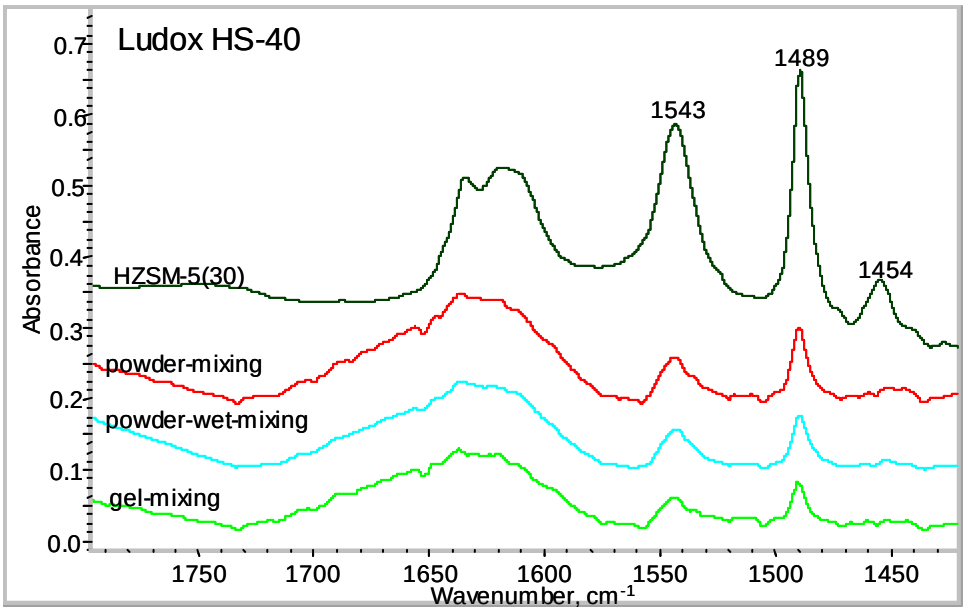

Fig. 5.1.6 Spectra of pyridine adsorption on SiO_2-bound ZSM-5 catalysts made by different binding methods. ZSM-5: SiO_2/Al_2O_3=30; silica source: HS-40; SiO_2-binder in bound catalyst: 29 wt%.

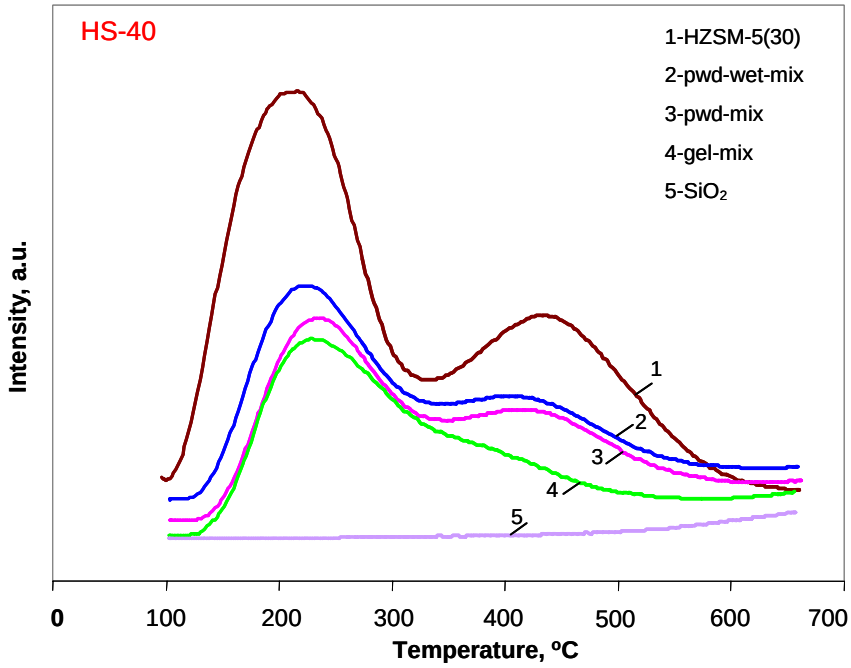

Fig. 5.1.7 NH_3-TPD profiles of SiO_2-bound ZSM-5 catalysts made by different binding methods. ZSM-5: SiO_2/Al_2O_3 =30; silica source: HS-40; SiO_2-binder in bound catalyst: 29 wt%.

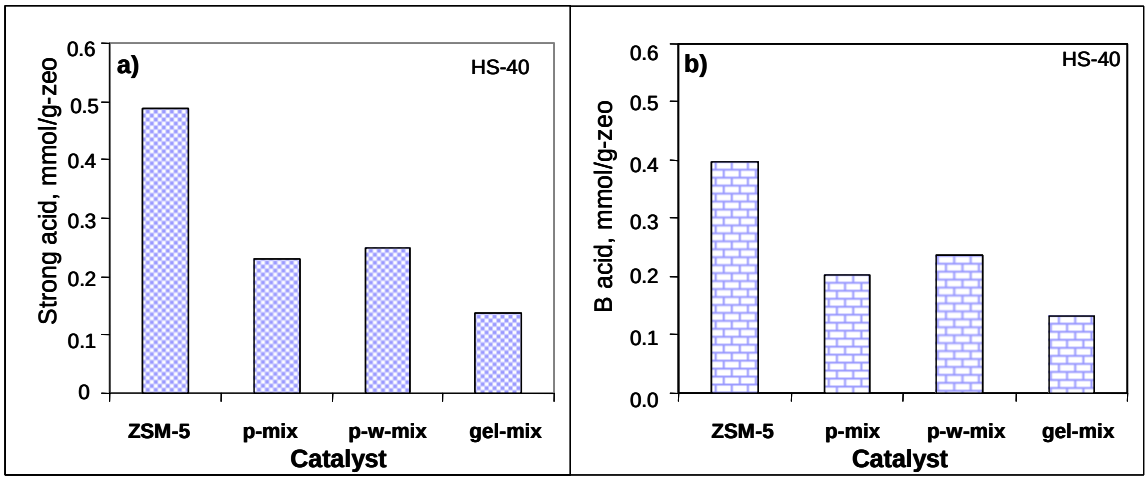

Fig. 5.1.8 (a) Strong acid site density and (b) strong Bronsted acid site density of SiO_2-bound ZSM-5 catalysts made by different binding methods. ZSM-5: SiO_2/Al_2O_3=30; silica source: HS-40; SiO_2-binder in bound catalyst: 29 wt%.

The gel-mixing method provides more intimate contact between zeolite crystals and silica particles than the other two methods, since small silica particles in gel will aggregate into bigger ones during preparation of SiO_2 for use in the powder-wet-mixing and the powder-mixing methods. However, during the aggregation, some sodium and potassium cations are encapsulated in the particles, allowing less alkaline metal content in the solution (suspension) of the binding mixture in the powder-wet-mixing method than in the gel-mixing method. The more contacts between the zeolite crystals and the SiO_2 binder particles, the more reaction between SiO_2 and extra-framework alumina in the zeolite would happen, and thus more acidic sites could be produced. However, the more sodium in the binder, the fewer acid sites will be present. Therefore, among the catalysts made by the three methods, the gel-mixing method produces the catalyst with

the least number of acid sites, and the powder-wet-mixing method produces the catalyst with the most acid sites.

5.1.2 Bound with Ludox AS-40

Similar results to HS-SiO_2-bound ZSM-5 were also found on AS-SiO_2-bound ZSM-5. FTIR spectra of AS-SiO_2-bound ZSM-5 samples made by the gel-mixing method are shown in Fig. 5.1.9. The 3602 cm^{-1} band intensity of all bound ZSM-5 catalysts is significantly reduced when Ludox AS-40 is embedded. Similar to HS-SiO_2-bound ZSM-5 catalysts, the 3658 cm^{-1} band shifts to a higher wavenumber position. However, if this band is not present in the parent ZSM-5, no new band near 3665 cm^{-1} is found. Again, this could be an indication that SiO_2 from the binder may react with extra-framework alumina in ZSM-5 during preparation of the bound catalysts.

The total acid site density and Bronsted acid density of the AS-SiO_2-bound ZSM-5 (with different SiO_2/Al_2O_3 ratios) made by the gel-mixing method are shown in Fig. 5.1.10. Both of the acid densities are reduced by embedding SiO_2 from Ludox AS-40.

Using three different binding methods and Ludox AS-40 as a silica binder, three bound ZSM-5 catalysts were made from a parent HZSM-5 with SiO_2/Al_2O_3=30. Figs. 5.1.11 and 5.1.12 show the IR spectra of the catalysts and the pyridine adsorption, respectively. It is clear that all of the binding methods lead to catalysts of much less intensity at 3602 cm^{-1} and 1543 cm^{-1} (both indicating Bronsted acid), and almost vanishing of the 1454 cm^{-1} band (indicating Lewis acid). This means that the Bronsted acid sites are significantly reduced and Lewis acid sites are almost vanishing. Extra-

framework aluminum in zeolite could be a source of Lewis acid. The disappearance of Lewis acid (featured by 1454 cm^{-1} band) and a new band near 3665 cm^{-1} may provide evidence, as in the case of HS-SiO_2-bound catalysts, that silica from the binder may react with extra-frame aluminum in the zeolite. However, the catalysts made by the powder-wet-mixing and powder-mixing methods show higher intensity at 1454 cm^{-1} than the catalyst made by gel-mixing method, as shown in Fig. 5.1.12. This is also true in the case of HS-SiO_2-bound ZSM-5 catalysts as shown in Fig. 5.1.6. This is because the gel-mixing method can provide more intimate contact between the binder particles and the zeolite crystals and thus result in more reactions between them, as discussed in the previous section.

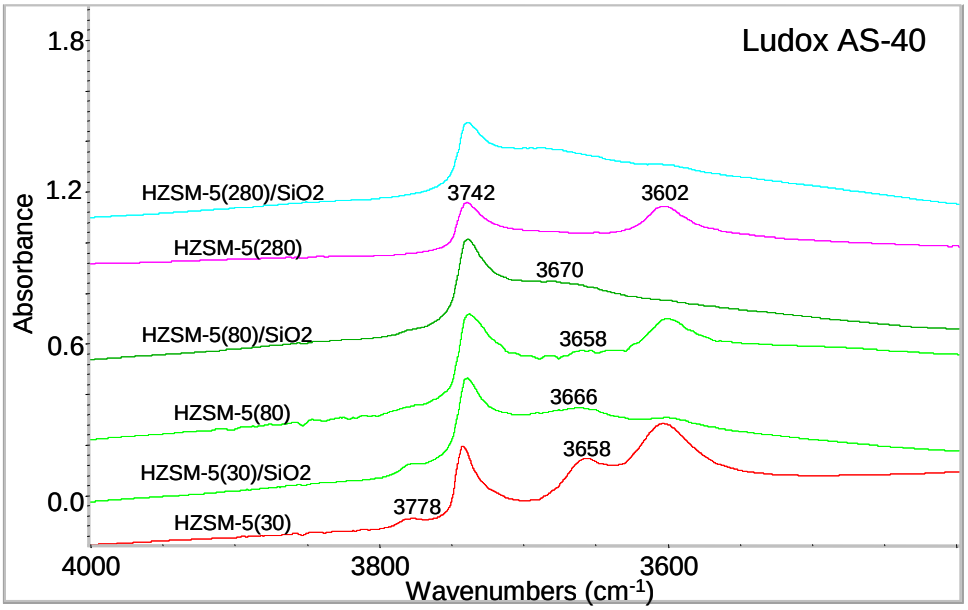

Fig. 5.1.9 FTIR spectra of ZSM-5 and SiO_2-bound ZSM-5. SiO_2: Ludox AS-40; ZSM-5: SiO_2/Al_2O_3 ratio of 30, 80, and 280; Binding method: gel-mixing; SiO_2-binder in bound catalyst: 29 wt%.

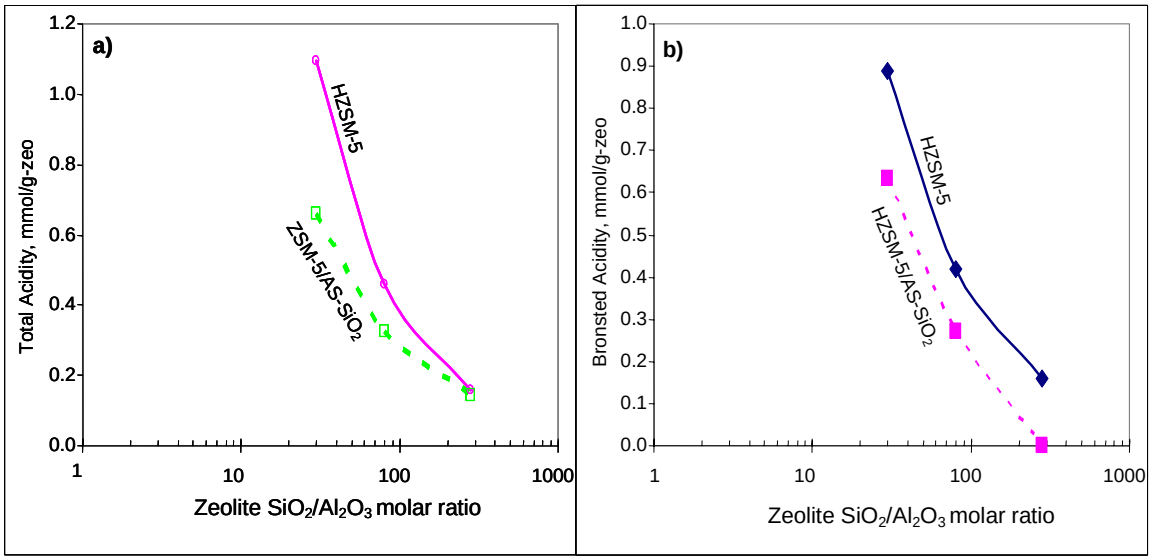

Fig. 5.1.10 (a) Total acid site density and (b) Bronsted acid site density of SiO_2-bound ZSM-5 catalysts. Binding method: gel-mixing; silica source: AS-40; SiO_2-binder in bound catalyst: 29 wt%.

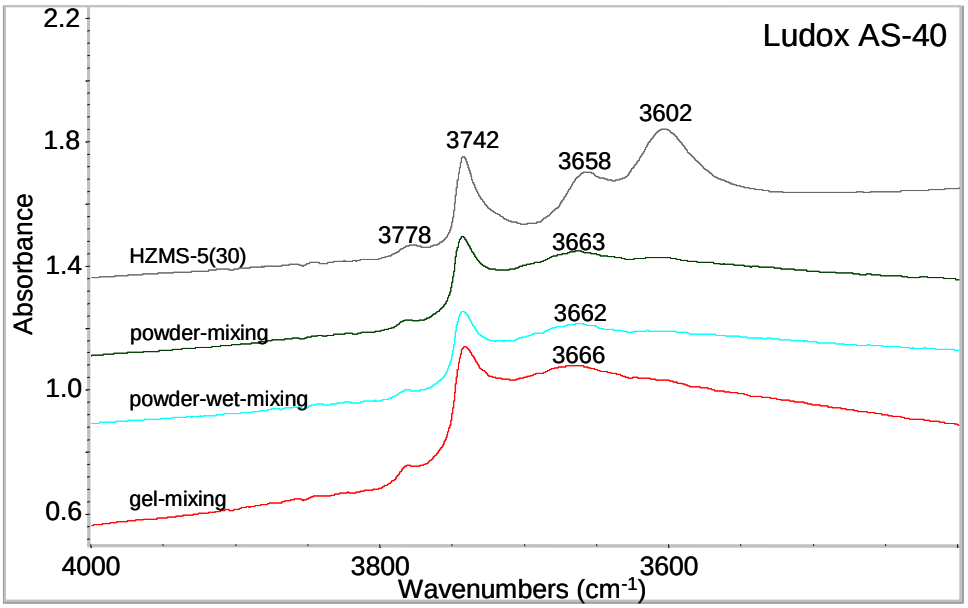

Fig. 5.1.11 IR spectra of SiO_2-bound ZSM-5 (SiO_2/Al_2O_3 ratio of 30) catalysts made by different binding methods. The silica source: Ludox AS-40. SiO_2-binder in bound catalyst: 29 wt%.

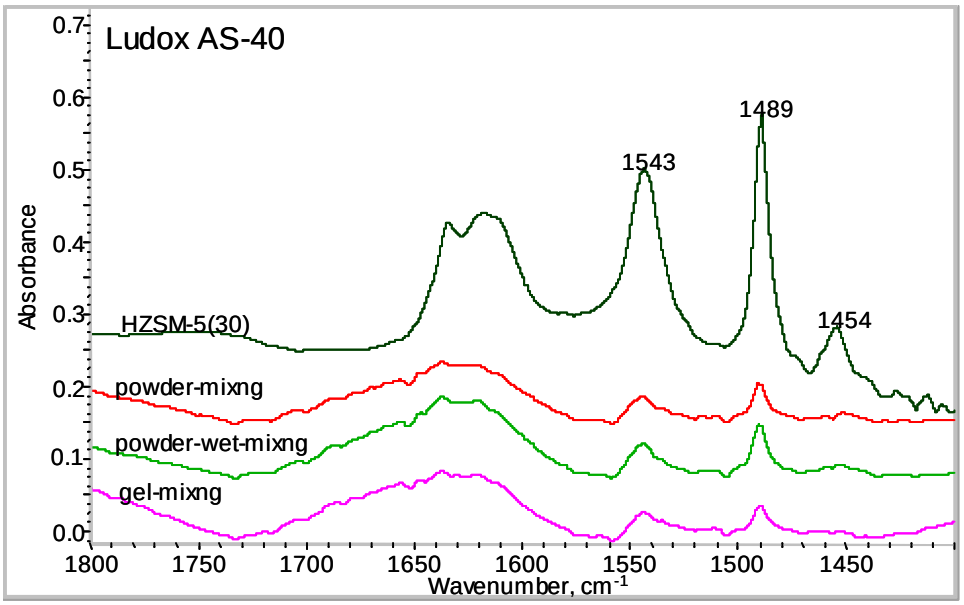

Fig. 5.1.12 Spectra of pyridine adsorption on AS-SiO_2-bound ZSM-5 catalysts made by different binding methods. ZSM-5: SiO_2/Al_2O_3=30; silica source: AS-40; SiO_2-binder in bound catalyst: 29 wt%.

As in the case of HS-SiO_2-bound ZSM-5 catalysts, AS-SiO_2-bound ZSM-5 catalysts show similar NH_3-TPD profiles, which are shown in Fig 5.1.13. The powder-wet-mixing and powder-mixing methods lead to catalysts with similar NH_3-TPD profiles, while the gel-mixing method leads to a catalyst with a smaller high-temperature peak, at which the peak temperature is also lower than those on the other two catalysts. Although Ludox AS-40 contains much less alkaline metal cations than HS-40, it still contains about 0.104 wt% of Na and K, which are responsible for the decrease of strong acid sites. As discussed in the previous section, the concentration of alkaline metal cations is at the highest in the case of the gel-mixing method among the three binding methods.

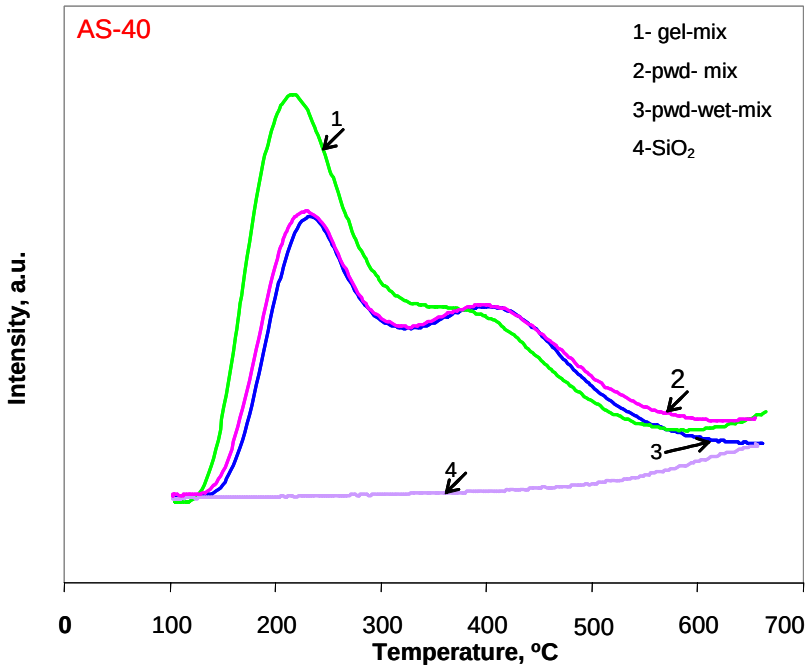

Fig. 5.1.13 NH_3-TPD profiles of AS-SiO_2-bound ZSM-5 catalysts made by different binding methods. ZSM-5: SiO_2/Al_2O_3 molar ratio of 30; silica source: AS-40; SiO_2-binder in bound catalyst: 29 wt%.

5.1.3 Comparison between Ludox HS-40 and AS-40

The major difference between Ludox AS-40 and HS-40 is the content of alkaline metal cations. AS-40 contained sodium and potassium of 0.068 wt%, while HS-40 contained 0.352 wt%. This difference of the alkaline metal content results in the catalysts having different behaviors in acidity. Fig. 5.1.14 shows NH_3-TPD profiles of the ZSM-5 catalysts made from AS-40 and HS-40 by the gel-mixing method. HS-SiO_2-bound catalysts have less strong acid sites and more weak acid sites than AS-SiO_2-bound catalysts. However, the strength of the strong acid is the same, as indicated by the

temperature corresponding to the high temperature peak. Therefore, alkaline metal cations in the binder neutralize the strong acid sites.

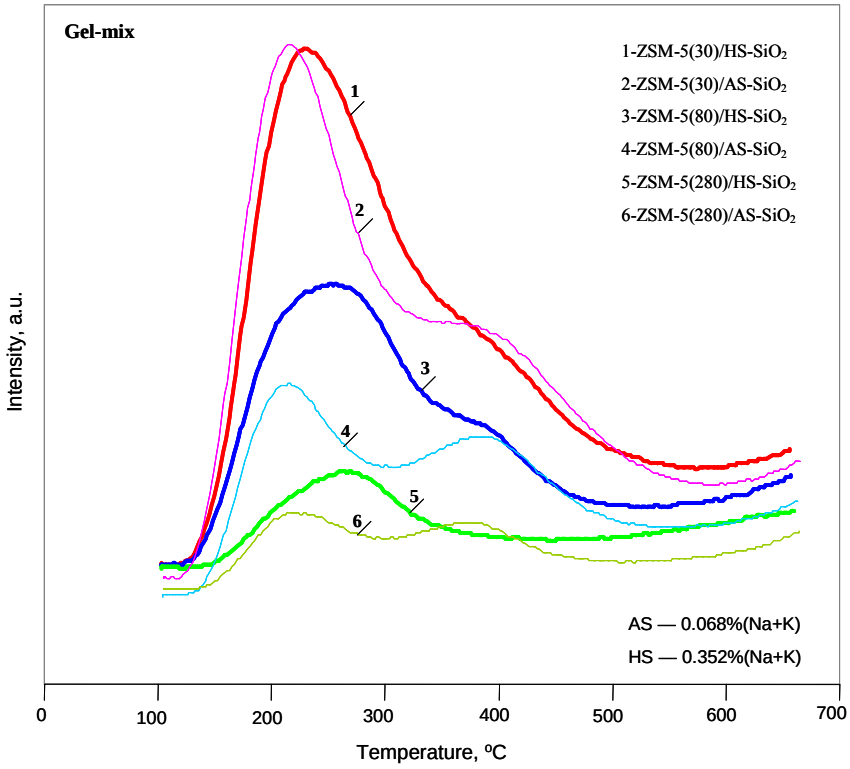

Fig. 5.1.14 NH_3-TPD profiles of SiO_2-bound ZSM-5 catalysts made by the gel-mixing method from Ludox AS-40 and Ludox HS-40. SiO_2 binder content in final catalyst: 29 wt%. The number in brackets denotes SiO_2/Al_2O_3 ratio of ZSM-5.

FTIR spectra of SiO_2-bound ZSM-5 samples made from different sources of silica and by different binding methods are shown in Figs 5.1.15. From this figure, it can be seen that, even though not very significantly, AS-SiO_2-bound ZSM-5 catalysts always have a higher intensity at the band near 3602 cm^{-1} than the HS-SiO_2-bound catalysts

especially in the case of gel-mixing method. The band near 3665 cm^{-1} looks almost the same for all of the catalysts, in addition to a little shift for the HS-SiO_2-bound catalyst made by the gel-mixing method.

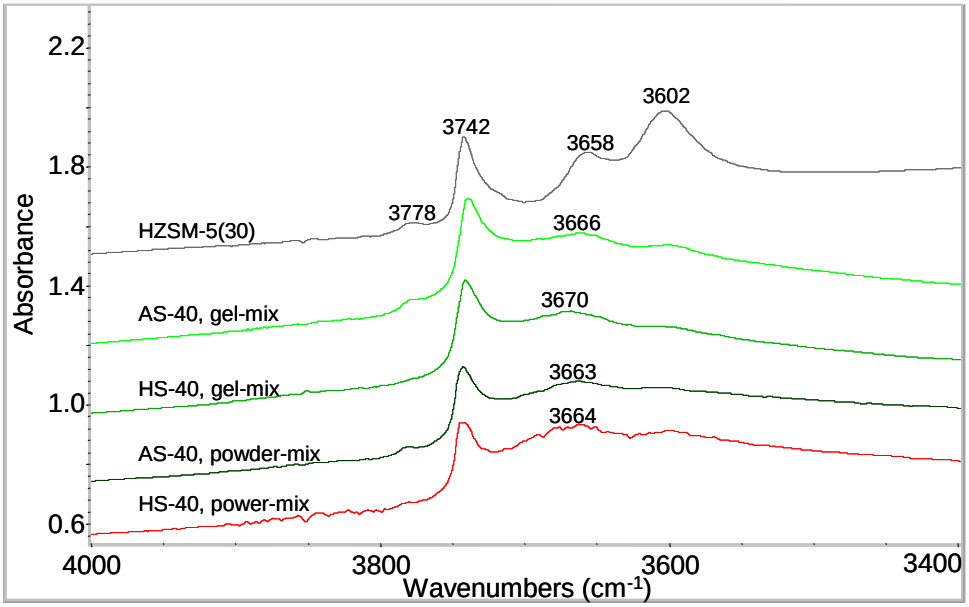

Fig. 5.1.15 Comparison of IR spectra of SiO_2-bound HZSM-5(30) made from AS-40 and HS-40.

The acidity comparison may be better expressed by Figs. 5.1.16 and 5.1.17. Based on the two figures, the strong acid site density (determined by NH_3-TPD experiment ramping from 235^oC) and Bronsted acid site density depend on binding methods and the alkaline metal content in the binder as well. However, by comparing AS-SiO_2-bound catalysts with HS-SiO_2-bound catalysts, the strong acid sites and Bronsted acid sites change significantly only when using the gel-mixing method. While

for the other two methods, it seems like the total acid sites and Bronsted acid sites have little relation with the alkaline metal content in the binder. Strong acid sites, which can be determined by running NH_3-TPD from a higher starting temperature such as 235^oC for ramping, also follow similar changes, which are shown in Fig. 5.1.18. This indicates that solid-state ion-exchange of alkaline metals in SiO_2 binder with protons in the zeolite occurs only to a limited degree during calcination of the bound catalysts. The acidity decrease due to alkaline metal neutralization primarily comes from solution ion-exchange with little contribution from solid-state ion-exchange.

The gel-mixing method provides a better condition than the other two binding methods in terms of solution ion-exchange. Some alkaline metal ions might be encapsulated in the SiO_2 particles when drying and calcining the Ludox gels to prepare SiO_2 powder for the powder-mixing and powder-wet-mixing methods, and could not come out into the solution in the powder-wet-mixing method. Ludox AS-40 had a pH of 9.1 and Ludox HS-40 had a pH of 9.8. The de-ionized water suspensions of SiO_2 powders made from Ludox AS-40 and HS-40 had pH values of 5.3 and 7.0, respectively. Therefore, the alkaline metal concentration in the solution in the case of the powder-wet-mixing method is much less than that in the case of the gel-mixing method. So the results on the powder-mixing and powder-wet-mixing methods are almost similar in terms of total acid sites, Bronsted acid sites, and strong acid sites.

The bound-catalysts, either HS-SiO_2-bound or AS-SiO_2-bound, made by a wet method (either the gel-mixing or the powder-wet-mixing) always have less Lewis acid sites than their corresponding catalysts made by a dry method (the powder-mixing). This

could be because the SiO_2 binder particles had better contacts with the zeolite crystals in the wet-mixing condition than the dry-mixing condition, and thus may have more reactions between the silica and extra-framework aluminum.

It is not clear yet that HS-SiO_2-bound catalysts always have less Lewis acid sites than AS-SiO_2-bound catalysts when a wet binding method is used.

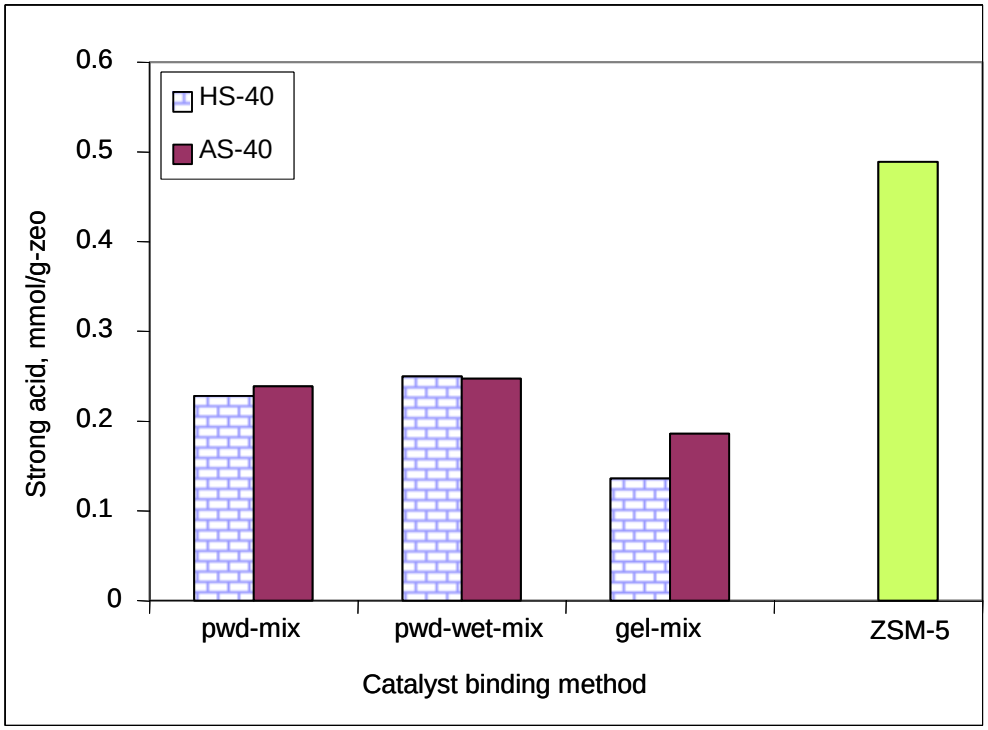

Fig. 5.1.16 Comparison on strong acid site density for AS-SiO_2-bound and HS-SiO_2-bound ZSM-5 (SiO_2/Al_2O_3=30); SiO_2 bonder content in the catalysts: 29 wt%.

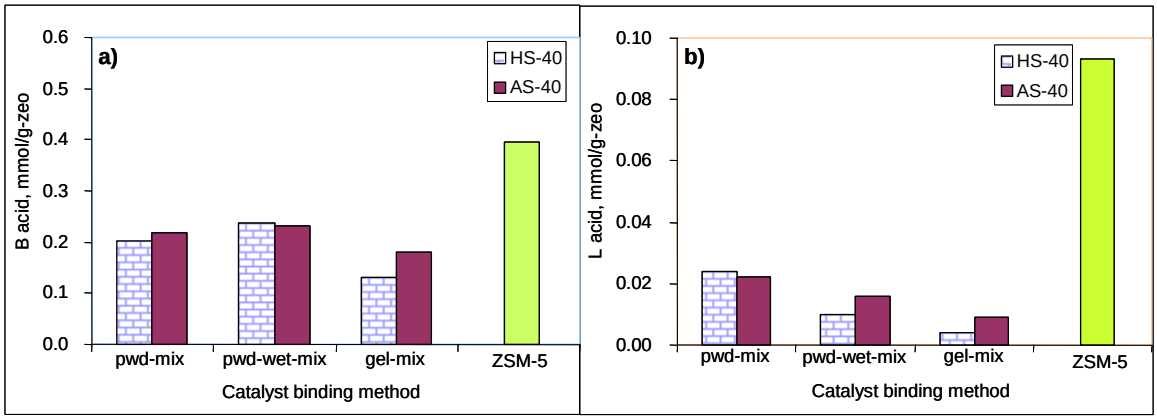

Fig. 5.1.17 Comparison on a) Bronsted acid density and b) Lewis acid density for AS-SiO_2-bound and HS-SiO_2-bound ZSM-5 (SiO_2/Al_2O_3=30); SiO_2 bonder content in the catalysts: 29 wt%.

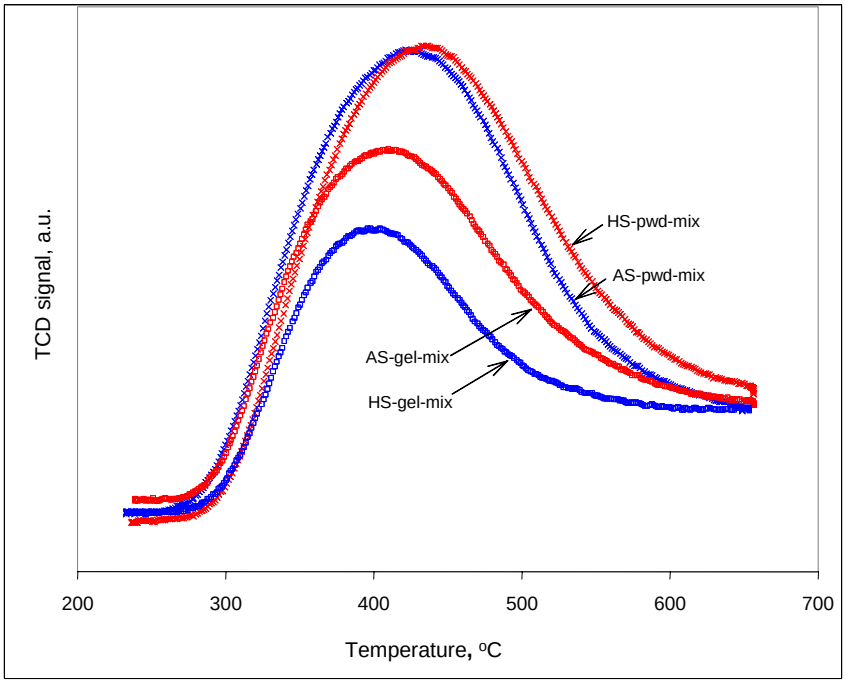

Fig. 5.1.18 Comparison of AS-SiO_2-bound with HS-SiO_2-bound ZSM-5(SiO_2/Al_2O_3=30). NH_3-TPD started from around 230°C to measure exclusively strong acids.

5.2 Alumina-bound Zeolites ZSM-5 and Y

5.2.1 Commercial Alumina-bound Catalysts

Figs. 5.2.1 and 5.2.2 show the FTIR spectra of commercial alumina-bound ZSM-5 and Y catalysts. Alumina binder content is 20 wt% in all of the commercial catalysts. In these alumina-bound ZSM-5 catalysts, it looks like the IR absorption bands on the bound catalysts are superimposed by the zeolites and γ-Al_2O_3. No new absorption band in the OH vibration range apparently shows up. This is similar to previous observation by Zholobenko et al. (1992) who claimed the IR spectra of an alumina-bound pentasil zeolite was a superimposed spectra from alumina and zeolite. However, in alumina-bound Y catalysts, a new IR band near 3600 cm^{-1} is formed as shown in Fig. 5.2.2. This IR band has been assigned to extra-framework alumina. This means that alumina from the binder may react with SiO_2 present in parent zeolite.

NH_3-TPD profiles of the catalysts are shown in Fig. 5.2.3. Comparing with the parent zeolites, the alumina-bound zeolite catalysts do not change much in peak temperatures of both the low-temperature peak and the high-temperature peak in NH_3-TPD profiles, indicating the acid strength of the zeolites remains the same after alumina binder is embedded.

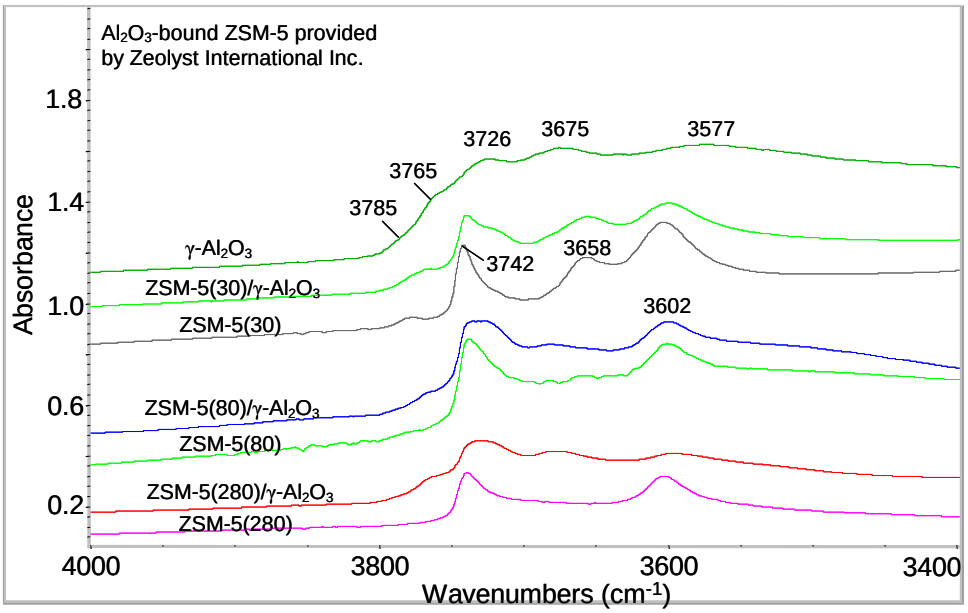

Fig. 5.2.1 IR spectra of Al_2O_3-bound ZSM-5 catalysts manufactured by Zeolyst International Inc. Number in brackets denotes the SiO_2/Al_2O_3 molar ratio of ZSM-5. Alumina binder content: 20 wt%.

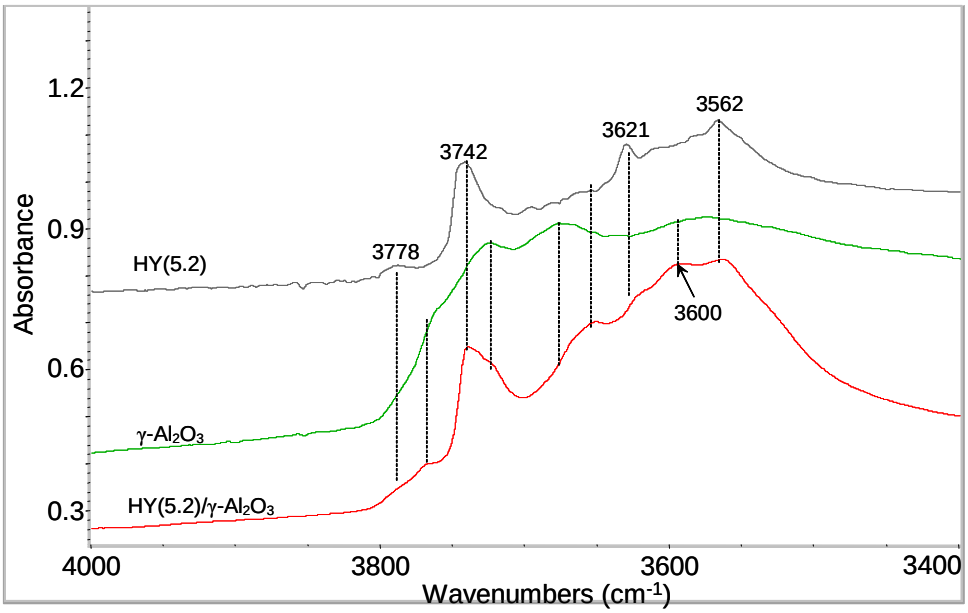

Fig. 5.2.2 IR spectra of Al_2O_3-bound Y(SiO_2/Al_2O_3=5.2) manufactured by Zeolyst International Inc. Alumina binder content: 20 wt%.

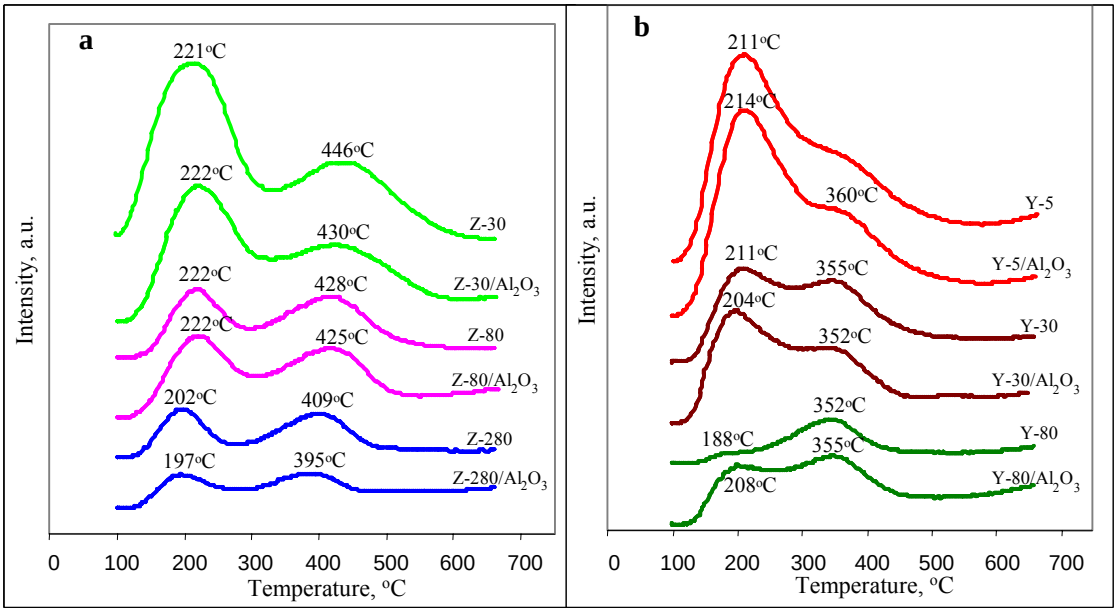

Fig.5.2.3 NH_3-TPD profiles for alumina-bound ZSM-5(a) and Y(b). Numbers following the letter Z or Y denote SiO_2/Al_2O_3 molar ratio of the zeolite. Alumina binder content: 20 wt% (from Wu et al., 2002).

The total acid density, Bronsted acid density and Lewis acid density of the commercial catalysts are shown in Figs. 5.2.4 and 5.2.5. The total acidities of both alumina-bound Y and ZSM-5 increase compared with the parent zeolites. However, the total acidity for alumina-bound Y zeolite has a slightly more enhancement than alumina-bound ZSM-5. For alumina-bound zeolites, the increase in total acidity does not seem to change with SiO_2/Al_2O_3 ratio of the parent zeolites.

Bronsted acidity is increased only for alumina-bound Y and does not change for alumina-bound ZSM-5, as shown in Fig.5.2.5. The reaction of Al_2O_3 from the binder with SiO_2 in the zeolite at high temperature such as at calcination, which results in new Bronsted acid sites featured by the IR band near 3600 cm^{-1} as shown in Fig. 5.2.2, might

be responsible for the increase in Bronsted acid density. This reaction mechanism was proposed by Shihabi et al. (1985) and Chang et al. (1984). The reason that the alumina-bound Y samples had more enhancement in Bronsted acid sites may be due to more free SiO_2 (non-frame silica) or framework silicon present in Y than in ZSM-5.

Lewis acidity is increased for alumina-bound Y and ZSM-5 zeolites, as shown in Fig.5.2.6. This is easy to understand since the binder alumina has Lewis acidity as shown in Fig. 5.2.8. From Figs. 5.2.4 to 5.3.6, one can attribute the total acidity increase of alumina-bound ZSM-5 mainly to the increase in Lewis acidity and that of alumina-bound Y to the increase in both Lewis and Bronsted acidity.

It should be pointed out that these commercial alumina-bound catalysts had low sodium contents. The alumina-bound ZSM-5 catalysts contained sodium at 0.02~0.05 wt%, and the alumina-bound Y catalysts contained sodium at about 0.04 wt% with an exception of an alumina-bound Y (SiO_2/Al_2O_3=5.2) catalyst which contained sodium at 0.13 wt%.

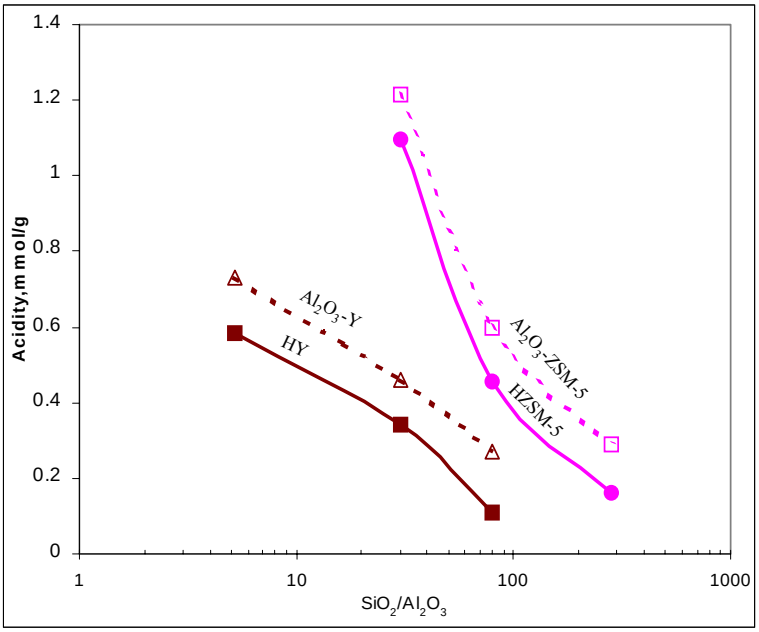

Fig. 5.2.4 Total acidity of commercial alumina-bound zeolites. Alumina binder content: 20 wt%.

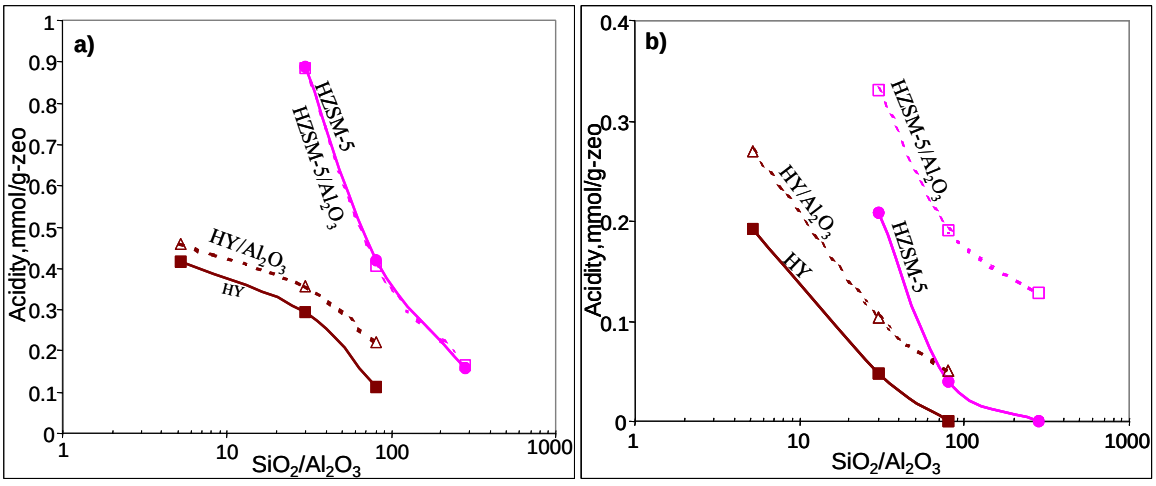

Fig. 5.2.5 Bronsted acidity (a) and Lewis acidity (b) of commercial alumina-bound zeolites (from Wu et al., 2002).

5.2.2 Lab-made Alumina-bound ZSM-5 Catalysts

Using HZSM-5 with SiO_2/Al_2O_3 ratio of 30 and different binding methods as used in binding silica, boehmite and γ-Al_2O_3 (made from calcination of the boehmite) are used as binders. Alumina binder content is 30 wt% in all of the alumina-bound catalysts made in the laboratory. With γ-Al_2O_3, only the powder-wet-mixing method is used; while with boehmite, the powder-wet-mixing and the powder-mixing methods are used. It should be noted that the alumina contains alkaline metals Na and K of 0.104 wt%. These alumina binders are used directly without further proton-exchange to reduce alkaline metal content. With these metals present in the binders, alkaline metal influence on acidity in different binding methods can be studied.

Figs.5.2.6 and 5.2.7 show the IR spectra of bound ZSM-5 catalysts and pyridine adsorption on these catalysts made by different binding methods using γ-Al_2O_3 and boehmite. The intensity of the IR band near 3600 cm^{-1} and IR band near 1542 cm^{-1} is significantly reduced in all of the catalysts compared to the parent ZSM-5. These two bands are related to Bronsted acidity. However, even though the intensity of the band near 1452 cm^{-1} (Lewis acid sites) is also reduced, it is not reduced as much as the band near 1542 cm^{-1}. This means that Bronsted acidity is reduced much more than Lewis acidity. From the results obtained from commercial alumina-bound zeolite catalysts as discussed in the previous section, Lewis acidity should increase and Bronsted acidity should not change much for ZMS-5. However, as just mentioned above, the alumina binder used here contained alkaline metals which neutralized some acid sites. From the

relative intensity of the bands at 1452 cm^{-1} and 1542 cm^{-1} in Fig. 5.2.7, one can conclude that alkaline metal cations mainly neutralize Bronsted acid sites.

It is clearly shown in Figs. 5.2.7 to 5.2.9 that the binding method has little influence on acidity when using alumina as a binder. Moreover, using boehmite or calcined boehmite to bind ZSM-5 does not make any considerable difference in terms of acidity. This implies that alumina phase status has no influence on the acidity of the alumina-bound catalysts. However, the strong acidity of ZSM-5 is significantly reduced in all of the cases due to the presence of alkaline metals in the alumina binder.

In the powder-mixing method, no water solution existed when mixing the binder powder and ZSM-5 powder. This means that no solution ion-exchange should occur. However, the fact of the change of acidity of the catalyst made by the powder-mixing method strongly suggests that the ion-exchange of alkaline metal cations in the alumina binder with protons in ZSM-5 occurred through solid-state ion-exchange.

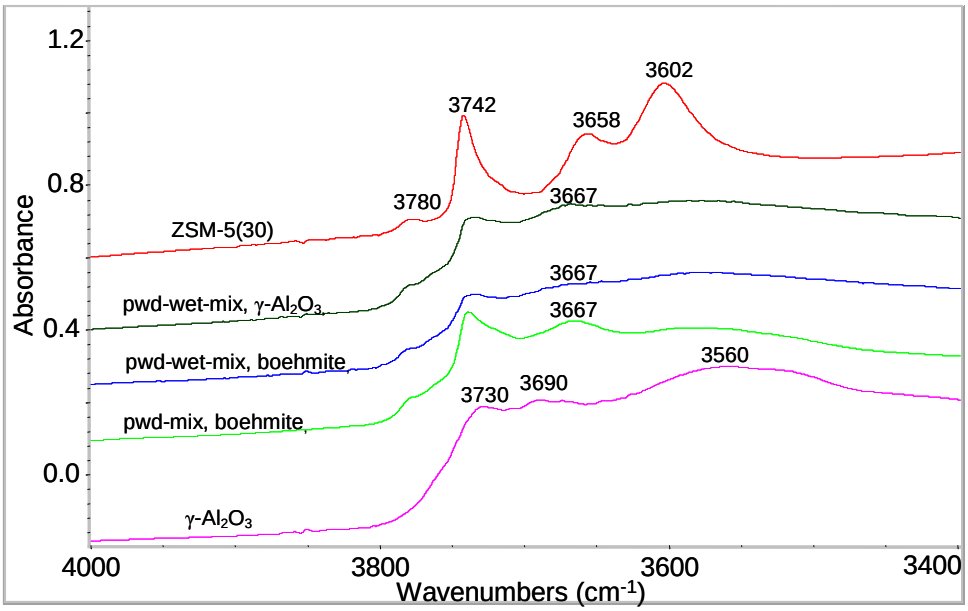

Fig. 5.2.6 IR spectra of Al_2O_3-bound ZSM-5(SiO_2/Al_2O_3=30) catalysts made in laboratory by different binding methods. Al_2O_3 binder: 30 wt%.

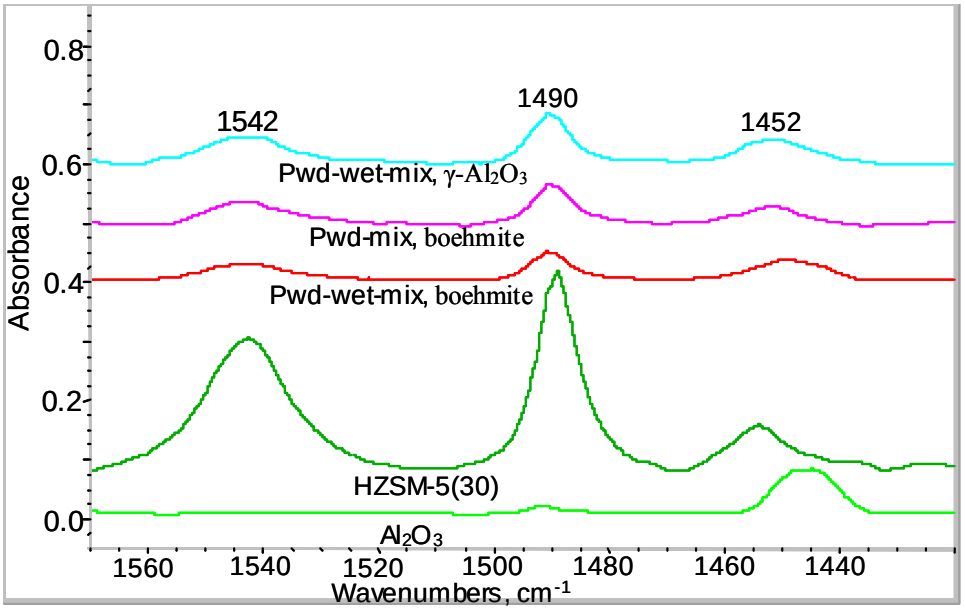

Fig. 5.2.7 IR spectra of pyridine adsorption on Al_2O_3-bound ZSM-5(SiO_2/Al_2O_3=30) catalysts made in laboratory by different binding methods. Al_2O_3 binder: 30 wt%.

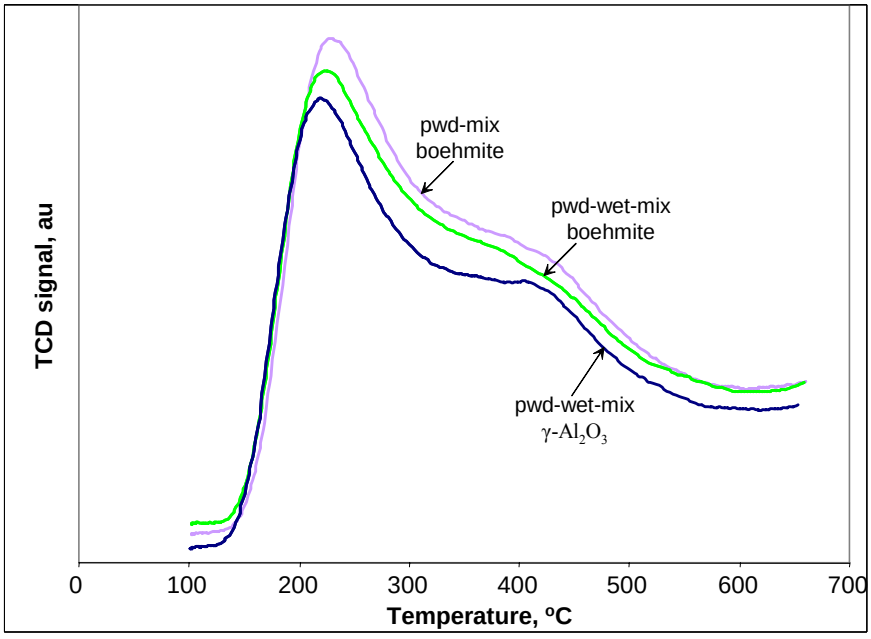

Fig. 5.2.8 Comparison of NH_3-TPD profiles of alumina-bound ZSM-5 (SiO_2/Al_2O_3=30) catalysts made by different methods. Al_2O_3 binder: 30 wt%.

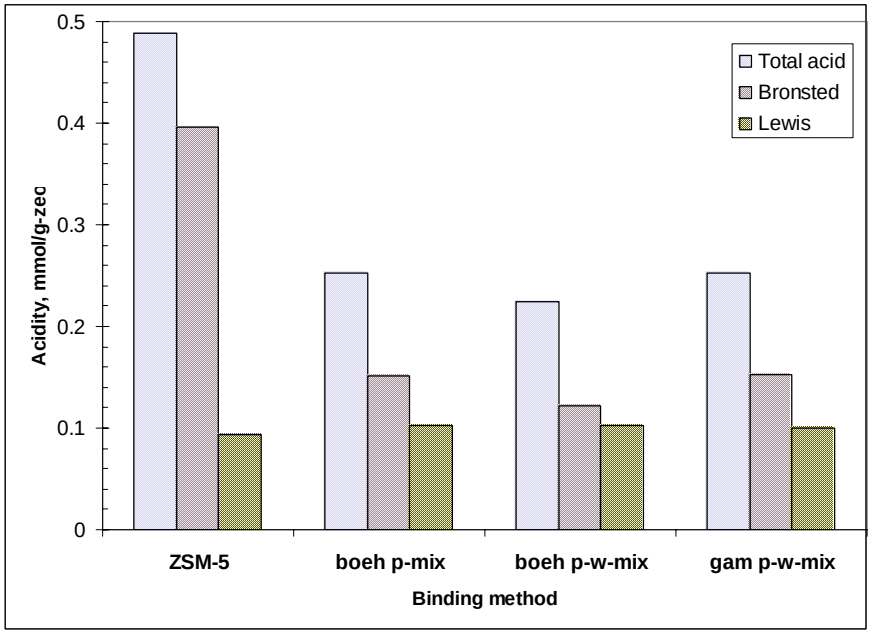

Fig. 5.2.9 Acidity of HZSM-5 and alumina-bound HZSM-5 (SiO_2/Al_2O_3=30) made by different binding methods and alumina sources. Binder content: 30wt%. Total acidity is determined by NH_3-TPD starting from 235°C.

5.3 Comparison between Binding with Silica and Alumina

As discussed in the above section, when using alumina as a binder, binding method and the phase status of alumina have little influence on acidity. This can allow one to compare any of the alumina-bound catalysts made in the laboratory to a silica-bound catalyst. Figs. 5.3.1 and 5.3.2 show the comparison. The alkaline metal content of the alumina binder lies between that of Ludox HS-40 and AS-40. Therefore the acidity, which can be assessed by an NH_3-TPD profile, of an alumina-bound ZSM-5 catalyst should also lie in between the HS-SiO_2-bound ZSM-5 and AS-SiO_2-bound ZSM-5. However, it is not the case. Alumina-bound ZSM-5 catalysts have fewer strong acid sites than either HS-SiO_2-bound ZSM-5 or AS-SiO_2-bound ZSM-5, as shown in Fig. 5.3.2. The significant decrease in strong acidity of alumina-bound ZSM-5 is the evidence that alkaline metal cations remove strong acid sites in ZSM-5. Since both the powder-wet-mixing method, which provides an aqueous solution, and the powder-mixing method, which does not provide an aqueous solution, produce the same acidity of catalysts, solid-state ion-exchange between alkaline metal cations in the alumina binder and protons in ZSM-5 must have occurred during calcination. Compared to silica-bound catalysts, in which the solid-state ion-exchange does not happen to a significant degree, one may conclude that alkaline metal cations have more mobility in alumina than in silica.

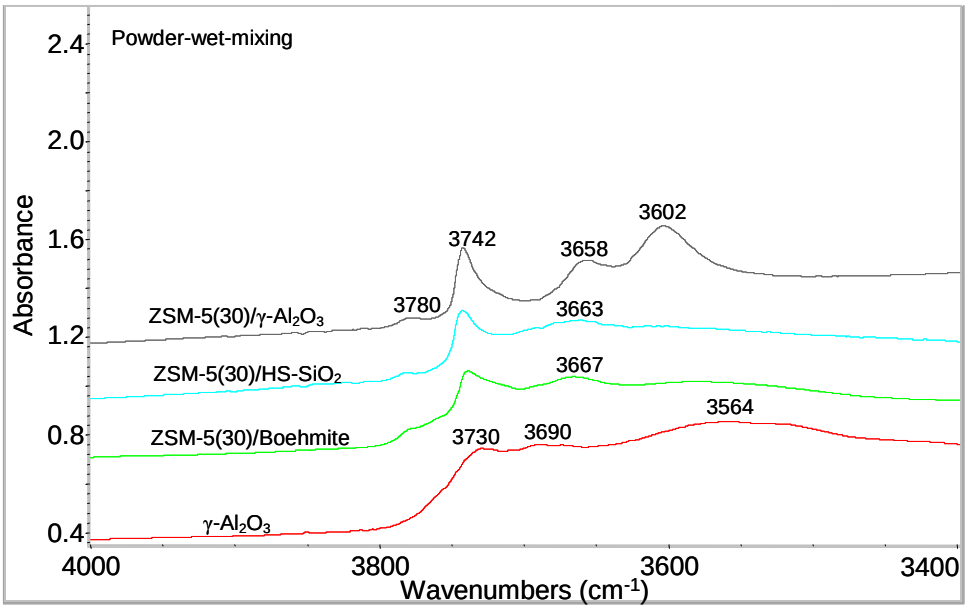

Fig. 5.3.1 Comparison of IR spectra of the bound catalysts for SiO_2 with Al_2O_3 binders made by the powder-wet-mixing method. Binder content: 29~30 wt%.

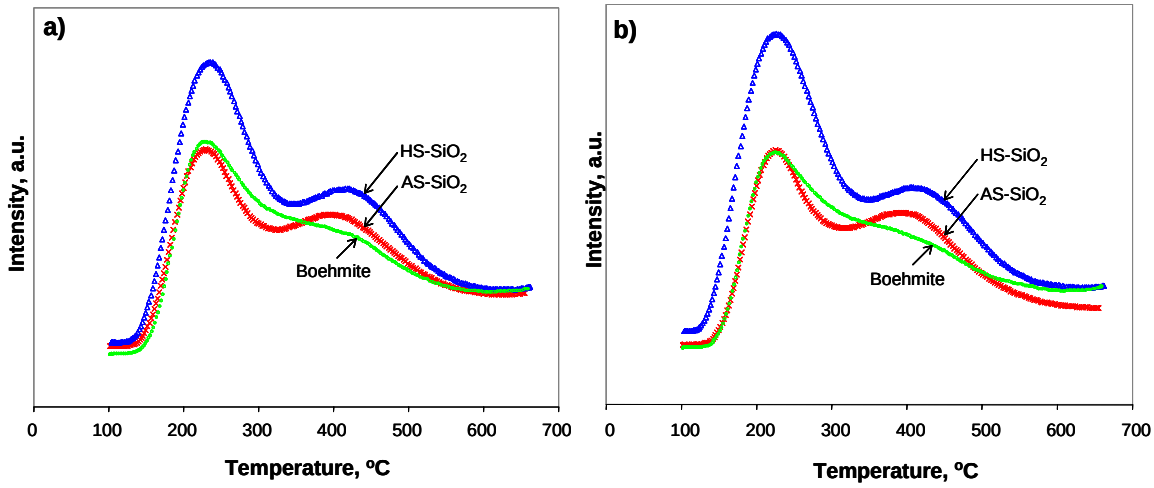

Fig. 5.3.2 Comparison on NH_3-TPD profiles of ZSM-5 (SiO_2/Al_2O_3=30) catalysts bound with silica and alumina by: (a) the powder-mixing method, and (b) the powder-wet-mixing method. Binder content: about 29~30 wt%.

CHAPTER VI

TEXTURE OF BOUND ZEOLITES

In this chapter, textures of zeolites ZSM-5 and Y and their silica-bound and alumina-bound counterparts are reported. To investigate the textures of these catalysts, BET surface area, micropore surface area, mesopore/macropore surface area, micropore volume, and mesopore/macropore volume are analyzed using a Micromeritics BET machine with nitrogen as an adsorbate. The binders used are silica and alumina, respectively. Binding methods are the gel-mixing, powder-wet-mixing, and powder-mixing, which have been described in Chapter III.

6.1 Silica-binder

6.1.1 Micropore Properties

Micropore surface area and pore volume are determined using a t-plot method. Micropore distribution is determined using Horvath-Kawazoe approach with the cylindrical pore model. Pore volume distribution as a function of pore diameter in the mesopore and macropore size range is attained using the BJH (Barrett-Joyner-Halenda) method from the desorption isotherm (Webb, et al, 1997). Fig.6.1.1 shows micropore surface areas of silica-bound ZSM-5 (SiO_2/Al_2O_3=30) catalysts made from Ludox HS-40 and AS-40 using different binding methods. The micropore surface areas of these SiO_2-bound catalysts are less than the predicted value of about 220 m^2/g-cat, which is calculated from the catalyst composition and the micropore surface areas of the binder (the binder in fact has almost no micropore surface area) and the zeolite. Mieville (

1972) has shown that a simply mechanical mixture (without drying and calcination) of a micropore material and a mesopore material has an additive surface area and pore volume, i.e., the pore volume and surface area of the mixture is equal to the weighed summation of the micropore and mesopore materials. The reduced micropore surface area of a silica-bound zeolite catalyst may imply that some changes to the micropores of the zeolite might have occurred during the preparation of the bound catalyst, such as in calcination. However, the micropore surface areas of the SiO_2-bound ZSM-5 catalysts do not seem to change significantly for different SiO_2 sources and binding methods. The micropore surface areas of all of the SiO_2-bound catalysts fall in a range which is about (19 ± 5)% less than the predicted value.

Micropore volumes of these catalysts are shown in Fig. 6.1.2. The predicted micropore volume is about 0.089 cc/g-catalyst. The micropore volume of the SiO_2-bound catalysts is less than the predicted value. As in the case of micropore surface areas, the micropore volumes of the SiO_2-bound ZSM-5 catalysts do not seem to change significantly with different SiO_2 sources and binding methods. The micropore volumes of all of the SiO_2-bound catalysts also fall in a range which is about (18 ± 5)% less than the predicted value.

Micropore blocking by a binder may be well demonstrated by micropore volume distribution. Micropore volume distribution of SiO_2-bound ZSM-5 catalysts made by different binding methods is shown in Fig. 6.1.3. It can be seen from the figure that even though the micropore volume distribution range is the same for all of the SiO_2-bound ZSM-5 catalysts, the gel-mixing method produces the catalysts (either from Ludox HS-

40 or AS-40) with a lower distribution density than the catalysts made by the other two methods, which produce the catalysts with almost the same micropore volume distribution density. This indicates that some micropores of the zeolite are blocked during embedding the zeolite to the silica binder, especially using the gel-mixing methods.

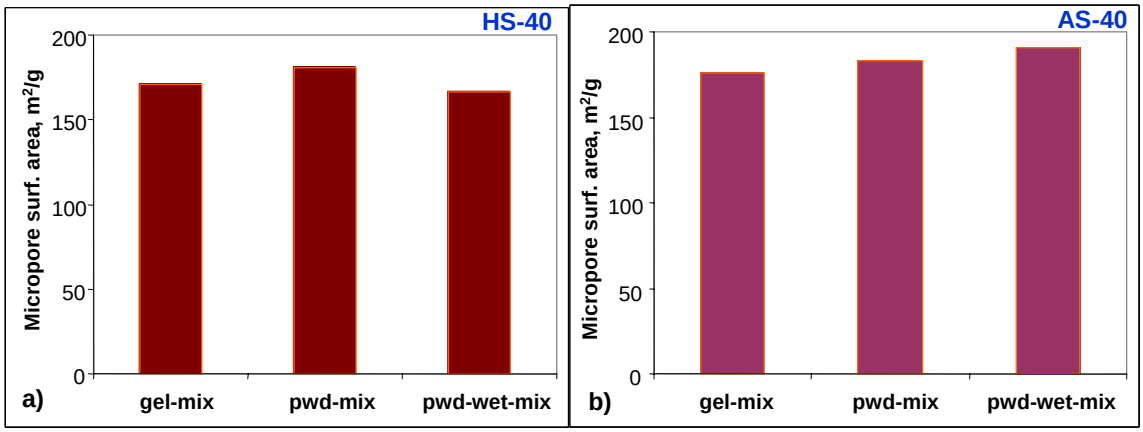

Fig. 6.1.1 Micropore surface area of silica-bound ZSM-5 (SiO_2/Al_2O_3=30). Silica binder: (a) Ludox HS-40 and (b) Ludox AS-40; binding method: gel-mixing, powder-mixing and powder-wet-mixing; binder content: 29wt%.

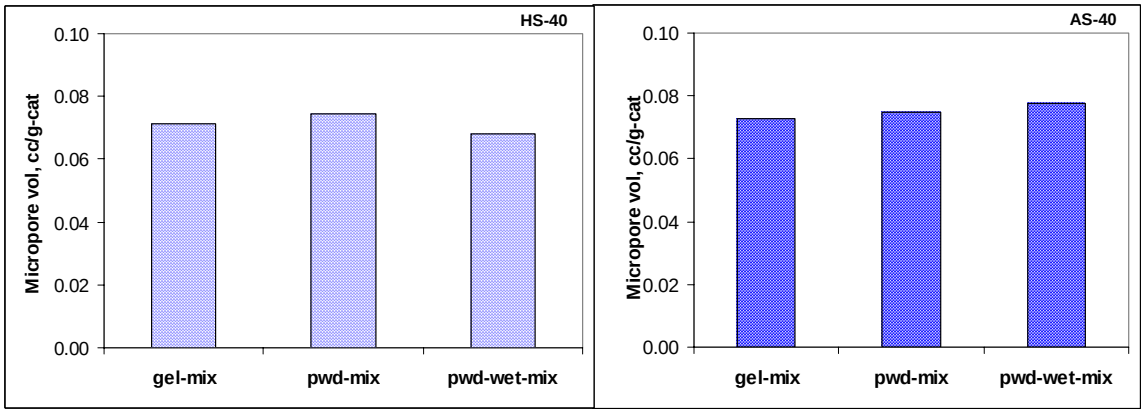

Fig. 6.1.2 Micropore volume of silica-bound ZSM-5 (SiO_2/Al_2O_3=30). Silica binder: (a) Ludox HS-40; (b) Ludox AS-40. Binder content: 29wt%.

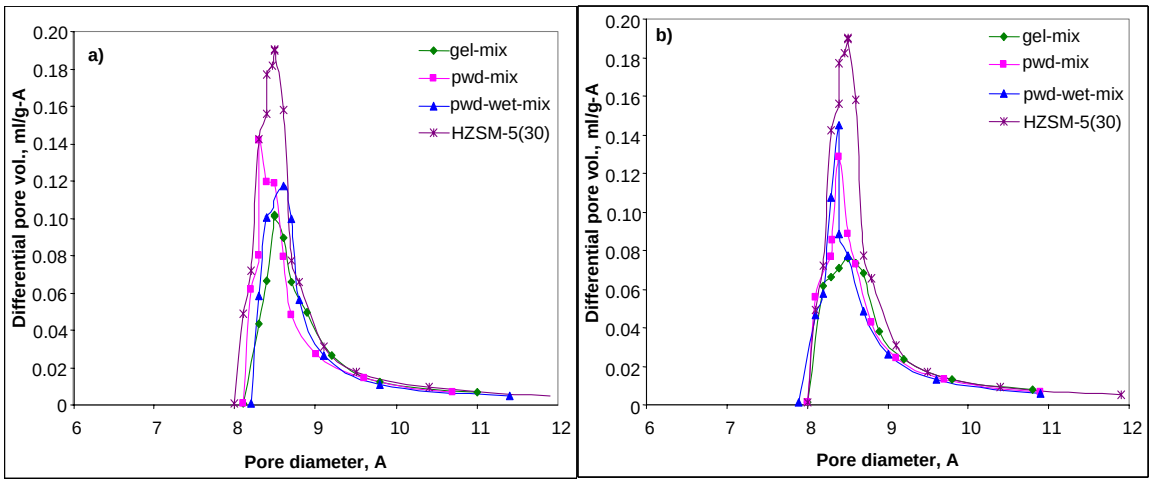

Fig. 6.1.3 Differential micropore volume of ZSM-5(SiO_2/Al_2O_3=30) bound with (a) Ludox HS-40 and (b) Ludox AS-40 by different binding methods. SiO_2 binder: 29 wt%.

From the facts that the micropore surface area and micropore volume are reduced almost by the same degree and the micropore volume distribution is in the same range of pore diameter, it can be concluded that the micropores of ZSM-5 are blocked rather than reduced in pore diameter. Should the micropore diameter of ZSM-5 be reduced, the micropore volume would be reduced to a greater degree than the micropore surface area for the SiO_2-bound ZSM-5 catalysts and the micropore volume distribution of ZSM-5 and the SiO_2-bound ZSM-5 catalysts would be in a smaller micropore diameter range. The experimental results show that the micropore volume distribution of the bound catalysts and ZSM-5 powder fall in the same micropore diameter range and the micropore volume and surface area are reduced to the same degree from the ZSM-5 powder.

The micropore blocking effect is also observed on zeolite Y with different SiO_2/Al_2O_3 ratios. The micropore pore volume and surface area of the bound Y catalysts are less than the predicted values, which would be around 70% of the corresponding value of the zeolite, since binder content is about 70 wt%. Figs. 6.1.4 and 6.1.5 show the micropore volume distribution, micropore volumes, and surface areas of zeolite Y and SiO_2-bound Y with different SiO_2/Al_2O_3 ratios.

One thing needs to be noted regarding Figs.6.1.3 and 6.1.4 that the pore diameters of ZSM-5 and Y are bigger (about 3 Å) than the literature value of about 5.5 Å for ZSM-5 and 6.5 Å for Y (Meier et al.1996). This is because the Horvath-Kawazoe approach with cylindrical geometry has some assumptions that do not match the pore systems of ZSM-5 and Y, for instance, the method assumes that the pore channels are not intersect and the pore channels are perfect cylindrical. However, the pore diameters are close to the literature values if using a slit pore geometry, which is not true in the actual pore system of ZSM-5. Even though the measured pore diameters are larger than the literature values, the discussion here would not be affected since the basis for the discussion is the same.

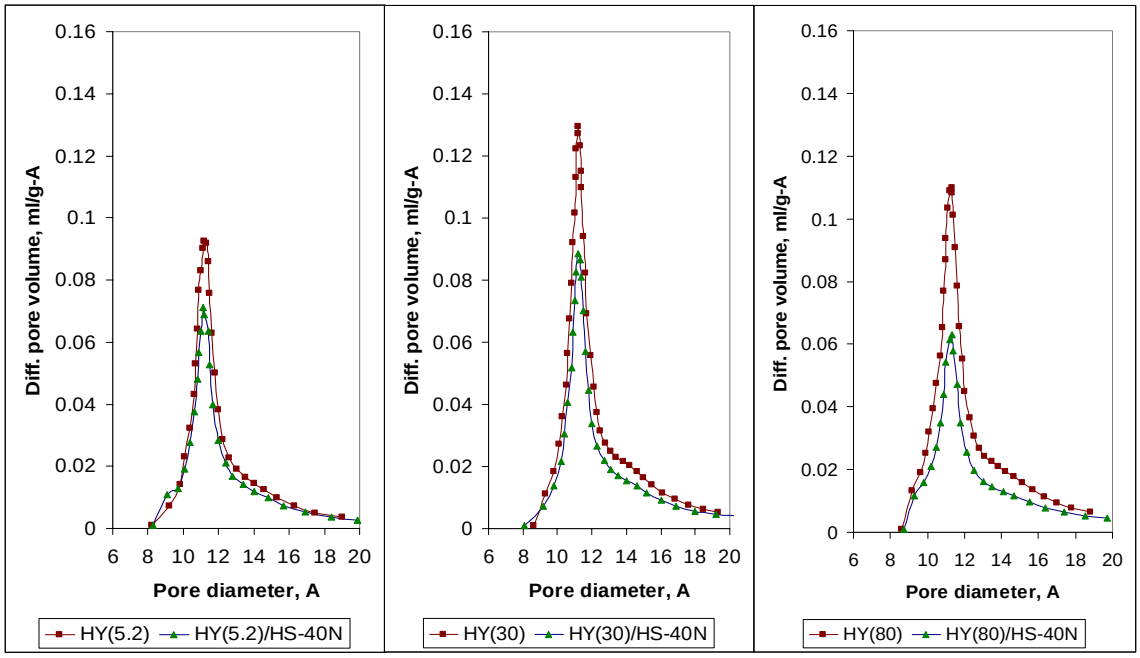

Fig. 6.1.4 Differential pore volume of micropores in zeolite Y and silica-bound Y with different SiO_2/Al_2O_3 ratios. Silica binder: Ludox HS-40; binding method: gel-mixing; binder content: 29wt%.

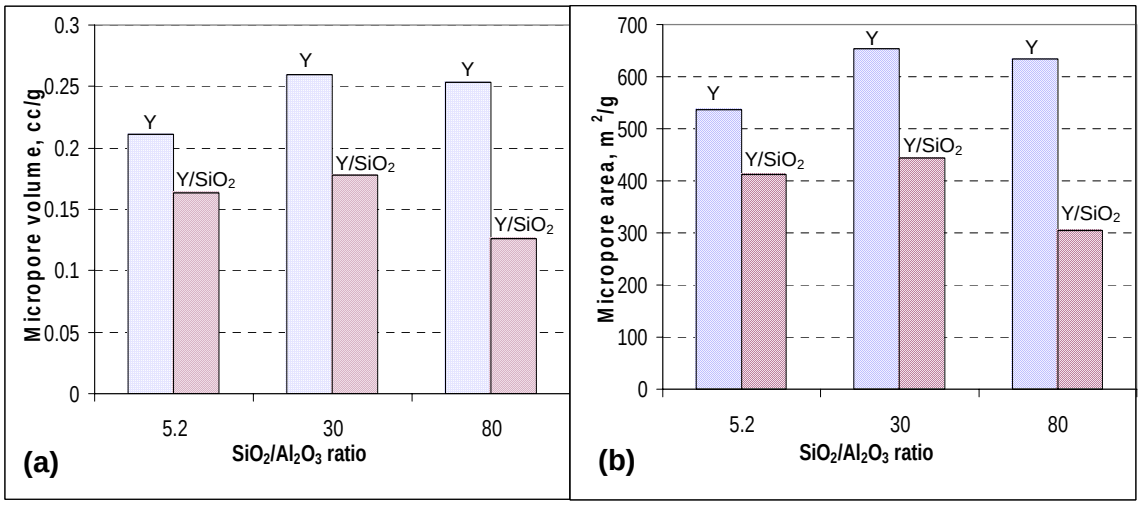

Fig. 6.1.5 (a) Micropore volume and (b) surface area of zeolite Y bound with Ludox HS-40 by the gel-mixing method. Silica binder content: 29 wt%.

6.1.2 Mesopore and Macropore Properties

Meso- and macropore surface areas (or external surface area as called in the t-plot method) were determined by the t-plot method for ZSM-5 bound with Ludox HS-40 and Ludox AS-40 by different binding methods. The results are shown in Fig. 6.1.6. Among the three binding methods, the gel-mixing method always leads to more meso/macropore surface area than the other two methods. Figs. 6.1.7 and 6.1.8 show mesopore pore volume distribution and surface area distribution of ZSM-5 bound with Ludox HS-40 and AS-40 by different binding methods, respectively. The gel-mixing method gives a wider mesopore distribution than the other two methods as well as larger mesopores than those in the binder itself. The gel-mixing method uses a smaller particle of SiO_2 than the other two methods since the SiO_2 particles in the gel are only partially aggregated. While in the other two methods, the SiO_2 particles were obtained by drying and calcining the silica gels (Ludox AS-40 and Ludox HS-40) and larger SiO_2 particles were produced during the drying and calcination processes.

For the zeolite Y, Fig. 6.1.9 shows the comparison of meso/macropore surface area of zeolite with its SiO_2-bound counterparts. The SiO_2-bound Y catalysts are made from Ludox HS-40 by the gel-mixing method.

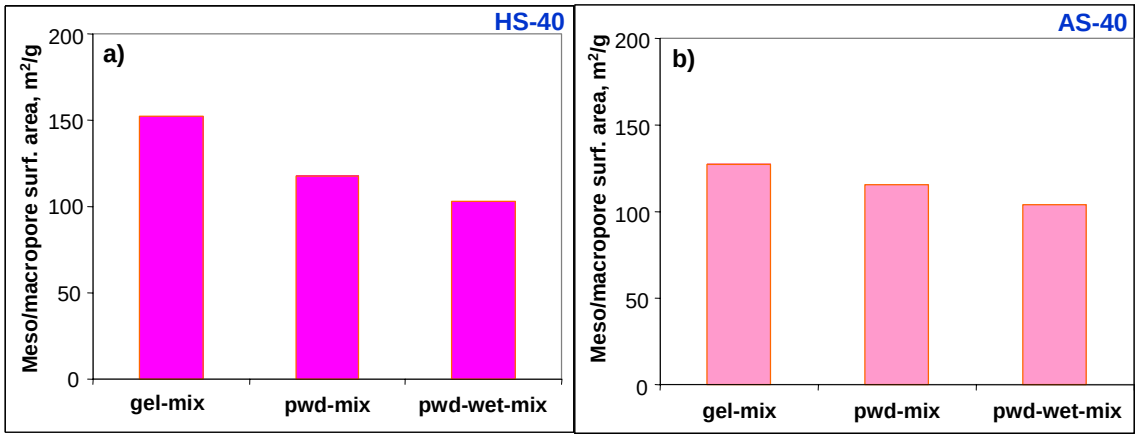

Fig. 6.1.6 Mesopore and macropore surface area of ZSM-5 (SiO_2/Al_2O_3=30) bound with (a) Ludox HS-40 and (b) Ludox AS-40 by different binding methods. Silica binder content: 29 wt%.

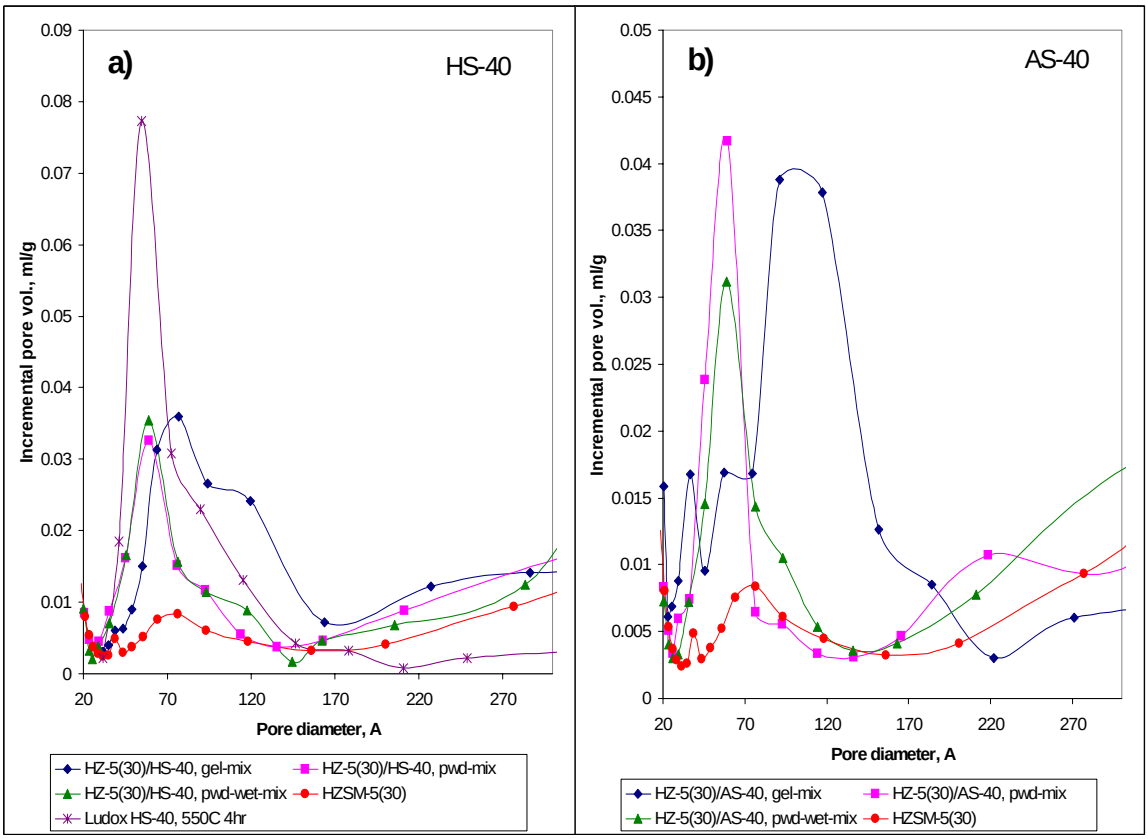

Fig. 6.1.7 Mesopore volume distribution of ZSM-5 bound with (a) Ludox HS-40 and (b) Ludox AS-40 by different binding methods. Silica binder content: 29 wt%.

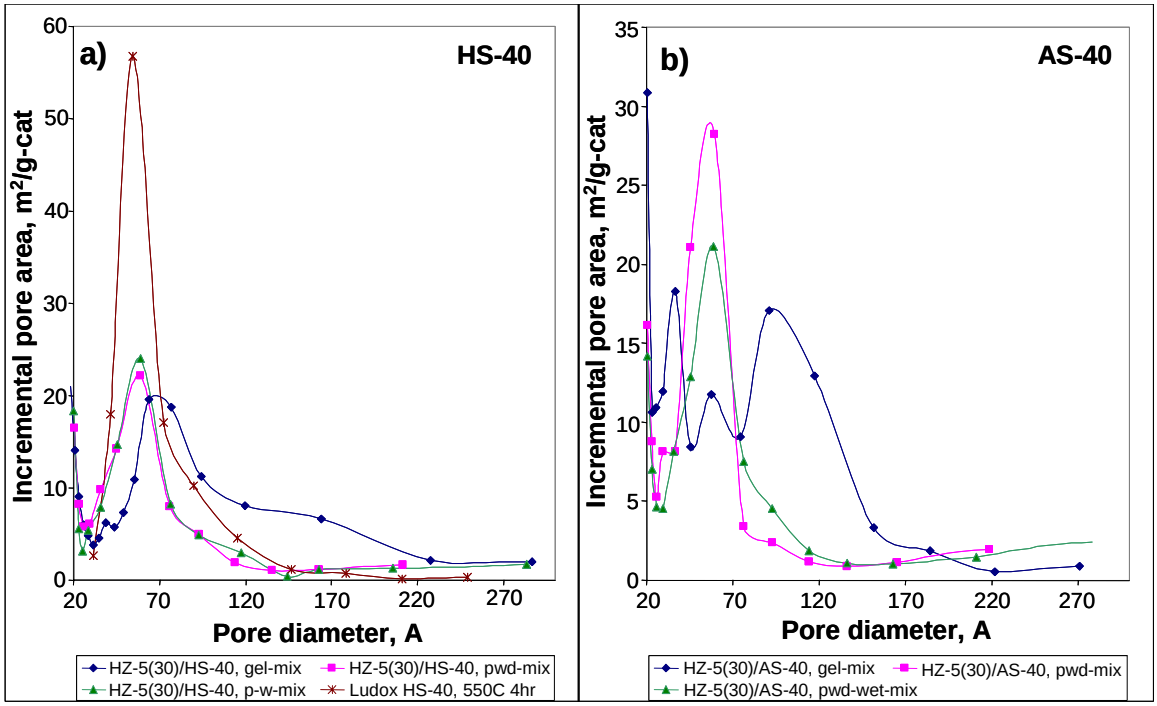

Fig. 6.1.8 Mesopore surface area distribution of ZSM-5 bound with (a) Ludox HS-40 and (b) Ludox AS-40 by different binding methods. Silica binder content: 29 wt%.

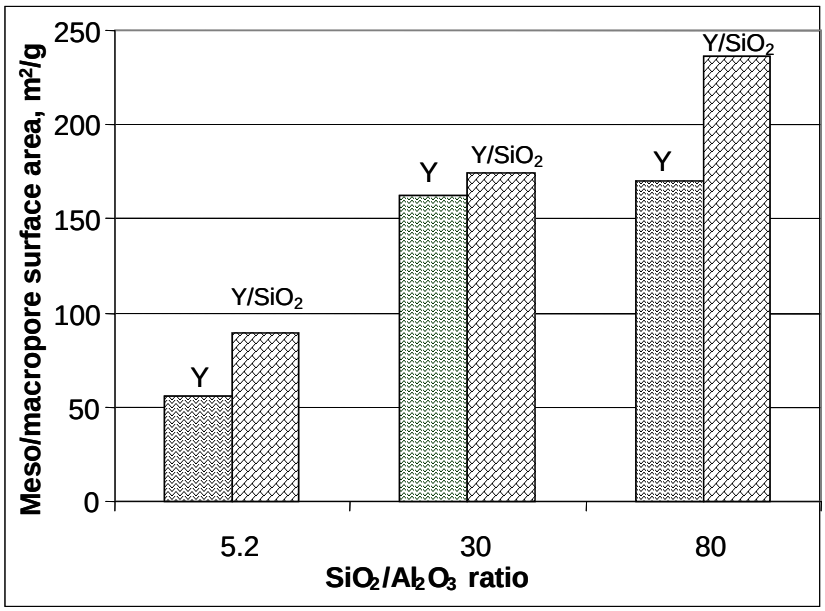

Fig. 6.1.9 Mesopore and macropore surface area of Y with different SiO_2/Al_2O_3 ratios bound with Ludox HS-40 by gel-mixing method. Silica binder content: 29 wt%.

6.2 Alumina Binder

6.2.1 Micropore Properties

When alumina is used as a binder, not much variation is observed in micropore volume and micropore surface area for the different binding methods and different alumina binders, which are either γ-Al_2O_3 or boehmite. Figs. 6.2.1 and 6.2.2 show the micropore volume and surface area of the alumina-bound ZSM-5 and the micropore distribution. The predicted micropore surface area and the micropore volume of these catalysts are about 220 m^2/g-catalyst and 0.089 cc/g-catalyst, respectively. The measured values are less than the predictions, which indicate as in the case of silica binder that some micropores of ZSM-5 are blocked by the binder. The consistence of micropore surface area, micropore volume and micropore volume distribution among different binding methods and different alumina binders indicates that the micropore system of ZSM-5 is blocked to the same degree by the powder-mixing and powder-wet-mixing methods. This would further indicate that the contact situation between alumina particles and zeolite crystals is the same in both of the binding cases. The micropore surface area and micropore volume of all of the alumina-bound ZSM-5 catalysts are (26 ± 1)% and (23 ± 1)% less than the predicted values, respectively.

Fig. 6.2.2 clearly shows that the micropore volume distribution is the same for all of the alumina-bound ZSM-5 catalysts, and is in the same range of micropore diameter as in the ZSM-5 powder, indicating that the micropore diameter of the bound ZSM-5 is the same as that of the ZSM-5 powder.

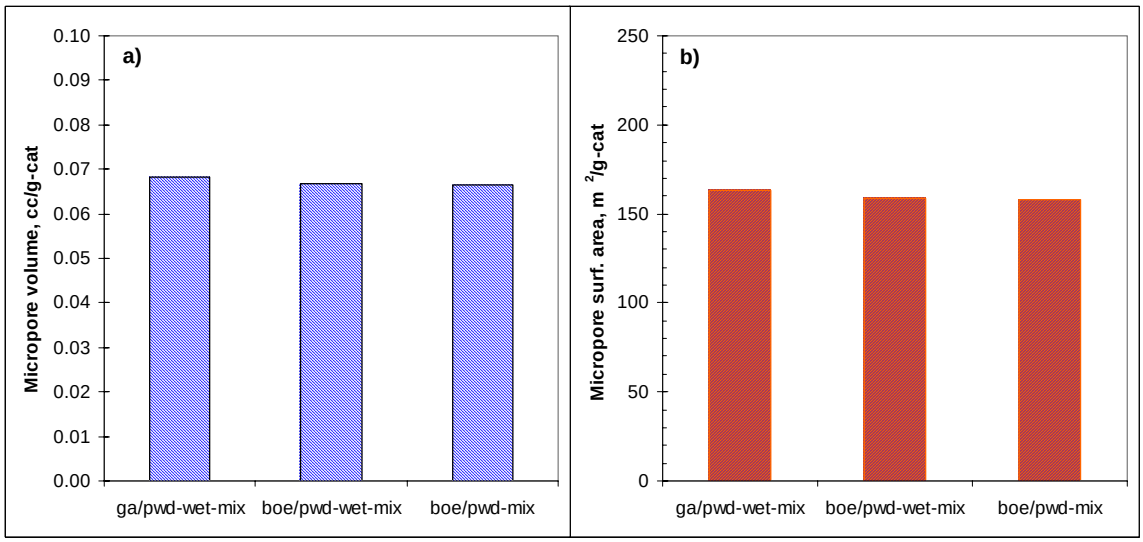

Fig. 6.2.1 Micropore volume (a) and micropore surface area (b) of Al_2O_3-bound ZSM-5. Legend: "ga" and "boe" denote "gamma" and "boehmite", respectively.

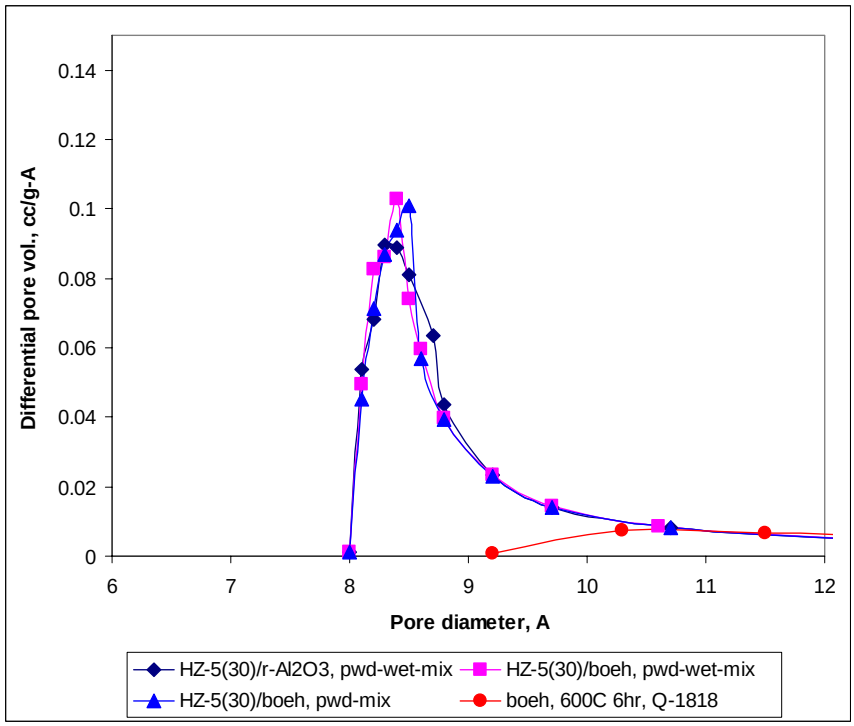

Fig. 6.2.2 Micropore volume distribution of Al_2O_3-bound ZSM-5. Legend: "boeh" denotes boehmite.

6.1.2 Mesopore and Macropore Properties

Figs. 6.2.3 and 6.2.4 show mesopore volume distribution and meso/macropore volume and surface area of the alumina-bound ZSM-5 catalysts. The mesopore volume distribution range is the same as the binder. However, the meso/macropore volumes and surface areas are larger than the predicted values of 0.261 cc/g-catalyst and 135 m^2/g-catalyst, respectively, indicating that larger void spaces are created on binding.

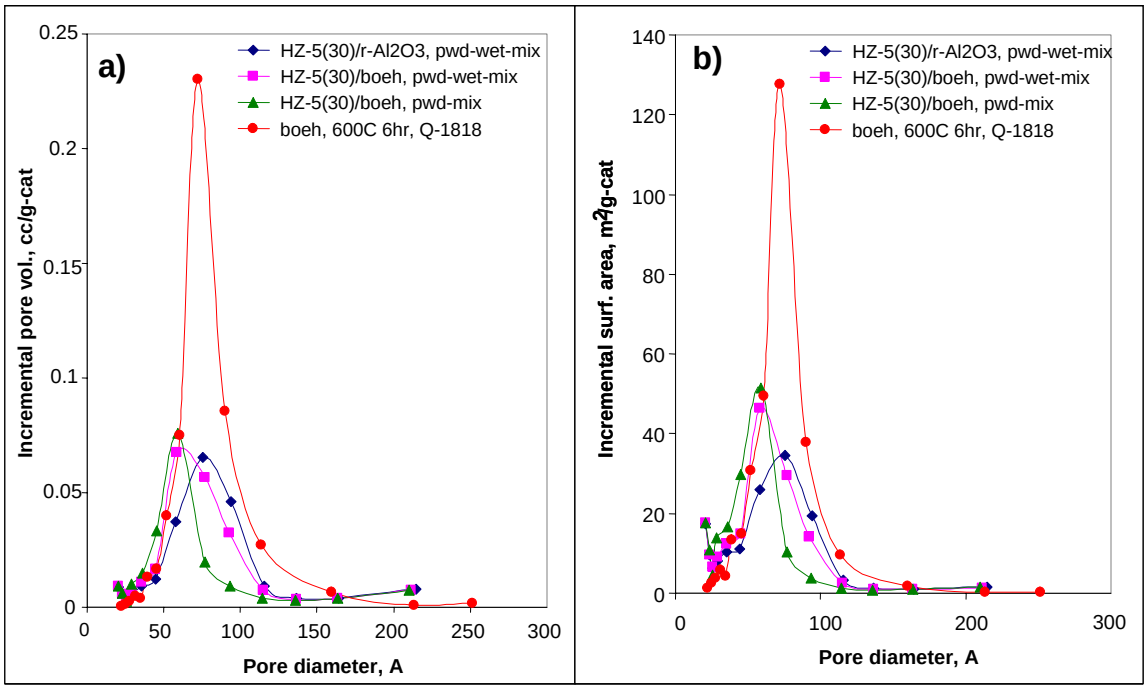

Fig. 6.2.3 Mesopore pore volume (a) and mesopore surface area (b) distribution of Al_2O_3-bound ZSM-5. Legend: "boeh" denotes boehmite.

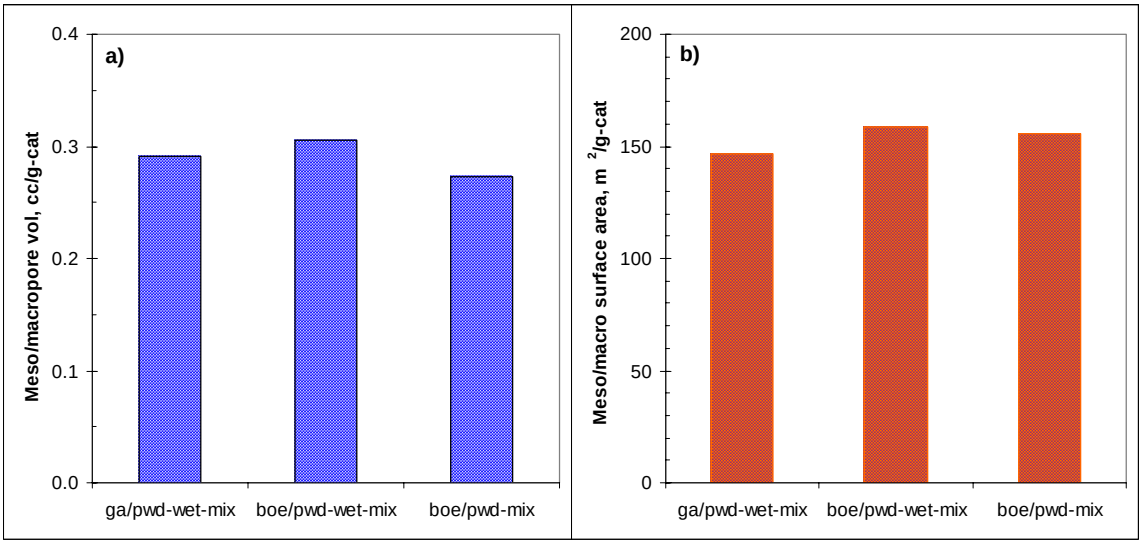

Fig. 6.2.4 (a) Meso/macropore volume and (b) surface area of Al_2O_3-bound ZSM-5. Legend: "ga" and "boe" denote "gamma" and "boehmite", respectively.

CHAPTER VII

BUTANE TRANSFORMATION

In this chapter, the catalytic activities of silica-bound and alumina-bound ZSM-5 (SiO_2/Al_2O_3=30) are investigated with butane transformation. In order to make a comparison, butane transformation on unbound ZSM-5 was also conducted. The procedure and apparatus used for conducting the reaction and product analysis were described in Chapter IV. Note that methane was used as a tie component in the GC calculation. The binders used were silica and alumina, respectively. Binding methods were the gel-mixing, powder-wet-mixing, and powder-mixing, which were described in Chapter III. The acidity and texture of these catalysts were reported in Chapters V and VI, respectively.

7.1 Chemistry

The primary reactions in butane conversion may involve cracking of butane into propylene and methane or ethylene and ethane, disproportionation of butane into pentane and propane, and isomerization of n-butane into iso-butane. Butane disproportionation is more dependent on strong acid site density of a catalyst than butane cracking (mono-molecular reaction) since two adjacent acidic sites are needed to start disproportionation (bi-molecular reaction) (Guisnet and Gnep, 1996). Ethylene, propylene, propane and pentanes formed from the primary reactions may undergo further reactions. The secondary reactions may involve oligomerization, isomerization, cracking, hydrogen

transfer, dehydrocyclization, aromatization, and coking (which leads to catalyst deactivation), etc. At low conversions, the primary reactions will be predominant.

Primary reactions:

$n\text{-}C_4H_{10} \rightarrow C_3H_6+CH_4$	(cracking)	(7-1)
$n\text{-}C_4H_{10} \rightarrow C_2H_4+C_2H_6$	(cracking)	(7-2)
$2\ n\text{-}C_4H_{10} \rightarrow C_5H_{12}+C_3H_8$	(disproportionation)	(7-3)
$n\text{-}C_4H_{10} \rightarrow i\text{-}C_4H_{10}$	(isomerization)	(7-4)

Secondary reactions:

$i\text{-}C_5H_{12} \rightarrow C_3H_8+C_2H_4$	(cracking)	(7-5)
$C_3H_8 \rightarrow C_2H_4+CH_4$	(cracking)	(7-6)
$2C_2H_4 \rightarrow n\text{-}C_4H_8$	(oligomerization)	(7-7)
$C_2H_4+C_3H_6 \rightarrow i\text{-}C_5H_{10}$	(oligomerization)	(7-8)
$i\text{-}C_4H_8 + i\text{-}C_5H_{12} \rightarrow i\text{-}C_4H_{10}+i\text{-}C_5H_{10}$	(hydrogen transfer)	(7-9)
$n\text{-}C_4H_8 \rightarrow i\text{-}C_4H_8$	(isomerization)	(7-10)
$C_6H_{12} \rightarrow C_2H_4+C_4H_8$	(cracking)	(7-11)
Olefins $\rightarrow$ Aromatics + H_2	(dehydrocyclization)	(7-12)

Table 7.1.1 lists some of the reactions and their standard heats of reaction and standard free energies. In the temperature range, except for cracking reactions (Reactions 7-1, 7-2, 7-5, 7-6, 7-11) that are very endothermic, the other reactions are exothermic or

have small heats of reaction. Oligomerizations (Reactions 7-7 and 7-8) have large exothermic heats of reaction.

The effect of temperature on the equilibria of the reactions is different. For cracking reactions, a high temperature is favored; while for oligomerization, a low temperature is favored. For hydrogen transfer reactions and isomerization reactions, the effect of temperature on reaction equilibrium is not as significant as on the other reactions.

Table 7.1.1 Reactions and thermodynamics of butane transformation (ideal-gas reaction).

Primary reactions	ΔH_R^o, Kcal/mol				ΔG_R^o, Kcal/mol			
	500K	600K	700K	800K	500K	600K	700K	800K
$n\text{-}C_4H_{10} \rightarrow C_3H_6+CH_4$	17.01	16.81	16.59	16.36	0.05	-3.32	-6.65	-9.95
$n\text{-}C_4H_{10} \rightarrow C_2H_4+C_2H_6$	22.21	22.04	21.84	21.64	5.86	2.61	-0.61	-3.81
$2n\text{-}C_4H_{10} \rightarrow i\text{-}C_5H_{12}+C_3H_8$	-1.47	-1.47	-1.46	-1.42	-0.62	-0.43	-0.27	-0.10
$n\text{-}C_4H_{10} \rightarrow i\text{-}C_4H_{10}$	-1.97	-1.94	-1.92	-1.89	-0.16	0.21	0.56	0.92
Secondary reactions								
$i\text{-}C_5H_{12} \rightarrow C_3H_8+C_2H_4$	24.39	24.21	24.01	23.79	7.23	3.81	0.43	-2.93
$C_3H_8 \rightarrow C_2H_4+CH_4$	19.46	19.36	19.23	19.06	3.17	-0.09	-3.31	-6.52
$2C_2H_4 \rightarrow n\text{-}C_4H_8$	-44.28	-44.81	-45.21	-45.5	-16.96	-11.44	-5.84	-0.2
$C_2H_4+C_3H_6 \rightarrow i\text{-}C_5H_{10}$	-25.82	-25.64	-25.44	-25.23	-8.56	-5.13	-1.73	1.64
$i\text{-}C_4H_8+i\text{-}C_5H_{12} \rightarrow i\text{-}C_4H_{10}+i\text{-}C_5H_{10}$	0.11	0.12	0.13	0.14	0.50	0.57	0.65	0.72
$n\text{-}C_4H_8 \rightarrow i\text{-}C_4H_8$	-3.9	-3.87	-3.86	-3.86	-2.61	-2.36	-2.11	-1.85
$3C_2H_4 \rightarrow C_6H_6 + 3H_2$	-15.88	-15.09	-14.41	-13.8	-18.51	-19.1	-19.83	-20.63
$2C_3H_6 \rightarrow C_6H_6 + 3H_2$	11.94	12.75	13.42	13.97	-5.66	-9.26	-12.99	-16.8

7.2 On HS-SiO_2-bound ZSM-5 Catalysts

Butane transformation was evaluated on HZSM-5 and its HS-SiO_2-bound ZSM-5 made by different binding methods at a total reaction pressure of 1 atm, Ar/C_4H_{10} molar ratio of 5.4, and C_4-$WHSV_{zeo}$ of 1.5 h^{-1} (the weight hourly space velocity is based on the mass of butane fed and the mass of zeolite in the reactor). Butane conversions at different temperatures over these catalysts are shown in Fig. 7.2.1. The activity of HZSM-5 is significantly reduced when HZSM-5 is bound with SiO_2. However, the degree of decrease in activity of the catalysts depends on the binding methods used in the catalyst preparation. The powder-mixing and powder-wet-mixing methods produce catalysts with much higher activities than the gel-mixing method; while the powder-mixing and powder-wet-mixing methods produce the catalysts with similar activities with the former a slightly higher activity. The activity changes over these catalysts correspond to the acidity changes on these catalysts as discussed in Chapter V. The strong acidity and the Bronsted acidity of HS-SiO_2-bound ZSM-5 decrease, and the gel-mixing method produces the lowest acidities of strong acid and Bronsted acid.

Table 7.2.1 lists the apparent activation energy of butane conversion over these catalysts assuming the apparent kinetics is a first-order reaction. The activation energy of HZSM-5 is increased by about 30~45% by the powder-mixing and powder-wet-mixing methods or increased by 13l% by the gel-mixing method, after SiO_2 (Ludox HS-40) is bound with the HZSM-5 powder with binder content of 29wt%.

The change of activity of these catalysts can be attributed to the different physio-chemical properties of these catalysts that vary in two factors. One is the difference in

acidity and the other is in textural difference. As discussed in Chapter 6, the SiO_2-bound ZSM-5 catalysts have much less acidity than HZSM-5 and about 19% less surface area than the predicted value, which indicates some micropores of ZSM-5 are blocked.

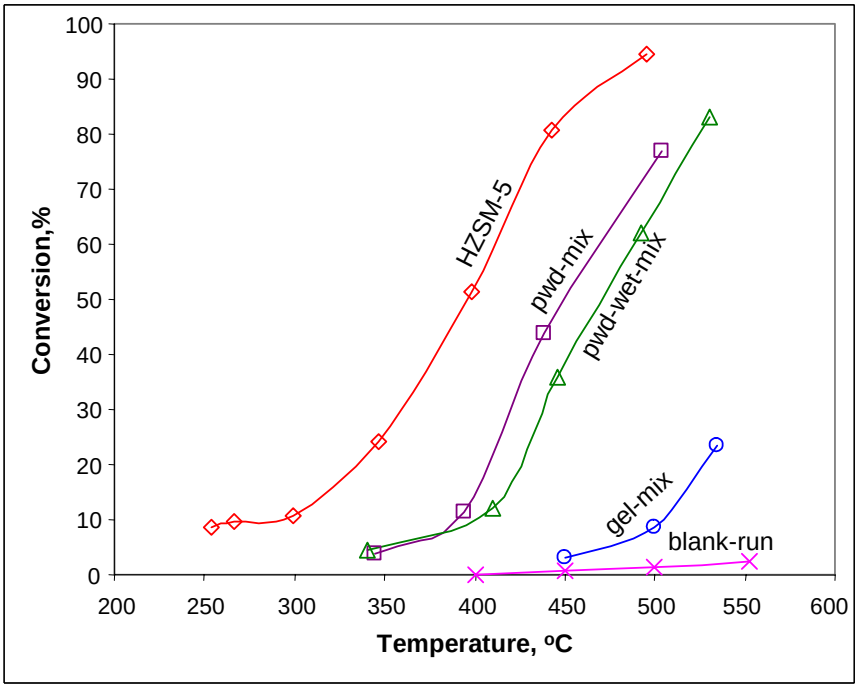

Fig. 7.2.1 Butane conversion over unbound and bound HZSM-5 (SiO_2/Al_2O_3=30) made from Ludox HS-40 by different binding methods. Binder content: 29 wt%; total reaction pressure: 1 atm; Ar/C_4H_{10} molar ratio=5.4; C_4-$WHSV_{zeo}$=1.5 h^{-1}.

Table 7.2.1 Apparent activation energy of butane cracking (first-order reaction) on SiO_2-bound ZSM-5 (SiO_2/Al_2O_3=30). Binder content: 29 wt%. Silica binder source: Ludox HS-40.

Catalyst	HZSM-5	ZSM-5/SiO_2	ZSM-5/SiO_2	ZSM-5/SiO_2
Binding method	No binder	Powder-mix	Pwd-wet-mix	Gel-mix
E, KJ/mol*	67.2±4.4	99±22	87±10	156±16

* With 90% confidence.

Table 7.2.2 lists a typical product distribution over these catalysts at about 445^{o}C. Aromatic hydrocarbons are not formed on the catalyst made by the gel-mixing method; however, they are generated on the other catalysts. Aromatic hydrocarbons are formed through tertiary reactions of secondary olefinic products through reactions such as dehydrocyclization and hydrogen transfer reactions. These reactions take place on strong acid sites. The gel-mixing method produces the least number of strong acid sites among the three binding methods. Therefore, no aromatic hydrocarbons are formed on the catalyst made by the gel-mixing method. From this table, one may conclude that isomerization of n-butane occurs to a small extend, since iso-butane is a small percentage in the products. Therefore, the major primary reactions for butane transformation over these catalysts are cracking and disproportionation.

Table 7.2.2 Product distribution of butane conversion over HZSM-5 and SiO_2-bound ZSM-5 made by different binding methods, mol%. Reaction temperature 445^{o}C; TOS=120 min; Ar/C_4H_{10} molar ratio=5.4; and C_4-$WHSV_{zeo}$=1.5 h^{-1}; silica source: Ludox HS-40.

Component	HZSM-5	pwd-mix	pwd-wet-mix	gel-mix
hydrogen	12.00	13.63	1.13	0
methane	9.20	9.71	10.20	19.76
ethane	10.46	11.57	13.22	22.91
ethylene	4.54	9.50	11.81	20.96
propane	50.07	38.08	43.25	3.69
propylene	3.34	6.70	8.66	14.94
isobutane	3.86	3.46	4.23	6.58
butenes	1.20	2.68	3.66	11.16
C_5	0.68	1.07	1.43	0.00
C_6	0.00	0.00	0.00	0.00
aromatics	4.66	3.60	2.42	0.00
Conversion, %	78.75	43.04	34.38	3.03

It should be noted that C_5 and C_6 hydrocarbons in the products are primarily aliphatic isomers. If there were no further cracking of pentanes, the amount of propane and the amount of pentanes in the products would have been in equimolar composition, which is the result of disproportionation. Table 7.2.2 illustrates that propane concentration is always higher than pentane concentration, indicating cracking of pentanes occurs to a significant extent.

Since methane and ethane are produced primarily from cracking reactions, and propane is produced primarily from disproportionation reaction, the ratio of methane plus ethane to propane can be used as a measure to check the competition between cracking and disproportionation. Table 7.2.3 shows the ratio over these different catalysts. As can be seen the ratio is much higher on the catalyst made by the gel-mixing method. The higher ratio indicates that the cracking reactions are more than the disproportionation reactions. Guisnet and Gnep (1996) proposed that disproportionation depends on the strong acid site density since it involves two acid sites catalysis. The catalyst made by the gel-mixing method has fewer strong acid sites than the catalysts made by the other two methods, as shown in Chapter V; therefore, fewer disproportionation reactions occur than cracking reactions, as indicated by the higher ratio. On the other hand, HZSM-5 has a higher strong acid site density and thus should have more disproportionation reactions, and consequently a lower ratio. However, the extent of cracking and disproportionation on HZSM-5 is, of course, larger than on the other catalysts since the strong acidity of HZSM-5 is much higher.

The catalyst deactivation rate is almost the same for all of the catalysts. No significant loss of activity is found on these catalysts over the time range tested. The conversion change with time on stream is shown in Fig. 7.2.2.

Table 7.2.3 $(C_1+C_2^0)/C_3^0$ molar ratio over HS-SiO_2-bound ZSM-5. Reaction temperature=445°C; total pressure=1 atm; Ar/C_4H_{10} molar ratio=5.4.

TOS, min	10	60	120	180	240	300
HZSM-5	0.38	0.39	0.39	0.39	0.39	0.39
pwd-mix	0.53	0.56	0.53	0.54	0.54	0.53
pwd-wet-mix	--	0.48	0.45	0.54	0.49	--
gel-mix	10.7	10.0	11.6	16.5	23.8	19.6

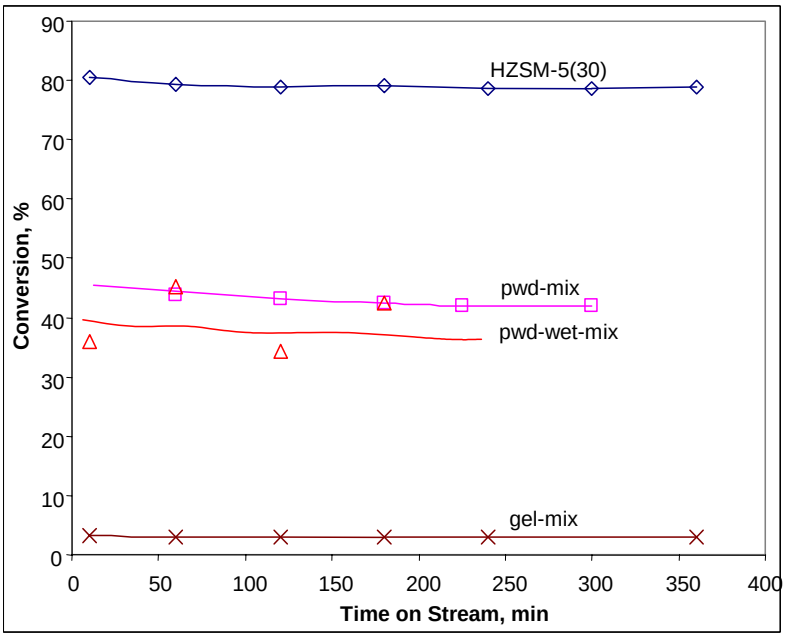

Fig.7.2.2 Conversion change with time on stream over different HZSM-5 catalysts for butane transformation. T=445°C; total pressure=1 atm; Ar/C_4H_{10} molar ratio=5.4; and C_4-$WHSV_{zeo}$=1.5 h^{-1}; silica source: Ludox HS-40. Binding methods are indicated by the legends.

7.3 On Al_2O_3-bound ZSM-5 Catalysts

The butane conversion over HZSM-5 and alumina-bound HZSM-5 (SiO_2/Al_2O_3=30) is shown in Fig. 7.3.1. As in the case of SiO_2-bound ZSM-5 catalysts, the decreased activity of the alumina-bound catalysts is mainly due to the lower acidity of these catalysts. The catalyst made from boehmite by the powder-wet-mixing method has the lowest strong and Bronsted acidities, as discussed in Chapter V, and therefore has the lowest activity among these catalysts.

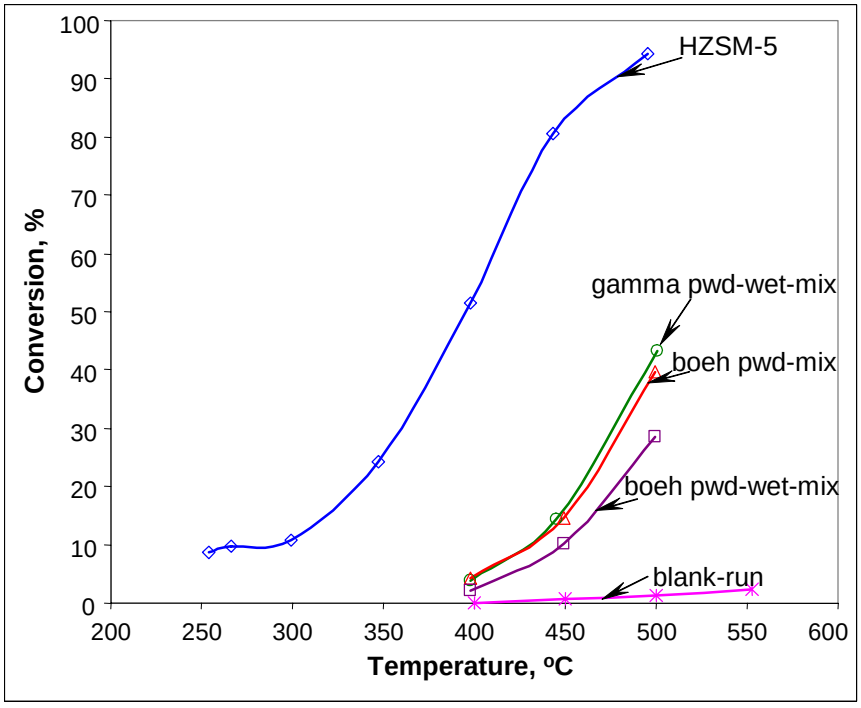

Fig. 7.3.1 Butane conversion on different HZSM-5 (SiO_2/Al_2O_3=30) catalyst. Alumina binder: 30wt% and sources: boehmite and γ-Al_2O_3; total pressure=1 atm; Ar/C_4H_{10} molar ratio=5.4; and C_4-$WHSV_{zeo}$=1.5 h^{-1}.

Comparing Fig. 7.3.1 with Fig.7.2.1, one can see that alumina-bound catalysts have less conversion than SiO_2-bound catalysts (except for the gel-mixing method). The acidities of both alumina-bound catalysts and SiO_2-bound catalysts have been discussed in Chapter V. For example, by the powder-mixing method, HS-SiO_2-bound ZSM-5 catalyst has a lower total strong and Lewis acidities but higher Bronsted acidity than alumina-bound ZSM-5, as indicated in Table 7.3.1. The former catalyst shows a higher butane conversion than the later catalyst at the same temperature. This indicates that butane transformation takes place on Bronsted acid sites.

Another factor that may also play a role in the decrease of activity of the alumina-bound catalysts is the micropore blockage by the binder. As discussed in Chapter VI, the alumina-bound ZSM-5 reduces micropore surface area of ZSM-5 by about 26%; while SiO_2-bound ZSM-5 reduces the micropore surface area by 19%.

The alumina-bound catalysts remain activity during the time period tested (normally a test ran about 5 hours), as indicated by the constant conversion of butane over the time period investigated.

Table 7.3.1 Comparison of acidity of SiO_2-bound and alumina-bound ZSM-5 catalysts made by the powder-mixing method.

Catalyst	Total strong acidity mmol/g-zeo	Bronsted acidity mmol/g-zeo	Lewis acidity mmol/g-zeo
HS-SiO_2-HZSM-5	0.229	0.203	0.024
Boehmite-HZSM-5	0.253	0.151	0.102
HZSM-5 (powder)	0.489	0.396	0.093

Again, a higher ratio of $(C_1+C_2^0)/C_3^0$ is found on an alumina-bound catalyst which has lower acid densities of both total strong acid and Bronsted acid, indicating a greater extent of cracking than disproportionation on the catalyst. Fig. 7.3.2 shows the ratio over the alumina-bound catalysts.

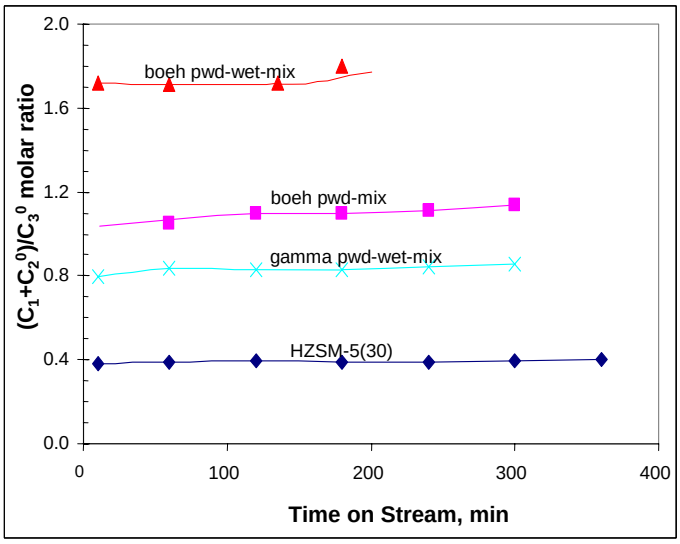

Fig. 7.3.2 Competition of cracking with disproportionation over different catalysts. T=445°C; total pressure=1 atm; Ar/C_4H_{10} molar ratio=5.4; and C_4-$WHSV_{zeo}$=1.5 h^{-1}.

7.4 Butane Conversion and Acidity of Catalysts

In NH_3-TPD experiments, the total acidity can be obtained by integrating the area under the curve of an NH_3-TPD profile. However, if the weak acid and strong acid (or the low temperature peak and the high temperature peak) are not well distinguished, as shown in Fig.7.4.1 for some zeolites, some mathematical methods have to be taken to deconvolute the curve into separate peaks. However, there are different criteria that have

been used for the deconvolution. Some used a symmetrical peak method (Lonyi and Valyon, 2001; Katada et al, 1997), some used an energy set method (Costa, et al., 1999), and others used a criterion that fits the profiles while the maxima and widths of the peaks are held constant (Romero et al., 1999). Apparently from Fig.7.4.1, these criteria do not give the same area (or acidity) after deconvolution. Therefore, some NH_3-TPD experiments in this work were performed by ramping from a higher temperature at about 235^oC. In this case, the deconvolution problem can be skipped and only strong acid sites are measured.

Butane conversion on different catalysts bound with silica and alumina is summarized in Table 7.4.1. In this table, the 105^oC Bronsted acidity and 105^oC Lewis acidity are determined from NH_3-TPD experiments ramping from 105^oC, and the 235^oC Bronsted acidity and 235^oC Lewis acidity are determined from NH_3-TPD experiments ramping from 235^oC. The calculation method for acidities has been described in Chapter III. Among these acidities, only strong (235^oC) Bronsted acid site density is found closely related to butane conversion, as shown in Fig.7.4.2, indicating only strong Bronsted acid is responsible for activating butane molecules.

Since strong Bronsted acid is the one to catalyze butane conversion, therefore, it is natural to expect that the strong Bronsted acid site density should be related to the competition between cracking and disproportionation. As discussed in the previous sections, the $(C_1+C_2^o)/C_3^o$ ratio can be used to reflect the competition. The relation of the $(C_1+C_2^o)/C_3^o$ ratio with strong acids is shown in Fig.7.4.3. Again, among the acids, only strong Bronsted acid site density is found closely related to the ratio.

From the above discussion, one can conclude that butane transformation occurs on strong Bronsted acid sites. The more strong Bronsted acid sites a catalyst has, the greater extent of disproportionation reaction takes place on this catalyst.

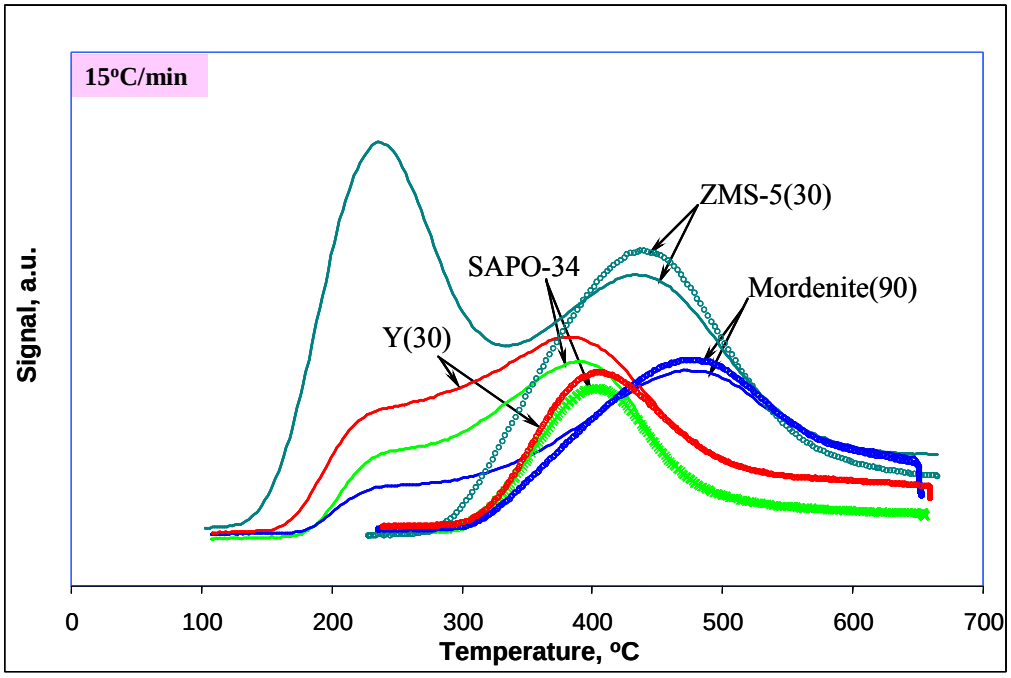

Fig.7.4.1 Comparison of NH_3-TPD experiment ramping from 105°C and 235°C for different zeolitic materials. Temperature ramping rate: 15°C/min. The number in the brackets denotes the SiO_2/Al_2O_3 ratio.

Table 7.4.1 Butane conversion and acidities of the catalysts. Reaction T=445°C; total pressure=1 atm; Ar/C_4H_{10} molar ratio=5.4; and C_4-$WHSV_{zeo}$=1.5 h^{-1}.

Catalysts	Conversion %	105°C L acid mmol/g-zeo	105°C B acid mmol/g-zeo	235°C L acid mmol/g-zeo	235°C B acid mmol/g-zeo
HZSM-5(30) powder	83	0.208	0.888	0.396	0.396
ZSM-5(30)/SiO_2-HS-40 pwd-mix	50	0.08	0.678	0.203	0.203
ZSM-5(30)/SiO_2-HS-40 pwd-wet-mix	38	0.029	0.727	0.237	0.237
ZSM-5(30)/γ-Al_2O_3 pwd-wet-mix	21	0.216	0.329	0.152	0.152
ZSM-5(30)/boehmite pwd-mix	19	0.221	0.33	0.151	0.151
ZSM-5(30)//boehmite pwd-wet-mix	10	0.246	0.294	0.122	0.122
ZSM-5(30)/SiO_2-HS-40 gel-mix	3	0.024	0.687	0.131	0.131
r-Al_2O_3	0.6	0.164	0	0	0

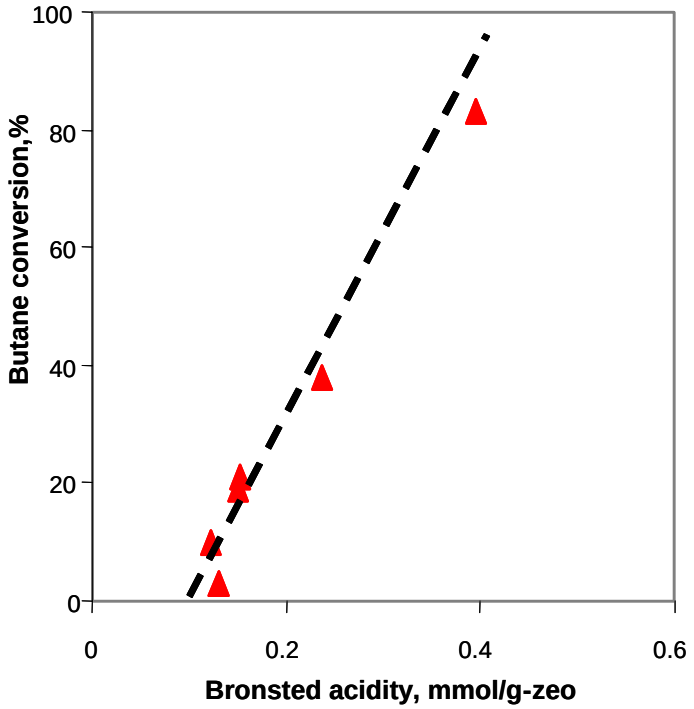

Fig.7.4.2 Relation of butane conversion and strong (235°C) Bronsted acidity of catalysts. Reaction T=445°C; total pressure=1 atm; Ar/C_4H_{10} molar ratio=5.4; and C_4-$WHSV_{zeo}$=1.5 h^{-1}.

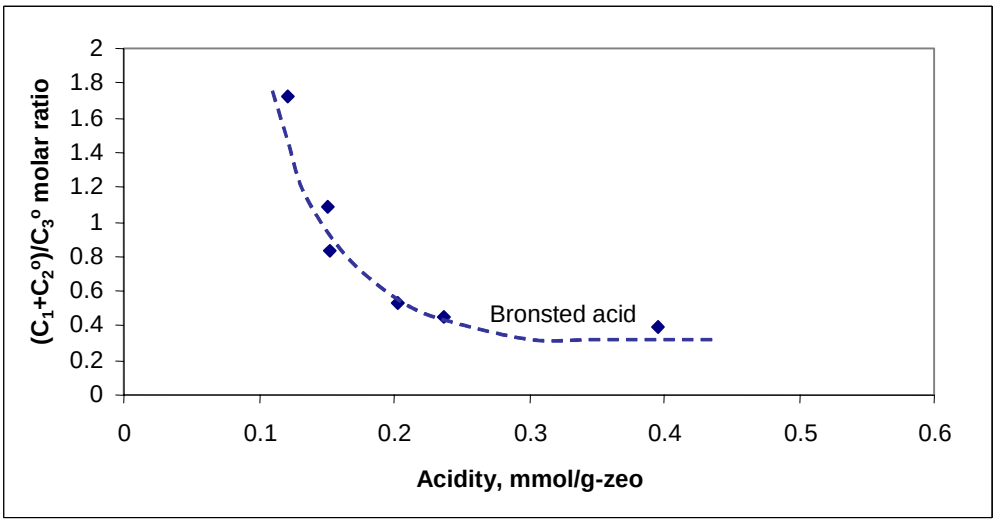

Fig. 7.4.3 Relation of $(C_1+C_2^o)/C_3^o$ ratio with strong Bronsted acidity of catalysts for butane conversion. T=445^{o}C; total pressure=1 atm; Ar/C_4H_{10} molar ratio=5.4; and C_4-$WHSV_{zeo}$=1.5 h^{-1}.

CHAPTER VIII

ETHYLENE OLIGOMERIZATION

In this chapter, the catalytic activity of silica-bound and alumina-bound ZSM-5 (SiO_2/Al_2O_3=30) are investigated for ethylene oligomerization. In order to make a comparison, ethylene oligomerization on unbound ZSM-5 is also studied. The apparatus used for conducting the reaction and product analysis method have been described in Chapter IV. Note that ethylene was used as a tie component in GC data processing when ethylene conversion was less than 80%; otherwise, methane was used as a tie component. The binders used are silica and alumina, respectively. Binding methods are gel-mixing, powder-wet-mixing, and powder-mixing, which have been described in Chapter III.

8.1 Chemistry

Quan et al. (1988) studied in detail the chemistry of olefin oligomerization. The main reaction is ethylene oligomerization, which is assumed to occur as follows (for demonstration and simplicity, only normal hydrocarbons are expressed herein):

$2C_2H_4 \rightarrow$ n-C_4H_8	ΔH^o_{600K}=-24.91 Kcal/mol;	ΔG^o_{600K} =-5.93 Kcal/mol
C_2H_4+n-$C_4H_8 \rightarrow$n-C_6H_{12}	ΔH^o_{600K} =-22.05 Kcal/mol;	ΔG^o_{600K} =-2.43 Kcal/mol
C_2H_4+n-$C_6H_{12} \rightarrow$n-C_8H_{16}	ΔH^o_{600K} =-22.02 Kcal/mol;	ΔG^o_{600K} =-2.17 Kcal/mol

The main reactions are strongly exothermic. Side reactions include hydrogen transfer, disproportionation, further oligomerization of primary products, cyclization,

and aromatization and cracking which take place at higher temperatures. For example, some of the side reactions are listed below:

$n\text{-}C_4H_8+n\text{-}C_6H_{12}\rightarrow n\text{-}C_4H_{10}+cy\text{-}C_6H_{10}$	ΔH^o_{600K}=-21.79 Kcal/mol; ΔG^o_{600K}=-11.26 Kcal/mol
$cy\text{-}C_6H_{10}+n\text{-}C_4H_8 \rightarrow C_6H_6+n\text{-}C_4H_{10}+H_2$	ΔH^o_{600K}= - 8.38 Kcal/mol; ΔG^o_{600K}=-22.79 Kcal/mol
$2\ n\text{-}C_4H_8 \rightarrow C_3H_6+i\text{-}C_5H_{10}$	ΔH^o_{600K}= -3.66 Kcal/mol; ΔG^o_{600K}= -3.11 Kcal/mol
$n\text{-}C_6H_{12} \rightarrow C_3H_6+C_3H_6$	ΔH^o_{600K}=+19.12 Kcal/mol; ΔG^o_{600K}= -1.49 Kcal/mol
$n\text{-}C_8H_{16} \rightarrow C_3H_6+ n\text{-}C_5H_{10}$	ΔH^o_{600K}=+19.14 Kcal/mol; ΔG^o_{600K}= -1.66 Kcal/mol
$cy\text{-}C_6H_{10} \rightarrow C_6H_6+2H_2$	ΔH^o_{600K}=+22.64 Kcal/mol; ΔG^o_{600K}=-11.14 Kcal/mol
$p\text{-}C_6H_{12} \rightarrow cy\text{-}C_6H_{12}$	ΔH^o_{600K}=-20.41 Kcal/mol; ΔG^o_{600K}= -6.56 Kcal/mol
$cy\text{-}C_6H_{12} \rightarrow cy\text{-}C_6H_{10}+H_2$	ΔH^o_{600K}=+29.64 Kcal/mol; ΔG^o_{600k}= +6.95 Kcal/mol

Cracking and dehydrogenation are strongly endothermic reactions. The former is thermodynamically favorable, while the later is not. Cyclization is also exothermic. Other reactions such as isomerization and disproportionation have a little heat of reaction and are reversible reactions.

8.2 On SiO_2-bound ZSM-5 Catalysts

8.2.1 HS-SiO_2-bound ZSM-5

Fig.8.2.1 shows ethylene conversion over HS-SiO_2-bound ZSM-5 catalysts at a reaction temperature of 300^{o}C. The activity of HZSM-5 is significantly reduced when silica Ludox HS-40 is used as a binder. However, the degree of activity decrease depends on the binding methods. The gel-mixing method gives the least active catalyst, while the other two methods produce catalysts with similar activity. All of the catalysts lose activity gradually as the time on stream increases, as shown in Fig. 8.2.1.

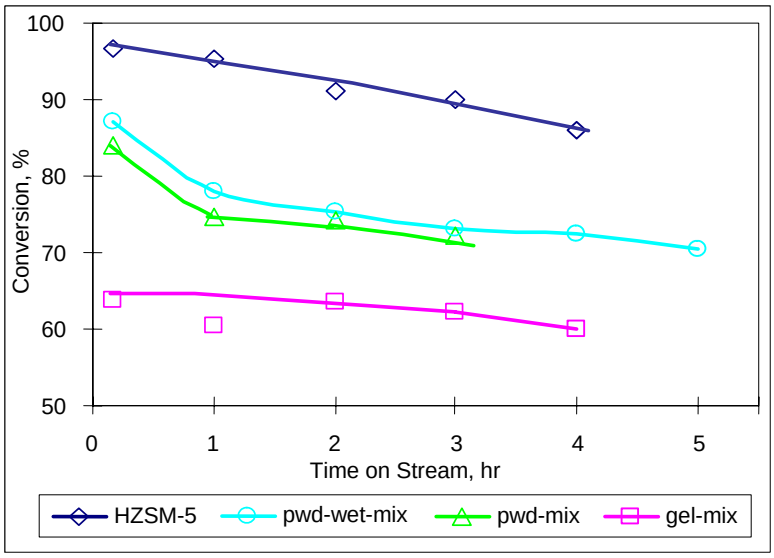

Fig.8.2.1 Comparison of HZSM-5 with HS-SiO_2-bound ZSM-5 catalysts at T=300°C. Total pressure: 1 atm; Ar/C_2H_4 molar ratio=4.78; $C_2^=$-$WHSV_{zeo}$=1.97 h^{-1}.

The effect of temperature on ethylene conversion and comparison of HZSM-5 with HS-SiO_2-bound ZSM-5 made by the gel-mixing method is shown in Fig. 8.2.2. As reaction temperature decreases, ethylene conversion dramatically declines as expected.

Table 8.2.1 lists the product distribution over these catalysts at 300°C at time on stream of 10 minutes. The propane and aromatics concentrations are lower and the propylene concentration is higher on the catalyst made by the gel-mixing method than on the other catalysts including HZSM-5. It has been shown in Chapter V that the gel-mixing method produces a catalyst with the least strong acidity and Bronsted acidity. Aromatics are formed on strong acid sites, and therefore their formation is inhibited on the gel-mix catalyst. Propylene is primarily formed from cracking of octenes. Since methane and ethane concentrations in the products are small, cracking of alkanes at this reaction condition occurs to a limited extent.

Table 8.2.1 Product distribution of ethylene oligomerization over HZSM-5 and HS-SiO_2-bound ZSM-5 made by different binding methods, mol%. T=300°C; TOS=10 min; Ar/C_2H_4 molar ratio=4.78; and $C_2^=$-$WHSV_{zeo}$=1.97 h^{-1}; silica source: Ludox HS-40; binder content: 29 wt%.

Component	HZSM-5	pwd-wet-mix	pwd-mix	gel-mix
hydrogen	0.00	0.00	0.00	0.00
methane	0.00	0.00	0.00	0.00
ethane	1.24	2.50	1.11	1.15
propane	10.97	3.80	4.07	1.53
propylene	7.25	11.19	8.56	19.66
isobutane	19.24	12.53	13.82	7.64
n-butane	4.99	2.45	2.56	1.03
butenes	11.86	21.59	16.63	33.20
C_5	20.99	21.96	21.00	16.16
C_6	1.58	10.26	10.29	12.09
C^+_7 non aromatics	7.20	11.16	9.31	7.53
Aromatics	14.68	14.54	12.64	7.53
i-C_4^0/n-C_4^0	3.85	5.11	5.40	7.40
$C^=_2$ conversion,%	96.73	87.13	84.10	63.74

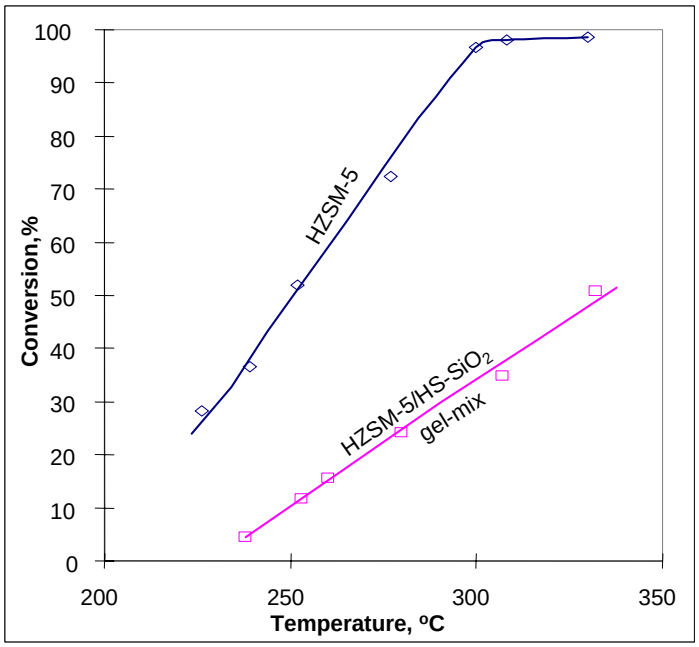

Fig. 8.2.2 Comparison of HZSM-5 with HS-SiO_2-bound ZSM-5 made by gel-mixing binding method. Total pressure: 1 atm; Ar/C_2H_4 molar ratio=4.78; TOS=10min; $C_2^=$-$WHSV_{zeo}$=1.97 h^{-1}.

Aromatic hydrocarbons and alkanes are formed through hydrogen transfer reactions which take place on strong acid sites. The acidity of the gel-mix catalyst is consistent with the experimental results when these products are considered.

As in the case of butane conversion, the decreased acidity and micropore blockage of HS-SiO_2-bound catalysts are the reasons for the decreased activity. The acidity change in the catalysts also results in changes in product distribution. A catalyst with fewer strong acid sites produces a product with more olefins and less aromatics from the conversion of ethylene.

8.2.2 AS-SiO_2-bound ZSM-5

The activity of SiO_2-bound ZSM-5 (SiO_2/Al_2O_3=30) catalysts made with Ludox AS-40 by different binding methods is illustrated in Fig.8.2.3 along with HZSM-5 for comparison. The activity of ZSM-5 is reduced after SiO_2 is embedded, as indicated by the lower ethylene conversions. As has been discussed in Chapter V, AS-SiO_2-ZSM-5 catalysts have less strong acid sites and strong Bronsted acid sites than HZSM-5. Therefore, the decreased activity can be inferred from the decreased acidity of these catalysts.

Another factor that may also make a contribution to the decreased activity of the SiO_2-bound catalysts is the reduced micropore surface area. As discussed in Chapter VI, SiO_2-bound catalysts have a micropore surface area of about 19% less than that of HZSM-5. It has been discussed in Chapter VI that the reduced surface area is a result of micropore blockage rather than micropore diameter shrinkage. The catalysts made from

Ludox AS-40 have more strong acid sites than the catalysts made from Ludox HS-40; therefore, they are more active, as indicated by the higher ethylene conversions.

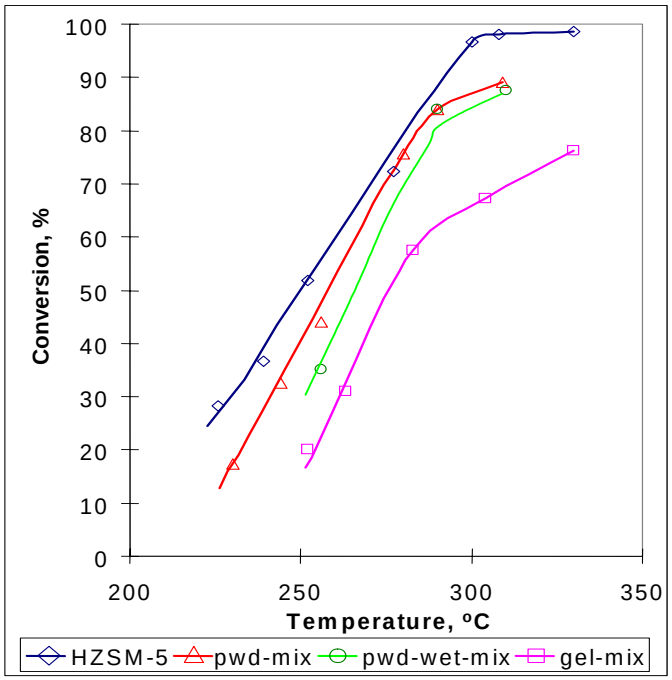

Fig. 8.2.3 Ethylene conversion over AS-SiO_2-bound ZSM-5(SiO_2/Al_2O_3=30) catalysts made by different binding methods. Total pressure: 1 atm; Ar/C_2H_4 molar ratio=4.78; TOS=10min; $C_2^=$-$WHSV_{zeo}$=1.97 h^{-1}.

The change of product distribution with reaction temperature is shown in Fig.8.2.4. In the product distribution, as reaction temperature increases, propylene and butenes decrease and alkanes and aromatics increase, indicating as expected more secondary reactions are occurring at higher temperatures. Note that, no hydrogen and methane were detected in the products for the reaction temperature range tested,

implying that deep cracking and dehydrogenation might not be occurring to a noticeable extent. The aromatics and alkanes are therefore formed primarily from hydrogen transfer between olefinic molecules. Among the aromatic hydrocarbons in the products, benzene is the predominant component at low reaction temperatures. As the reaction temperature increases, alkyl benzene starts to appear in the aromatic hydrocarbons.

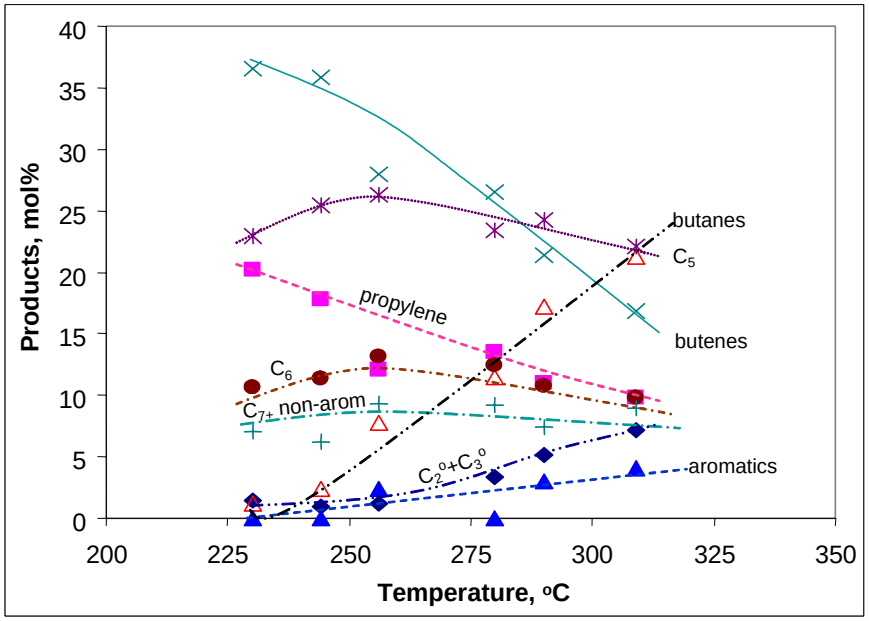

Fig. 8.2.4 Product distribution change with reaction temperature over AS-SiO2-bound ZSM-5(SiO_2/Al_2O_3=30) made by powder-mixing method. Total pressure=1 atm; Ar/C_2H_4 molar ratio=4.78; TOS=10min; $C_2^=$-$WHSV_{zeo}$=1.97 h^{-1}.

The effect of space time (the reciprocal of space velocity) on ethylene conversion is shown in Fig.8.2.5. When space time decreases, ethylene conversion decreases, because of the shorter residence time. Note that the space time is based on ethylene fed

and the mass of zeolite loaded into the reactor instead of the total feeding and the total mass of the catalyst.

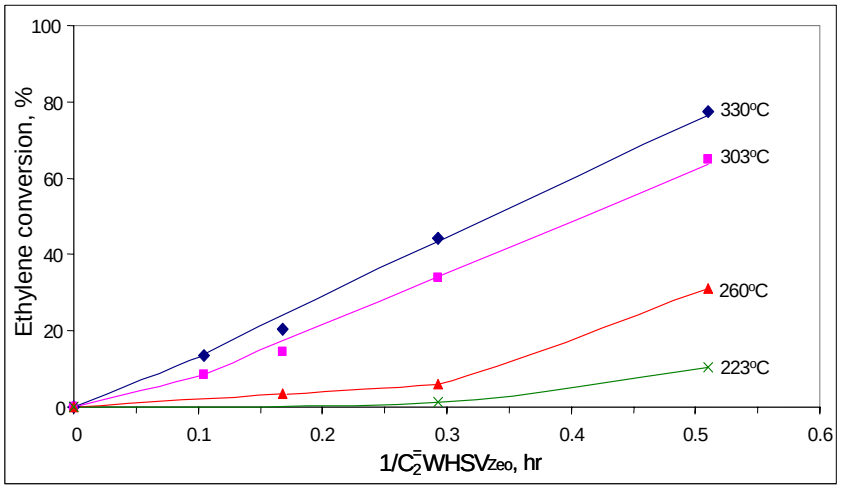

Fig.8.2.5 Ethylene conversion dependence on space time. Catalyst: pwd-mix AS-SiO_2-bound ZSM-5. Total pressure=1 atm; Ar/C_2H_4 molar ratio=4.78; TOS=10min.

Fig.8.2.6 shows how products change with ethylene conversion. It is apparent that butenes, propylene and C_5 are the major products at the reaction temperature of 303^{o}C. From this feature of the product distribution, ethylene dimerization and cracking of C_8 olefins are rapid reactions. The fact that the concentration of C_6 hydrocarbons in the products is much lower than that of C_5 hydrocarbons in a wide range of ethylene conversion suggests that the rate of oligomerization of butenes with ethylene would be much lower than the dimerization of butenes. Therefore, the possible major reactions involved in the initial steps in the conversion of ethylene can be as follows:

$$2C_2H_4 \rightarrow C_4H_8$$

$$2C_4H_8 \rightarrow n\text{-}C_8H_{16}$$

$$C_8H_{16} \rightarrow C_3H_6 + C_5H_{10}$$

The last reaction should be a fast reaction; otherwise, C_{7+} hydrocarbons would have been at a higher concentration in the products.

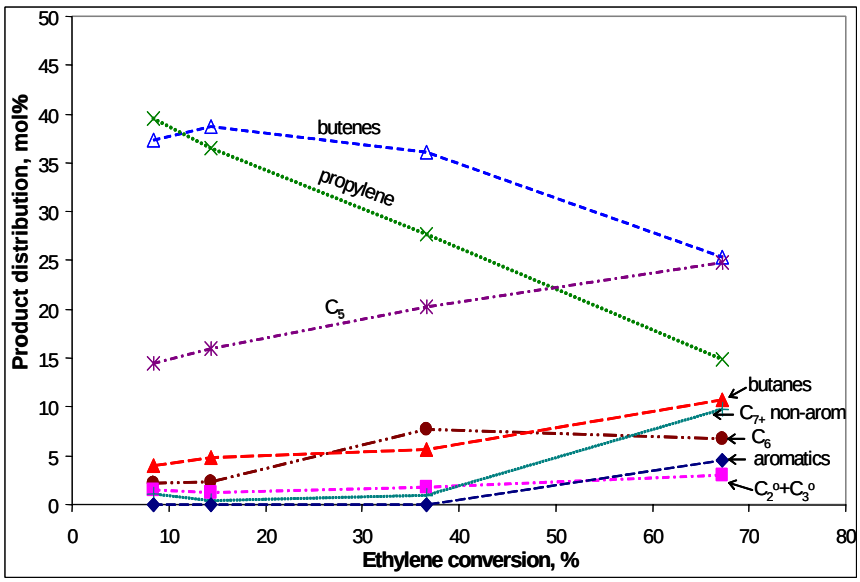

Fig.8.2.6 Product distribution at different ethylene conversions at 303°C on AS-SiO_2-bound ZSM-5 catalyst made by gel-mix method. Total pressure=1 atm; Ar/C_2H_4 molar ratio=4.78; TOS=10min.

8.3 On Al_2O_3-bound ZSM-5 Catalysts

Ethylene conversion was also evaluated on alumina-bound ZSM-5 (SiO_2/Al_2O_3=30) catalysts. Ethylene conversion is shown in Fig.8.3.1. The ethylene conversion levels on these catalysts correspond to the acidities of these catalysts as described in Chapter V. Micropore blockage of ZSM-5 by the alumina binder also has a role in the decreased activity of the bound catalysts.

In order to further verify the effect of micropore blockage of ZSM-5 by alumina binder on ethylene conversion, a commercial alumina-bound ZSM-5 (SiO_2/Al_2O_3=30) catalyst (denoted as "extrudate") is also tested and the results are shown in Fig.8.3.1. As discussed in Chapter V, this commercial catalyst has the same amount of Bronsted acidity as HZSM-5, but has a slightly lower activity (ethylene conversion) than HZSM-5 as shown in Fig.8.3.1. This difference in activity between these two catalysts should be attributed to the micropore blockage of ZSM-5 by the alumina binder.

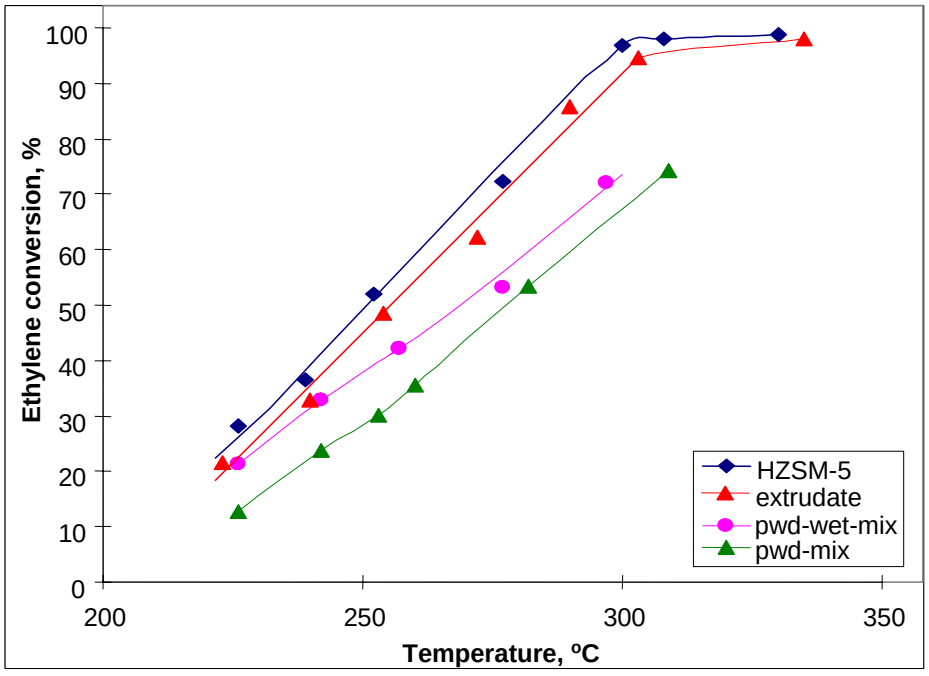

Fig. 8.3.1 Ethylene conversion over alumina-bound ZSM-5(SiO_2/Al_2O_3=30) catalysts made by different binding methods. Total pressure: 1 atm; Ar/C_2H_4 molar ratio=4.78; TOS=10min; $C_2^=$-$WHSV_{zeo}$=1.97 h^{-1}. The legend "extrudate" refers to a commercial alumina-bound ZSM-5 catalyst (binder 20 wt%).

8.4 Ethylene Conversion and Catalyst Acidity

Ethylene conversion is found to be highly dependent on Bronsted acid site density as shown in Fig.8.4.1. No close relationship between Lewis acidity and ethylene conversion is found, as indicated by the scattered points in Fig.8.4.1 for Lewis acids. This result is similar to that obtained by Amin and Anggoro (2002) who used FTIR to characterize the hydroxyl groups for Bronsted acid sites and found that ethylene conversion and gasoline selectivity were related to the Bronsted acid sites of the dealuminated ZSM-5. Both 105^{o}C Bronsted acidity (the total Bronsted acidity) and the 235^{o}C Bronsted acidity (the strong Bronsted acidity) correlated closely to ethylene conversion. From this result, one may conclude that the conversion of ethylene primarily occur on both strong and weak Bronsted acid sites. Note that the site densities of 105^{o}C Bronsted acid and Lewis acid are determined from an NH_3-TPD experiment starting from 105^{o}C (to get the total acid sites) and a pyridine-FTIR experiment (to get the Bronsted/Lewis acid site ratio). Similarly, the 235^{o}C Bronsted and Lewis acid sites are determined from a separate NH_3-TPD experiment starting from 235^{o}C to obtain the total acid sites. The Bronsted/Lewis acid site ratio is taken the same one as used in 105^{o}C.

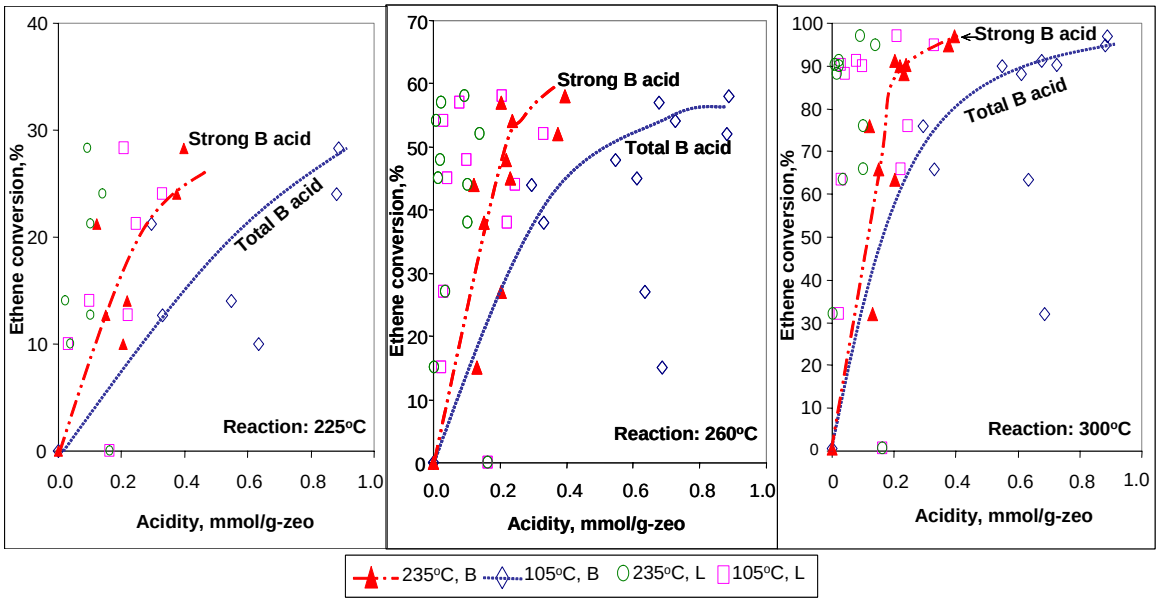

Fig.8.4.1 Relation of ethylene conversion at reaction temperature of 225°C, 260°C and 300°C with Bronsted acidity and Lewis acidity. The temperature indicted by the legends refers to the starting temperature of NH_3-TPD for acidity measurement. Reaction condition: total pressure: 1 atm; Ar/C_2H_4 molar ratio=4.78.

8.5 Catalyst Deactivation

The catalysts either unbound ZSM-5 or bound ZSM-5 deactivate rapidly with time on stream for ethylene conversion. What were the reasons that cause the catalysts lose their activities? In order to answer this question, some catalysts were taken out of the reactor without regeneration after they had been in the reactor for several hours with the diluted ethylene feed. The catalysts were analyzed on a BET machine and FTIR spectrometer, respectively. Table 8.5.1 and Figs. 8.5.1 and 8.5.2 show the results.

Table 8.5.1 Surface area and pore volume of fresh and partially deactivated catalysts.

Catalyst	BET m^2/g-cat	Micropore surface area m^2/g-cat	Meso/macro surface area m^2/g-cat	Micropore volume ml/g-cat	BJH 17-3000Å* m^2/g-cat
HZMS-5(30)/SiO_2 HS-gel-mix fresh	322	176	145	0.0738	164
HZMS-5(30)/SiO_2 HS-gel-mix Ethene reaction at 253°C for 4hrs	311	176	135	0.0729	143
HZSM-5(30) Powder fresh	411	308	104	0.1240	101
HZSM-5(30) Powder Ethene reaction at 254°C for 5hrs	374	252	122	0.1025	89
HZSM-5(30) Powder Ethene reaction at 300°C for 4hrs	243	159	84	0.0647	74

* Pore diameter range.

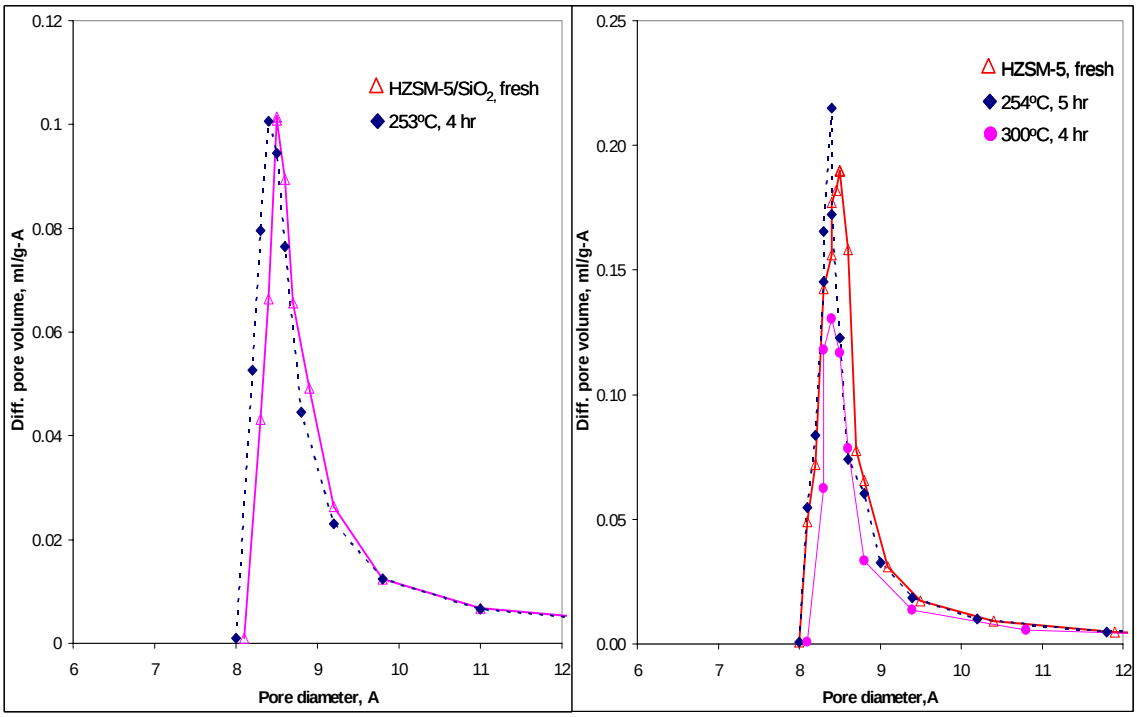

Fig. 8.5.1 Micropore volume distribution on fresh and partially deactivated SiO_2-bound ZSM-5 (left) and ZSM-5 (right) catalysts. The temperature and time denoted by the legends refer to reaction temperature and time on stream at which the catalyst was used for ethylene conversion.

From Table 8.5.1 it can be seen that micropore surface area and micropore volume are decreased for the deactivated catalysts. Since HS-SiO_2-bound ZSM-5 made by the gel-mixing method has a low activity, the surface area and micropore volume of the used catalyst do not change significantly compared with the fresh catalyst because of the low conversion of ethylene. However, on used HZSM-5 the micropore surface area and pore volume are reduced significantly, depending reaction condition. Higher reaction temperature results in higher ethylene conversion and more reduction in micropore surface area and micropore volume.

Micropore volume distributions of the partially deactivated catalysts are shown in Fig.8.5.1. The micropore volume distributions on the partially deactivated catalysts look like that on SiO_2- or Al_2O_3-bound ZSM-5. Therefore, the catalysts lose their activity because of pore blockage rather than pore diameter reduction.

FTIR spectra of these partially deactivated catalysts are shown in Fig.8.5.2. No absorption band above 3000 cm^{-1} are observed, indicating no aromatic hydrocarbons are present in the partially deactivated catalysts. It is known that coke is a complex substance that contains polynuclear aromatics, which has C-H vibrations around 3030 cm^{-1}. Therefore, the deactivation of the catalysts is due to big non-aromatic hydrocarbon molecules rather than coke. These big molecules are formed, for instance, from ethylene polymerization. These bulky molecules are trapped in the pores and cause the catalyst to deactivate.

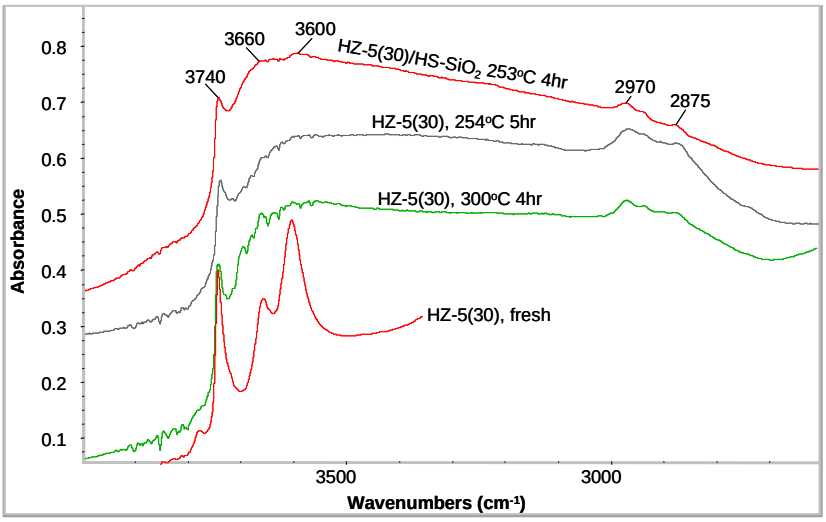

Fig. 8.5.2 IR spectra of fresh and partially deactivated catalysts from ethylene conversion. The legends denote the reaction temperature and time on stream for ethylene conversion. HZ-5(30) denotes HZSM-5 (SiO_2/Al_2O_3=30). HZ-5(30)/HS-SiO_2 was made by the gel-mixing method.

CHAPTER IX

CONCLUSION

Zeolites ZSM-5 and Y are bound with binders of SiO_2 (29 wt%) and Al_2O_3 (30 wt%) by different binding methods, namely gel-mixing, powder-wet-mixing and powder-wet-mixing. Acidity and texture of these bound catalysts are analyzed. Ethylene oligomerization and butane transformation (cracking and disproportionation) are used as probe reactions to examine the activity of the bound zeolite catalysts. From the results, the following conclusions can be drawn.

Some micropores of zeolite are blocked on embedding the zeolite powder to the silica or alumina binder. This occurs in the embedding process, probably in the calcination step. Micropore diameter of an embedded zeolite catalyst remains the same as the zeolite powder, that is, a binder does not change micropore size of the zeolite. Because of micropore blockage, micropore surface area and micropore volume of ZSM-5 (SiO_2/Al_2O_3=30) are reduced by about 19% and 18%, respectively, by a silica gel. While the micropore surface area and micropore volume of ZSM-5 are reduced by 26% and 23%, respectively, by an alumina binder.

Acidity of SiO_2-bound zeolite is reduced in terms of strong acid sites, and Lewis acid sites. SiO_2 from the binder may react with extra-framework alumina in zeolite to form a new acid center. Among the three different binding methods, the gel-mixing method provides a better contact between the zeolite crystals and the binder particles,

and thus more area for SiO_2 to react with extra-framework alumina, resulting less Lewis acid and more new acid sites than the other two binding methods.

The reduced acidity of silica-bound zeolite catalysts is due to alkaline metal cations present in the binder and the micropore blockage of the zeolite. Those metal cations neutralize acid sites, especially strong Bronsted acid sites. The metal cations in the binder come into zeolite to neutralize acid sites through ion-exchange in water solution in wet binding methods and through solid-state ion-exchange in calcination process. However, water solution ion-exchange is much easier to proceed than solid-state ion-exchange.

Alumina-bound zeolite catalysts have more Lewis acid sites and total acid sites than the zeolite powder itself. Bronsted acid sites of alumina-bound zeolite remain the same for ZSM-5 but increases for Y. The increased Bronsted acidity may come from the reaction of alumina from the binder with silica in zeolite (extra-framework); the increased Lewis acidity comes from the binder alumina which has only Lewis acid sites.

Alkaline metal content in a binder is a crucial factor that influences the acid site density. However, alkaline metal cations are more selective to neutralize Bronsted acid sites than to Lewis acid sites. Solid-state ion-exchange occurs more easily in alumina-bound catalysts than in silica-bound catalysts, indicating these metal cations migrate more easily in alumina than in silica.

Strong Bronsted acid site density is closely related to the catalyst catalytic activity for butane transformation (cracking and disproportionation). In ethylene oligomerization, both strong and weak Bronsted acidities are related to ethylene

conversion. The catalysts deactivate rapidly in ethylene oligomerization because some micropores of the zeolite are blocked by bulky oligomers formed inside the channels. In butane transformation, catalysts deactivates slowly.

On the bound ZSM-5 catalysts, for butane transformation, only cracking and disproportionation reactions occur to a significant extent and isomerization does not; in ethylene oligomerization, ethylene dimerization and butenes disproportionation are the major reactions.

LITERATURE CITED

Absil, R.P.L; Angevine, P.J; Herbst, J.A, et al.,U.S. Patent 5,053,374, 1991

Amin, N. A. S.; Anggoro, D. D., *J. Nat. Gas Chemistry* **2002**, *11*, 79-86

Anderson, J.R and Pratt, K.C, *Introduction to Characterization and Testing of Catalysts;* Academic Press: Australia, 1985.

Beck, J.S.; Vartuli, J.C.; Roth W.J.; Leonowicz, M.E.; Kresge, C.T.; Schmitt, K.D.; Chu, C.T-W.; Olson, D.H.; Sheppard, E.W.; McCullen, S.B.; Higgins, J.B., Schlenker, J. K., *J. Am. Chem. Soc*. **1992**, *114*, 10834

Canizares, P.; Duran, A.; Dorado, F.; Carmona, M., *Appl. Clay Science* **2000**, 16, 273-287

Cao, Y.; Lu, L.; Cheng, W.; Yang, D., *Acta Petrolei SINICA (Petroleum Processing Section)*, special issue, **1997**, 111-117

Chang, C. D.; Chu, C. T-W.; Miale, J. N.; Bridger, R. F.; Calvert, R. B., *J. Am. Chem. Soc*. **1984**, *106*, 8143-8146

Choudhary, V.R.; Devadas, P.; Kinage, A.K; Guisnet, M., *Appl. Catal. A: General*, **1997**, *162*, 223-233

Clerici, M. G., *Eurasian Chemico-Technological Journal* **2001**, *3*(4), 231-239

Climent, M. J.; Comra, A.; Velty, A.; Suarter, M., *J. Catal*. **2000**, *196*, 345-351

Climent, M. J.; Comra, A.; Garcia, H.; Guil-Lopez, R.; Iborra, S.; Fornés, V., *J. Catal.* **2001**, *197*, 385-393

Corma, A., *J. Catal*. **2003**, *216*, 289-312

Corma. A.; Fornes, V.; Rey, F., *Appl. Catal.* **1990**a, *59*, 267-274

Corma, A.; Grande, M.; Fornes, V.; Cartlidge, S., *Appl. Catal*., **1990**c, *66*, 247-255

Corma, A.; Grande, M.; Fornes, V.; Cartlidge, S.; Shatlock, M. P., *Appl. Catal*. **1990**b, *66*, 45-57

Costa, C.; Lopes, J.M.; Lemos, F.; Ribeiro, F. R., *J. Mol. Catal A: Chemcial* **1999**, *144*, 221-231

Dagade, S. P.; Waghmode, S. B.; Kadam, V. S.; Dongare, M. K., *Appl. Catal. A: General* **2002**, *226*, 49-61

Davis, M. E.; Saldarriaga, C.; Montes, C.; Garces, J.; Crowder, C., *Nature* **1988**, *331*, 698-701

Degnan Jr, T. F., *J. Catal*. **2003**, *216*, 32-46

De la Puente, G.; Sousa-Aguiar, E. F.; Costa, A. F.; Sedran, U., *Appl. Catal. A: General* **2003**, *242*, 381-391

Dessau, R. M., Schlenker, J. L.; Higgins, J. B., *Zeolites* **1990**, *10*, 522-530

Devadas, P.; Kinage, A.K.; Choudhary, V.R., *Recent Advances in Applied Aspects of Industrial Catalysis*, Ed. by T.S.R. Prasada Rao and G. Murali Dhar, Studies in Surface Science and Catalysis, Vol. 113, 425-432, Elsevier Science B.V.: New York, 1998

Dietz, W. A., *J. Gas Chrom*. **1967**, *5*(2), 68-72

Dorado, F.; Romero, R.; Canizares, P., *Applied Catalysis: A: General* **2002**, *236*, 235-243

Esterman, M.; McCusker, L. B.; Baerlocher, C.; Merrouche, A.; Kessler, H., *Nature* **1991**, *352*, 320-322

Falabella Sousa-Aguiar, E.; Almeida, D.; Bezerra, M.B.; Murta V., *Lat. Am. Appl. Res.* **1996**, *26*(2), 99-105

Fougerit, M. J.; Gnep, N. S.; Guisnet, M. ; Amigues, P., Duplan, J. L.; Hugues, F., *Zeolites and Related Microporous Materials: State of the Art 1994*, Ed. by J. Weitkamp; H. G. Karge; H. Pfeifer and W. Hoelderich, Studies in surface science and catalysis, Vol. 84, 1723-1730, Elsevier Science BV: New York, 1994

Gelin, P.; Des Courieres, T., *Appl. Catal*. **1991**, *72*, 179-192

Gelin, P; Gueguen, C., *Appl. Catal*. **1988**, *38*, 225-233

Guann, R. J.; Green, L. A.; Tabak, S. A.; Krambeck, F. J., *Ind. Eng. Chem. Res.* **1988**, *27* (4), 565-570

Guisnet, M.; Gnep, N. S., *Appl. Catal.* **1996**, *146*, 33-64

Guisnet, M.; Ayrault, P.; Datka, J., *Polish J. Chem.* **1997**, *71*(10), 1445-1461

Guisnet, M.; Moreau, V.; Magnoux, P., *Bulletin of the Polish Academy of Sciences, Chemistry* **2002**, *50*(2), 203-218

Hewin International, *Zeolites—Industry Trends and World Markets in 2010*, John Wiley & Sons, Inc.: New York, 2000

Jacobs, Peter A., *Carboniogenic Activity of Zeolites*, Elsevier Sci. Pub. Co.: New York, 1977

Katada, N.; Igi, H.; Kim, J. H.; Niwa M., *J. Phys. Chem. B* **1997**, *101* (31), 5969-5977

Klint, D.; Bovin, J-O., *Materials Research Bulletin* **1999**, *34*(5), 721-731

Kotrel, S.; Rosynek, M. P; Lunsford, J. H., *J. Catal*. **1999**, *182*, 278-281

Kubicek, N.; Vaudry, F.; Chiche, B.H.; Hudec, P.; Renzo, F. Di; Schultz, P.; Fajula, F., *Appl. Catal*. **1998**, *175*, 159-171

Le Van Mao, R., *Micro. Meso. Mat* **1999**, *28*, 9-17

Lonyi, F.; Valyon J., *Micro. Meso. Mat*. **2001**, *47*, 293-301

Marchilly, C., *J. Catal*. **2003**, *216*, 47-62

Marler, D.O, U.S. Patent 5,182,242, 1993

Meier, W. M.; Olson, D. H.; Baerlocher, Ch., *Atlas of Zeolite Structure Types*, 4th edition, Elsevier: New York, 1996

Mieville, R. L., *Journal of Colloid Interface Science* **1972**, *41*(2), 371-373

Misk, M.; Joly, G.; Magnoux, P; Guisnet, M; Jullian, S., *Micro. Meso. Mat*. **2000**, *40*, 197-204

Moore, P. B.; Shen, J., *Nature* **1983**, *306*, 356-358

Noronha, Zuy Maria M.; Monteiro, J. L. F.; Gelin, P., *Micro. Meso. Mat.* **1998**, *23*, 331-334

Romero, M .D.; Calles, J. A.; Rodriguez, A.; de Lucas, A., *Microporous Materials*, **1997**, *9*, 221-228

Scherzer, J., in *Fluid Catalytic Cracking: Science and Technology* Ed. by J. S. Magee and M. M. Mictchell, Studies in Surface Science and Catalysis, Vol. 76, 145-182, Elsevier Science B.V.: New York, 1993

Shihabi, D.; Garwood, W.E.; Chu, P.; Miale, J.N.; Lago, R. M.; Chu, C.T-W.; Chang, C.D., *J. Catal*, **1985**, *93*, 471-474

Smith, J.V., *American Mineral Society, Special Paper*, **1963**, *1*, 281-305

Szostak, R. *Molecular Sieves, Principles of Synthesis and Identification*, Van Nostrand Reinhold Catalysis Series, Van Nostrand Reinhold: New York, 1989.

Tanabe, K.; Holderich, W. F., *Appl. Catal.A: General*, **1999**, *181*, 399-434

Uguina, M. A.; Sotelo, J. L.; Serrano, D. P., *Appl. Catal*. **1991**, *76*, 183-198

Webb, P. A.; Orr, C., *Analytical Methods in Fine Particle Technology*, Micromeritics Instrument Corp.: 1997

Wu, X.; Anthony, R. G., *J. Catal*. **1999**, *184*, 294-297

Wu, X.; Alkhawaldeh, A.; Anthony, R.G., *Scientific Bases for the Preparation of Heterogeneous Catalysts* Ed. by E. Gaigneaux et al., Stud. Surf. Sci. Catal., Vol. 143, 217-225, Elsevier Science B.V.: New York, 2002

Wu, X.; Shan, X; Dong, Q.; Chang, H.; Li, Z., "New Synthetic Route for Benzyl Methyl Ether and Benzyl Alcohol from Benzene and Formaldehyde on Shape-selective Catalysts", *Jingxi Huagong*, **2001**, *18*(2), 114-116 (Chinese)

Zholobenko, V.L.; Kustov, L.M.; Isaev, S.A.; Kazanskii, V.B., *Kinet. Catal. : A translation of kinet i kataliz.* **1992**, *33*(1), 194-196

VITA

Xianchun Wu was born in Xinmin County, Liaoning Province, China, in 1962 to Mr. Haishan Wu and Mrs. Shuren Li. He attended elementary school and middle school in Dahongqi, Xinmin County. In 1978, he was selected by the Xinmin Special High School where he was awarded with a high school diploma in the summer of 1980. He went to college right after high school in the summer of 1980, the Daqing Petroleum Institute, Daqing City, Heilongjiang Province, China, where he received a Bachelor degree in Petroleum Refining in 1984. In 1987, he started the graduate study program in Daqing Petroleum Institute and received a Master of Science in Organochemical Engineering in 1990. After he graduated, he was a lecturer, and later in 1996 was promoted to an associate professor of Daqing Petroleum Institute.

He worked for a short period (8 months) for Dr. Rayford G. Anthony in the Chemical Engineering Department of Texas A&M University, College Station, TX, as a visiting scholar in 1997-1998. In 1999, he came to work again in the department for research under the direction of Dr. Rayford G. Anthony. In Spring 2000, he became a Ph.D. student in the department.

He can be contacted through email at wu850@yahoo.com or by the following address: 2002 Longmire CT Apt. 9D, College Station, TX 77840.